

**Studies on High Voltage Cathode Materials for Advanced
Lithium-Ion Battery**

Thesis

Submitted by

Sourav Nag

Doctor of Philosophy (Engineering)

Fuel Cell and Battery Division

CSIR-Central Glass and Ceramic Research Institute

Kolkata – 700 032, India

Department of Chemical Engineering

Faculty Council of Engineering and Technology

Jadavpur University

Kolkata – 700 032, India

2022

**Studies on High Voltage Cathode Materials for Advanced
Lithium-Ion Battery**

Thesis

Submitted by

Sourav Nag

Registration Ref. No. D-7/E/179/15 of 15-16

Index No. 96/15/E

Doctor of Philosophy (Engineering)

Fuel Cell and Battery Division

CSIR-Central Glass and Ceramic Research Institute

Kolkata – 700 032, India

Department of Chemical Engineering

Faculty Council of Engineering and Technology

Jadavpur University

Kolkata – 700 032, India

2022

JADAVPUR UNIVERSITY

KOLKATA-700032, INDIA

Statement of Originality

I, **Sourav Nag**, registered on 5th May, 2015 do hereby declare that this thesis entitled “**Development of Novel Separator and Cathode Materials for Lithium-Ion Battery**” contains literature survey and original research work done by undersigned candidate as part of Doctoral studies.

All information in this thesis have been obtained and presented in accordance with existing academic rules and ethical conduct. I declare that, as required by these rules and conduct, I have fully cited and referred all materials and results that are not original to this work.

I also declare that I have checked this thesis as per the “Policy of Anti Plagiarism, Jadavpur University, 2020”, and the level of similarity as checked by iThenticate software is 9 %.

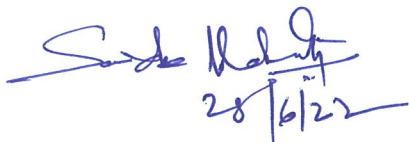


Signature of Candidate

Date: 27.06.2022

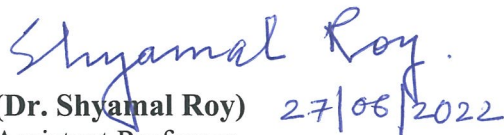
Certified by Supervisors

(Signature with date, seal)


28/6/22

(Dr. Sourindra Mahanty)

Former Senior Principal Scientist
Central Glass and Ceramic Research Institute
Council of Scientific & Industrial Research
Kolkata – 700 032


27/06/2022

(Dr. Shyamal Roy)

Assistant Professor
Chemical Engineering Department
Jadavpur University
Kolkata – 700 032

Assistant Professor
CHEMICAL ENGINEERING DEPARTMENT
JADAVPUR UNIVERSITY
Kolkata-700 032

JADAVPUR UNIVERSITY

KOLKATA-700032, INDIA

Certificate from Supervisors

This is certify that the thesis entitled “**Studies on High Voltage Cathode Materials for Advanced Lithium-ion Battery**” submitted by **Shri Sourav Nag** who got his name registered on 5th May, 2015 for the award of Ph.D (Engineering) degree of Jadavpur University, is absolutely based upon his work under the supervision of **Dr. Sourindra Mahanty** (Senior Principal Scientist, CSIR-Central Glass and Ceramic Research Institute, Kolkata 700 032) and **Dr. Shyamal Roy** (Assistant Prof, Chemical Engineering Department, Jadavpur University, Kolkata 700 032) and neither his thesis nor any part of the thesis has been submitted for any degree/diploma or any other academic award anywhere before.

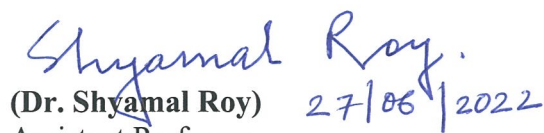
Signature of the Supervisors

Date with Official Seal



28/6/22

(Dr. Sourindra Mahanty)
Former Senior Principal Scientist
Central Glass and Ceramic Research Institute
Council of Scientific & Industrial Research
Kolkata – 700 032



27/06/2022

(Dr. Shyamal Roy)
Assistant Professor
Chemical Engineering Department
Jadavpur University
Kolkata – 700 032

Assistant Professor
CHEMICAL ENGINEERING DEPARTMENT
JADAVPUR UNIVERSITY
Kolkata-700 032

Dedicated

To

My Mentor

Daisaku Ikeda

President, Soka Gakkai International

Acknowledgement

First of all, I would like to express my sincere gratitude and indebtedness to my honorable supervisors Dr. Sourindra Mahanty and Dr. Shyamal Roy for their constant support, encouragement and valuable guidance during entire stages of this Ph.D research work. They invested their valuable time and effort to frame out the thesis work and I am giving my sincere regards and thank to them.

I thankfully acknowledge CSIR TAPSUN NWP0056 project (A network project involving several CSIR labs) for supporting the separator work which was carried out at the Fuel Cell & Battery Division at CSIR-CGCRI.

I would like to express my sincere gratitude to my departmental HOD, Prof. C. Guha, Prof. K. Kar Gupta, Prof. D. Roy, Prof. U Sarkar (Former HODs, Chemical Engineering Department) and Prof. R. Chakraborty (Present HOD, Chemical Engineering Department) for their kind help and encouragement to continue my research work and giving me the permission to use different equipment in different laboratories.

I would like to express my sincere gratitude to the Director, Central Glass and Ceramic Research Institute, Kolkata – 700 032 for her kind help and encouragement to continue my research work.

I would also like to convey my sincere gratitude to Dr. Atin Pramanik, Dr. Sandipan Maiti, Mr. Sudip Kumar Ghosh and all other staff members of Fuel Cell and Battery Division for their active support for carrying out the experimental work.

What I am today is because of my parents Late Pronay Kumar Nag and Mrs. Anajli Nag. Whatever success I have achieved in my life this is because of their unconditional support, care, and endless love with lots of blessings. Though, my father is not physically alive but his ethics, his advice and memory will always encourage me.

I would like to give thanks to my wife Ms. Shampa Nag for her un-ending support, love and encouragement during every moment of ups and downs of my life over past few years. Without her support and encouragement, it could not have been done. I would like to express my deepest gratitude and love to her for being with me as a wife and friend.

I also want to thank my daughter, Sharanya who makes me happy in all my work place and feel relaxed. I am also thankful to my colleagues Dr. Biswanath Kundu and Dr. Pradyot Datta who have constantly motivated me and have given their valuable time and effort in carrying out my thesis during the entire period.

Above all, I am grateful to my Mentor, Daisaku Ikeda for showering lots of blessing on me and with that I overcome all the barriers came in front of me during my entire period of research as well as in my life.


(SOURAV NAG)

Abstract

Developing alternate energy storage systems for transportation are motivated by a combination of socio-economic issues like environmental conservation to combat global warming, fast diminution of conventional non-renewable energy sources, rising cost of fossil fuel and concern for sustainable energy. Electrochemical energy storage may be considered as an important strategy while addressing the increasing demand for clean energy. In this complex situation Lithium-ion battery has come up as a potential alternative energy source that can be used in number of areas. However, the energy density of Li-ion battery is still much lower than that of fossil fuel. Therefore, at present the major challenge for the Li-ion battery research is focused on to increase the energy density along with power density to fulfil the demand for energies required for electric vehicles and high-end portable electronics. Now to satisfy the requirement of higher energy and power density, improved LIB materials are required with better electrochemical performance along with safety.

Cathode materials are the primary component responsible for increasing the energy and power density of rechargeable Li-ion batteries. The olivine structured LiMPO_4 (where $M = \text{Fe, Mn, Ni, or Co}$) has a great potential to serve this purpose. Among the various cathode materials, LiFePO_4 and the materials derived from LiFePO_4 are most widely used positive electrodes in LIBs. Along with LiFePO_4 , LiMnPO_4 is also gradually becoming attractive due to its high energy density (700 Whkg^{-1}), higher operational voltage at 4.1 V vs. Li, stability of traditional electrolyte solutions at this voltage electrochemically, improved safety due to existing strong P–O covalent bond, low cost and its environmentally benign nature. Having 20% higher redox potential compare to LiFePO_4 , LiMnPO_4 is considered as a potential cathode material while replacing LiFePO_4 in LIB. However,

the cyclic stability and rate performance of LiMnPO_4 are somewhat restricted due to its lower electronic and Li^+ ion conductivity.

In this work, LiMnPO_4 olivine structured cathode material at optimum pH condition with optimum content of conducting carbon in cathode material has been successfully prepared by low temperature (180°C) hydrothermal method. Optimum percent of La dopant in carbon containing cathode material is obtained based on electrochemical performance of the material. Physical and morphological characterization shows the structure and phase purity and their nano size morphology. Substitution of Mn^{2+} with La^{3+} in LiMnPO_4 improves the bulk conductivity as well as electronic mobility of the material than that of pure LiMnPO_4 .

During the past two decades, the development of lithium-ion battery research has been focused on exploring and improving the electrode materials and electrolytes. However, the separator, an indispensable component of Li-ion battery is not studied extensively. In general, a separator has major two functions, i.e., preventing the electronic connection between positive electrode and negative electrodes while providing transport pathways for Li^+ ion movements. Commercial separators for Li-ion batteries are usually made of polyolefin materials having two major drawbacks viz. low thermal stabilities and poor electrolyte wettability.

The development of advanced separator has been a major concern, in recent years for rechargeable lithium-ion batteries for varying areas of applications like portable electronics, electric vehicles and power grids. Having served the role of a physical barrier against the electronic conduction between cathode and anode in order to prevent electrical short circuiting, separator also holds the

liquid electrolyte which acts as a vehicle for Li^+ ions transport during charge/discharge cycles of Li-ion battery. The performance of Li-ion battery is largely dependent on the materials and structure of the separators.

In the present work, we have synthesized Boehmite ($\gamma\text{-AlO.OH}$) nanorods (length 90-140 nm; dia. ~15 nm) by a simple low-temperature (180°C) hydrothermal method and coated onto both sides of surface modified polypropylene (Celgard). The prepared composite separator has been tested in $\text{LiFePO}_4//\text{Li}$ half cells as well as in $\text{LiFePO}_4//\text{MCMB}$ full cells in coin cell configuration for understanding the influence of this separator on electrochemical performance. It is found that composite separator results in improved cell kinetics due to better electrolyte uptake and formation of a Li^+ ions buffer reservoir facilitating fast ion transport at high current rates.

Publication List

Publications included in Thesis

1. **S. Nag**, S. Roy, Conventional Cathode Materials for Advanced Lithium-ion Battery: A Review, *Journal of Materials Science* (2023) Manuscript Under Review.
2. **S. Nag**, S. Roy, La-doped LiMnPO₄/C cathode material for Lithium-ion battery, *Chemical Engineering Science*, 272 (2023) 118600 - 118606.
3. **S. Nag**, A. Pramanik, S. Roy, S. Mahanty, Enhancement of Li⁺ ion kinetics in boehmite nanofiber coated polypropylene separator in LiFePO₄ cells, *Journal of Solid State Chemistry*, 312 (2022) 123214 –123223.
4. **S. Nag**, S. Mahanty, Electrochemical properties of La-doped LiMnPO₄/C as lithium-ion battery cathode, Feb. 18-20, 2016, 27th Annual General Meeting of MRSI on Advanced Materials for Sustainable Application held at CSIR-NEIST, Jorhat, Assam.

Other publications

1. S. Mandal, S. Manna, K. Biswas, **S. Nag**, B. Ambade, Effect of gamma ray irradiation on optical and luminescence properties of CeO₂ doped bismuth glass, *Ceramics International*, (2023) DOI: <https://doi.org/10.1016/j.ceramint.2023.04.231>
2. S. Mandal, R. Chatterjee, **S. Nag**, S. Manna, S. Jana, K. Biswas, B. Ambade, Low Expansion Glass-Ceramics Using Industrial Waste and Low-cost Aluminosilicate Minerals: Fabrication and Characterizations, *Transaction of Indian Ceramic Society*, 82 (1) (2023) 46-55
3. **S. Nag**, S. Jana, M. Adhikary, S. Barik, A. Roy Chowdhury, S. Ghorui, B. Haldar, A. Ghosh, H. S. Tripathi and S. Mandal, Development of Mullite Based Refractory Pot for High Lead Containing Glass Melting, *Transaction of Indian Ceramic Society*, 80 (2) (2021) 150–156.

4. Q.A. Islam, **S. Nag**, R.N. Basu, Chemical Stability and Electrical Conductivity of $\text{Ba}_{0.8}\text{Ce}_{0.85-x}\text{Zr}_x\text{Tb}_{0.15}\text{O}_{3-\delta}$ Proton Conductors with ZnO as Sintering Aid, *Transaction of Indian Ceramic Society*, 75 (1) (2016) 25–32.
5. Q.A. Islam, S. Nag, R.N. Basu, Electrical properties of Tb-doped barium cerate, *Ceramics International*, 39 (6) (2013) 6433–6440.
6. Q.A. Islam, **S. Nag**, R.N. Basu, Study of electrical conductivity of Ca-substituted $\text{La}_2\text{Zr}_2\text{O}_7$, *Materials Research Bulletin*, 48 (2013) 3103–3107.
7. **S. Nag**, S. Mukhopadhyay, R.N. Basu, Development of mixed conducting dense nickel/Ca-doped lanthanum zirconate cermet for gas separation application, *Materials Research Bulletin*, 47 (2012) 925–929.

Table of Content

Content	Page No.
Statement of Originality	ii
Certificate from Supervisors	iii
Acknowledgement	v
Abstract	vii
Publications	x
Table of Content	xii
List of Figures	xvii
List of Tables	xxii
Nomenclature	xxiii

<u>Index No.</u>	<u>Content</u>	<u>Page No.</u>
CHAPTER 1: INTRODUCTION		
1.1	Challenges and Motivation	2
1.2	Research Objectives	5
CHAPTER 2: LITERATURE REVIEW		
2.1	Energy Storage Systems	12
2.1.1	Lead Acid Battery	14
2.1.2	Nickel-Cadmium Battery	14
2.1.3	Lithium-ion Battery	15

2.2 Approaches to and Challenges for Li-Ion batteries	18
2.2.1 Advantages of Nanomaterials	22
2.3 History of Li-Ion Batteries	24
2.4 Working Principal of Li-Ion Battery	27
2.5 Design of Cell and Various Configurations	29
2.6 Battery Specifications	33
2.7 Practical Parameters in Evaluating Battery Performance	34
2.7.1 Capacity and Rate Capability	34
2.7.2 Cyclability	36
2.7.3 Voltage	37
2.7.4 Energy Density	39
2.7.5 Power Density	40
2.7.6 Safety	40
2.7.7 Cost	40
2.8 Details of Battery Components	41
2.8.1 Cathode Materials	42
2.8.1.1 Requirements for Cathode materials	42
2.8.1.1.1 Layered Oxides	44
2.8.1.1.2 Spinel Structure	46
2.8.1.1.3 Olivine Structure	46
2.8.1.2 Brief Detail of Cathode	48
2.8.1.3 Recent Developments in Cathode Materials	51
2.8.1.3.1 LiNi_{1-y}Mn_yO₂	53

2.8.1.3.2	LiNi _{1/3} Mn _{1/3} Co _{1/3} O ₂	54
2.8.1.3.3	LiMnO ₂ (layered)/LiMn ₂ O ₄ (Spinel)	54
2.8.1.3.4	Li ₂ MnO ₃	56
2.8.1.3.5	Binary and Ternary Solid Solutions of Li ₂ MnO ₃	57
2.8.2	Anode Materials	58
2.8.2.1	Lithium Metal	59
2.8.2.2	Carbon-based Materials	59
2.8.2.2.1	Graphite	60
2.8.2.2.2	Graphene	61
2.8.2.3	Li- metal Alloys / Intermetallic Alloys	63
2.8.2.4	Tin-based Compounds	64
2.8.2.5	Transition Metal Oxides	65
2.8.2.6	Titanium Oxides based Anode Materials	66
2.8.2.7	Solid-Electrolyte Interphase	67
2.8.3	Separators	67
2.8.3.1	Fundamental Requirements of Separators	68
2.8.4	Electrolyte	77
2.9	Future Batteries	81
 CHAPTER 3: MATERIAL AND METHODS		
3.1	Objective of this Thesis Work	84
3.1.1	Cathode Material	84
3.1.2	Separator	86

3.2 Cathode Materials Synthesis and Characterization	88
3.2.1 Synthesis of Lanthanum doped Lithium Manganese Phosphate	88
Cathode Materials	
3.2.2 Structural Characterization	88
3.2.3 Microstructure & Morphology	88
3.2.4 Fabrication of LIB Coin Cell and Electrochemical Tests	89
3.2.4.1 Cell Fabrication	89
3.2.4.2 Electrochemical Measurements	89
3.3 Separator Materials Synthesis and Characterization	89
3.3.1 Synthesis of γ-AlO.OH	89
3.3.2 Preparation of γ-AlO.OH coated PP (ALO-PP) Separator,	90
LiFePO ₄ Cathode and MCMB Anode	
3.3.3 Material Characterization	90
3.3.4 Electrochemical Characterization	91
 CHAPTER 4: RESULTS AND DISCUSSION	
4.1 Cathode Materials	94
4.2 Separator	102
4.2.1 Structure and Morphology of Synthesized AlO.OH Powder	102
4.2.2 Structure and Morphology of γ-AlO.OH coated PP(ALO-PP)	106
4.2.3 Thermal, Chemical Stability and Electrolyte up-take of γ-	108
AlO.OH coated PP (ALO-PP)	
4.2.4 Mechanical Properties	110

4.2.5 Electrochemical Properties	114
CHAPTER 5: CONCLUSIONS AND FUTURE WORK	
5.1 Conclusions	124
5.2 Scope of Future Work	129
REFERENCES	131
APPENDIX	166

List of Figures

<u>Figure No.</u>	<u>Figure caption</u>	<u>Page No.</u>
Figure 1	Energy Density of Various Energy Storage Systems	13
Figure 2	Energy Density of Various Battery Technologies	15
Figure 3	Cost of Current Technologies Compared to DOE Targets	18
Figure 4	Voltage vs. Capacity for Various Cathode and Anode Materials	19
Figure 5	Dendrite Formation on Lithium Anode	25
Figure 6	Structure of Graphite Lithium Intercalation	26
Figure 7	Schematic of Charging and Discharging of Li-Ion Cell	28
Figure 8	Schematic Representation of Charge/Discharge Mechanism in Li-Ion Battery	28
Figure 9	Various Configurations of Battery a) Cylindrical type b) Coin type c) Prismatic type and d) Thin and Flat Polymer type	30
Figure 10	Coated Cathode and Anode for Sony 18650 LiCoO ₂ Battery	31
Figure 11	Battery Manufacturing Flow Chart	32
Figure 12	Effect of Coulombic Efficiency on Cyclability	35
Figure 13	Capacity Plots with Voltage	36
Figure 14	C/LiCoO ₂ (18650 type) Batteries Show Rate Capability at Constant Current	36
Figure 15	Different types of Discharge Curves Represented Schematically	38

Figure 16	Schematic Representation of Three Major types of Positive Electrode Materials	47
Figure 17	Graphene based Anode Material Showing Typical Charge-Discharge Profile	50
Figure 18	Layered Structured LiMO_2	51
Figure 19	Layered Structure of LiCoO_2	52
Figure 20	Unit Cell of $\text{LiMn}_y\text{Ni}_{1-y}\text{O}_2$ Showing Li Layer and Ni, Mn Layers	53
Figure 21	Layered LiMnO_2 and Spinel LiMn_2O_4 Structure	55
Figure 22	The Rock Salt Structure of Li_2MnO_3	57
Figure 23	Hexagonal Graphite as (a) Graphene Layers Stack Together and (b) Single Layer Graphene	60
Figure 24	Three types of Carbon used in Li-Ion Battery	63
Figure 25	Typical Polyolefin Separators Prepared by Wet Process (Solupor 8P01E) (left) and Dry Process (Celgard 2325) (right)	68
Figure 26	Schematic Representation of $\gamma\text{-AlOOH}$ Coated Separator Preparation	92
Figure 27	(a) X-ray Diffractogram and (b) FTIR Spectrum of Synthesized LiMnPO_4 at Different pH Condition	94
Figure 28	(a) TGA and (b) DTA of Synthesized LiMnPO_4 with Different Carbon Content	95
Figure 29	X-ray Diffractogram of LiMnPO_4/C Composite Produced by Hydrothermal Method	95

Figure 30	Electrochemical Charge Discharge Capacity of LiMnPO ₄ /C Composites	96
Figure 31	(a) X-ray Diffractogram and (b) DTA/TGA of Synthesized La doped LiMnPO ₄ /C Composite	97
Figure 32	Structure of LiMnPO ₄ /C With and Without Lanthanum	97
Figure 33	Particle Morphology of LiMnPO ₄ (a) Without doping and (b) With 1% La doping	98
Figure 34	X-ray Diffractogram and of Synthesized LiMnPO ₄ after in-situ Carbon Deposition and Lanthanum Doping	99
Figure 35	Electrochemical Charge Discharge Capacity of La-doped LiMnPO ₄ /C Composites	100
Figure 36	Electrochemical Rate Performance of LiMnPO ₄ /C Composites With and Without Lanthanum	100
Figure 37	Electrochemical Performance of LiMnPO ₄ /C Composites (a) Cyclability and (b) Coulombic Efficiency With and Without Lanthanum	101
Figure 38	(a) X-ray Diffractogram and (b) FTIR Spectrum of Synthesized γ -AlO.OH Powders	103
Figure 39	(a, b): FESEM Micrographs of Synthesized γ -AlO.OH Powder at different Magnifications	104
Figure 40	(a, b): Bright Field TEM images; (c) High Resolution TEM Image and (d) SAD Pattern of TEM of AlO.OH Powder	105

Figure 41	Adsorption-desorption Isotherms of γ -AlO.OH Powder along with its Pore Size Distribution	106
Figure 42	FESEM Micrographs of (a) PP and (b) ALO-PP-35	107
Figure 43	Adsorption-desorption Isotherms with pore Size Distribution of (a) Uncoated PP and (b) ALO-PP-35	107
Figure 44	(a) Photograph Showing (a) Comparative Thermal Stability of PP and ALO-PP (b) Variation of Thermal Stability and (c) Variation of Electrolyte Uptake of ALO-PP with Coating Thickness	109
Figure 45	Nanoindentation Profile of PP (19 μ m) and AlO.OH coated PP (35 μ m)	110
Figure 46	Variation of (a) Extensional Storage Modulus and (b) Elastic Modulus and (c) Poission's Ratio with Thickness of Coated Separator	112
Figure 47	Comparison of Electrochemical Properties with ALO-PP and PP as Separator (a) Initial Charge-discharge Capacity of LiFePO ₄ //Li cells at C/20 for varying Coating Thickness (b) Rate Capability of LiFePO ₄ //Li Cells between C/20 and C/2 and (c) Rate Capability of LiFePO ₄ //MCMB Cells between C/20 and C/2	117
Figure 48	Nyquist Plots for PP and ALO-PP-35 Soaked in Liquid Electrolyte. The Equivalent Circuit used to fit the Impedance data is given in the Inset	118

Figure 49	Cycling of LiFePO ₄ /Li Cell with PP and Coated Separators	119
Figure 50	Cycling Performances of LiFePO ₄ /Li Cell with Coated Separator (35 μm) with Conventional Polypropylene (19 μm) at Current Densities of (a) C/10, (b) C/5 and (c) C/2	120
Figure 51	Cycling Performance of LiFePO ₄ /CMS Graphite Cell	121
Figure 52	Cell Impedance of LiFePO ₄ /Li Half-cell with AIO-PP 35	121

List of Tables

<u>Table No.</u>	<u>Title of table</u>	<u>Page No.</u>
Table 1	Goals Set for Commercial Advanced Batteries for EVs till CY 2020: United States Advanced Battery Consortium (USABC) (2014)	17
Table 2	Properties of Various Anode Materials (Capacity Values are based On Delithiated State of Material except Lithium Metal	22
Table 3	Characteristics of Three Major Types of Positive Electrode Materials	48
Table 4	Properties of Commercially available Cathode Materials	49
Table 5	General Requirements for LIB Separators	71
Table 6	Common Lithium Salts and their Properties	78
Table 7	Performance Comparison of Future Battery Systems	81
Table 8	Impedance Parameter for PP and ALO-PP-35 Membranes	119
Table 9	Properties of LiFePO ₄ /Li Half-cell with ALO-PP-35 Membranes	122

Nomenclature

Whkg ⁻¹	Watt-hour per kilogram
V	Volt
dia.	Diameter
nm	Nanometer
MCMB	Meso carbon micro bead
°C	Degree centigrade
LIB	Lithium-ion battery
EV	Electric vehicle
HEV	Hybrid electric vehicle
GHG	Greenhouse gas
ICE	Internal combustion engine
DOH	Degree of hybridization
PHEV	Plug-in hybrid electric vehicle
mWhg ⁻¹	Mili-watt hour per gram
mAhg ⁻¹	Mili-ampere hour per gram
SHE	Standard hydrogen electrode
gcm ⁻³	Gram per centimeter cube
IEA	International Energy Agency
GW	Gigawatt
0D	Zero dimension
1D	One dimension

2D	Two dimension
C-rate	Rate of current
SEI	Solid electrolyte interphase
mm	Milimeter
PVDF	Polyvinylidene fluoride
C_g	Specific capacity
F	Faraday Constant
z	Number of charge transfer per mole of material
M	Molar mass of materials
C_{cell}	Specific capacity of cell
A	Amphere
E_{cell}	Voltage of cell
NaSICON	Na super-ionic conductor
S_{cm}^{-1}	Siemens per centimeter
LCO	Lithium cobalt oxide
LMO	Lithium manganese oxide
MTSC	Maximum theoretical specific capacity
$g\ mol^{-1}$	Gram per mole
FCC	Face centered cubic
E_0	Electrochemical potential
MCF	Mesophasepitch carbon fibre
VGCF	Vapour grown carbon fibre
MAG	Massive artificial graphite

HPG	Hierarchically porous graphite
DHPG	Doped hierarchically porous graphene
MWCNT	Multi wall carbon nano tube
cm^2s^{-1}	Centimeter square per second
μm	Micrometer
N_m	McMullin number
ρ_s	Electrolyte resistances in the presence of separator
ρ_e	Electrolyte resistances in absence of a separator
τ	Tortuosity
ϵ	Porosity of the separator
σ_i	Ionic conductivity
DEC	Diethylene carbonate
EC	Ethylene carbonate
PC	Propylene carbonate
DMC	Dimethyl carbonate
LiSICON	Lithium superionic conductor
TFSI	Trifluoromethanesulfonil imide
PE	polyethylene
PI	polyimide
NMP	n-methyl-2-pyrrolidone
PP	polypropylene
AIO-PP	AIO.OH coated polypropylene
DMSO	Dimethyl sulfoxide

TEGDME	Tetraethylene glycol dimethyl ether
GPa	Gigapascal
MD	Machine direction
N	Newton
MPa	Megapascal
Ω	Ohm
PEO	polyethylene oxide
PAN	polyacrylonitrile
PVDF-HFP	Polyvinylidene fluoride-co-hexafluoro propylene

CHAPTER 1
INTRODUCTION

CHAPTER 1

INTRODUCTION

Lithium-ion battery (LIB) systems have become the commonly used power sources for various electronic and electrical applications viz. portable electronics as well as transportation such as for electric vehicles (EVs) as well as hybrid electric vehicles (HEVs) etc. This is because of their high voltage, high energy and power density and long cycle life. In the area of renewable energy systems, LIB is regarded to be the most prospective energy storage device. Following is the history and commercialization of Lithium-ion battery. Whittingham from Exxon first conceived the concept of Li-ion battery and showed a working cell consisting of Li metal/TiS₂ 1970. In 1979 Goodenough first published the paper showing that LiCoO₂ can be used as an intercalation cathode. Following the year in 1980 Rachid Yazami first published the concept of using graphite anode in LIB and with this Lithium-ion battery technology underwent a revolutionary change in the direction of its commercialization. The first commercial LIB was developed by Sony Corporation in 1991. Nowadays, many devices, depending upon their applications use various types of LIBs. These applications include portable electronics to automotive to power grid. According to the prediction of International Energy Agency (IEA), the light-duty EV fleet is likely to grow from ~ 10 million in 2021 to 124–199 million in 2030 globally [1].

1.1 Challenges and Motivation

Combustion engine was the primary energy source for transportation because of its high energy and power densities in 20th century and also in the beginning of 21st century. However, the increasing rate of global warming and limiting supply of fossil fuels demand a sustainable alternative energy source. Electrochemical conversion (Fuel cells) and storage devices (Batteries

and Supercapacitors) can be considered as best alternatives to this direction. Battery technology has been commercialized and is recently being in use in electric and hybrid electric vehicles (EV/HEV). Out of various battery systems lithium-ion battery (LIB) showed the highest potential for the application in electric vehicle and advanced energy storage systems for clean electricity. However, significant increase in energy and power density is required for such high power applications [2-4]. Higher power density essentially decreases the Li-ion battery charging time, which is a primary consideration for electric vehicle. Specific power is the product of specific current and voltage. This can be increased either by raising the voltage by judiciously selecting the positive and negative electrode materials or by improving the rate of charging/discharging or by increasing both. One of the possible ways to increase the overall charge/discharge rate is to develop the positive electrode materials using nanoparticles instead of conventional microparticles [5, 6]. Although the use of nanoparticles as active materials promises higher power density for LIB, however, the nature of electrochemical storage in these nano engineered materials is not fully understood. To commercialize the LIB using nanoparticles as active materials for electrodes still require sophisticated electrode formulation for better understanding of charge storing mechanism. Therefore, this work is motivated by a need for a deeper understanding of the use of nanoparticles towards the formulation of cathode active materials to be used in Li-ion batteries.

The majority of electrical energy requirement as on today is fulfilled by fossil fuels. However, increasing demands for fuels along with its increased cost and resulting environmental pollution has created a pressure on world energy infrastructure. To combat this situation, a significant effort has been put forward to develop alternate renewable energy sources like solar cells, fuel cells etc. along with electrochemical energy storage systems such as Li-ion battery [7-10]. The wide

application of lithium-ion battery is mainly because of its light-weight and rechargeable property which is suitable for portable electronics such as laptop, mobiles, camera etc. Recently, this system is also being in use in hybrid electric vehicle (HEV). However, the energy and power density, operating voltage, capacity, safety and cost issues has put a limit towards its commercialization. In this research, focus has been given on to enhance the performance of olivine structure based cathode material for improving the energy density in addition to power density of cathode material.

The separator is an indispensable component in a battery, be it primary or rechargeable. It prevents the electronic connection between cathode and anode, while permitting ionic communication between electrodes. Porous structured insulators naturally do the job. Historically, felt, glass, asbestos, rubber, cellulose, wooden veneer, organic fibres, nylon and polyolefin have been used in lead-acid and alkaline batteries [11, 12]. In the era of LIBs, polyolefin microporous separators have prevailed since the very commencement of their commercialization in the early 1990s [11]. This is due to their satisfactory performance and socioeconomic feasibility. The initiation of research on LIB separators includes efforts made on the identification of alternative materials with good wettability for non-aqueous electrolytes and high thermal stabilities, and the modifications of polyolefin separators to achieve the same purposes. This has been well-summarized in several review papers [11, 13, 14]. However, the most drastic expansion of the separator research started after year 2010, when post-LIBs gained significant attention and modified separators were found capable of solving/mitigating certain problems associated with them, e.g., polysulfide shuttling [15] and Li dendrite growth [16]. The gained knowledge from the post-LIBs in return stimulated the development of advanced separators for high performance LIBs. In this research the focus has also been given on separator material for improved electrochemical performance and safety.

1.2 Research Objectives

The primary objective of this work is to understand the methods and procedures necessary to investigate the effect of nanoparticles on performance improvement of Li-ion battery cathode material. The investigation of critical issues associated with the use of nanoparticles as active material for positive electrode, namely, cathode formulation along with active material synthesis and its property evaluation are the goals of this work. This work would, therefore hopefully contribute to the improvement of devices requiring high power such as the EV/HEV and other electrochemical devices.

The objective of the separator work to investigate and develop a suitable surface modified polypropylene separator for advanced lithium-ion battery, which would not only serve its basic purpose of being an insulator against the electronic conduction between cathode and anode electrodes but also act as a buffer layer for Li^+ ion storage for improved electrochemical performance.

CHAPTER 2
LITERATURE REVIEW

CHAPTER 2

LITERATURE REVIEW

The energy and environmental issues are the two major concern at present and these issues have triggered the searching for alternative clean energy sources. Addressing these issues through the development of clean energy sources in turn manifests the societal and technological advancement. The continuously increasing demand for energy and rapid depletion of non-renewable energy resources have posed a threat on present day energy economy. Moreover, greenhouse gas emission associated with the use of non-renewable energy sources such as fossil fuels are considered as one of the major reasons for global warming [17, 18].

The revolution in transportation such as faster automobiles and airplanes have enhanced people's movement significantly in last two centuries. As this mode of transportations are primarily dependent on fossil fuels, therefore the utilization of fossil fuels has also increased steadily, which in turn generated a large volume of greenhouse gas (GHG) followed by causing the global warming as well. According to a report in 2011, the energy consumption in US transportation is around 28% and the major portion of this energy (93%) came from petroleum and this directly linked to the GHG emission of 28% [19, 20]. The increasing volume of GHG emission due to over usage of fossil fuels have therefore, become a limiting factor that has shaped the future of transportation. Therefore, moving from fossil fuels to alternative energy sources in the area of transportation require to address the following issues:

Energy security: Becoming self-reliant by gradually reducing/ eliminating the fuel import.

Preserving Environment: Technology development without negatively impacting the environment.

Revenue protection: Generate/increase the revenue by reducing operating cost of alternative renewable energy technology

While addressing these issues, various clean energy technologies have been evolved in the areas of electric vehicles and alternative propulsion systems based on fuel efficiency maintaining stringent emission standard. With the advent of hydrogen fuel cells and high energy density batteries, electric vehicles can be demonstrated as the possible replacement of conventional vehicles operated by internal combustion engine (ICE). Various energy systems can be used to provide electrical energy to run the electric vehicles having different power system design. One of the main advantages of electrically driven transport system is its significantly lower operational cost compared to conventional vehicles operated by ICE.

Hybrid/Electric Vehicle Designs: Electric vehicles have started its journey since more than a century ago. A Belgian electric vehicle was the first to be reported to cover 30 m/s in 1899 [21, 22]. The lack of progress in energy storage system had slowed down the development of EVs. However, with the advent of electrochemical energy storage system, the electric and hybrid vehicles once again re-emerged in the recent times. Unlike EVs for which the power source is electric propulsion system only, hybrid vehicles are powered by two or sometimes with more power sources. For hybrid electric vehicle (HEV) an electrical energy storage system is used to power a motor or a generator which then used in association with an ICE. Generally, such vehicles are classified based on degree of hybridization (DOH), which can be expressed as [23]:

DOH = It is the ratio of electric motor power to that of total power of electric motor and IC engine

Based on DOH, the hybrid vehicles are categorised as follows:

Mild hybrid: This type of vehicle has a stand by electric energy storage system to assist ICE.

The size of battery pack is moderate. This type of battery has lower driving range due to comparatively lower energy density, lower power output due to low power density and little improvement in fuel savings. The existing ICE vehicles can be made to mild hybrid with little modification. The commercially available mild hybrid vehicles are Toyota Prius and Honda Insights.

Plug-in hybrid: This type of vehicles run in all-electric driving range. However, an ICE or turbine is also available only to extend driving range or to recharge the battery whenever required. Here the battery pack is large with high power output. The other advantage is that battery is compatible for grid charging. PHEV contributes in maintaining a significant fuel economy; thus, in turn reduces GHG generation also. However, larger and higher weight of battery packs for this type of vehicles increases the cost of vehicle. The commercial vehicles in this category includes GM's Chevrolet Volt and Ford C-Max Energy.

Electric vehicle: This type of vehicles powered by only electric storage system without ICE. The battery pack is extremely large therefore having higher weight. Recharging of this type of battery is done from grid only. Theoretically there should not be any GHG emission from this type of vehicle. The challenges for EVs are high cost and lower driving range compare to conventional vehicles. Commercially available EVs are Nissan Leaf and Model S. The 2030 Agenda for Sustainable Development," which has been unanimously adopted in September 2015 at the United Nations Summit [24] includes Sustainable Development Goals (SDGs) which is consisting of 17 goals and 169 targets for resolving key social issues globally and realizing a sustainable world.

Out of these 17 goals, most SDGs are focused on energy and environment related problems which needs technological solutions. One of the most important SDG is to ensure energy-sustainable society, which requires the efficient use of renewable energy in infrastructure. However, the renewable energy such as solar and wind power is not stable and thus often causes frequency fluctuation in the power grid. Lithium-ion batteries are capable in mitigating this fluctuation and solving this problem. Among the various energy storage systems, compare to Lead acid, Ni–Cd and Ni-MH battery, LIB has higher energy and power density along with longer cycle life with relatively much lower environmental impact [25].

The battery research and development is an interdisciplinary area where industries and academia are required to work jointly by supporting each other for ensuring the maximum benefit in this sector. The primary attributes of a battery, which are required to be looked into before its installation in electric vehicles are its energy and power density, chemistry of the cell, cell design and cycle life. These attributes will determine the installation space for a battery in an electric vehicle along with its range with a full charged battery, high power pick up, safety and life span [26].

In spite of various advantages, one of the major factors that limit the lithium-ion battery performance is its operating temperature. For application in electric vehicle, the suitable operating temperature is in-between 15 – 35°C. Both, the too high as well as too low temperature are detrimental for lithium-ion battery when used in electric vehicle. At higher temperature, the growth of SEI is significant which leads to decomposition of electrodes, results reduction in capacity. Similarly, at lower temperature, the lithium plating and dendrite formation is significant, which

again reduce the capacity and power of lithium-ion battery. Therefore, for an effective and efficient utilization and sustainability of lithium-ion battery a battery temperature management system (BTMS) must be adapted [27].

Presently the electric vehicle market is increasing and is expected to surpass 300 million on-road vehicles by 2030 and this predict the installation capacity of LIB to reach at 3000 GWh by the end of this decade. Now as the voltage and capacity of a single cell is limited due to unavailability of the different LIB component materials, encompassing all respective properties together for each component, therefore at present the battery pack consists of hundreds of cells connected in parallel and series to meet the high energy and power density, particularly for electric vehicle application. In this present scenario, a strong and robust battery management system (BMS) is required to handle this high energy (>100 kWh) and high voltage (>300 V) battery packs. The battery state estimation, such as state-of-charge (SOC), state of-health (SOH), state-of-power (SOP), state-of-energy (SOE), and state of-safety (SOS), is the first and foremost factor of BMS for an efficient and sustainable battery pack [28]. In the recent days, the price of the lithium-ion battery raw materials has been increasing due to higher demand for electric vehicles. Worldwide Russia is one of the major producers of high-purity Ni and Co. However, on the verge of Russia Ukraine war started in February 2022, Europe and United States imposed various economic sanctions on Russia, which includes trading of various items required for manufacturing of lithium-ion battery. This results an abnormal soaring of the cost of raw materials for lithium-ion battery. This also motivated the researchers to search alternative source of raw materials [29].

Moreover, the life of lithium-ion battery generally spans in-between 1-3 years. After the battery become unusable, its generally thrown in the garbage or used as landfill. However, these used LIBs have created significant environmental threat as it contains toxic elements such as Li, Ni, Co as well as plastic materials and organic electrolyte. Therefore, the safe disposal of these used batteries or the environmentally benign and energy efficient recycling of the elements present in the battery are a serious concern of LIB market. A recent dated report shows that approximately 10,700 tons of waste LIB is generated in the year 2012 and this value is increasing on each passing year by 59% annually and with this rate of increment, it is expected to reach the LIB waste to 464,000 tons by 2025 [30]. Now a days, there is an increasing demand for spent lithium-ion battery. The energy that is stored in lithium-ion battery is renewable. However, the source of raw materials with which the LIB is manufactured is limited and are not renewable. Now as the demand for lithium-ion battery is increasing, particularly for its high end applications, such as in electric vehicles, the global market expects the growth of lithium-ion battery from > 2500 GWh in this decade during the years 2020–2030. This predicts a substantial increase in demands for LIB raw materials. Following this analysis, if the spent LIBs can be used as an alternative source of raw materials instead of mineral from mines, then this alternate raw materials solution can mitigate the number of problems linked with economic, environmental, sustainable and geographical issues that are related to lithium-ion battery [31].

2.1 Energy Storage Systems

The onboard energy storage system is the most critical part from design aspect of HEV. However, various choices are available for such onboard system. Based on DOH of the vehicle, the system varies from fuel cell to battery to supercapacitor etc. Flywheel and less favoured pneumatic power

can also be installed [32]. **Figure 1** shows a comparative study of energy density between various energy storage systems. Among these systems, batteries are the most favoured choice primarily because of the ease of their use in various applications utilising the available infrastructure.

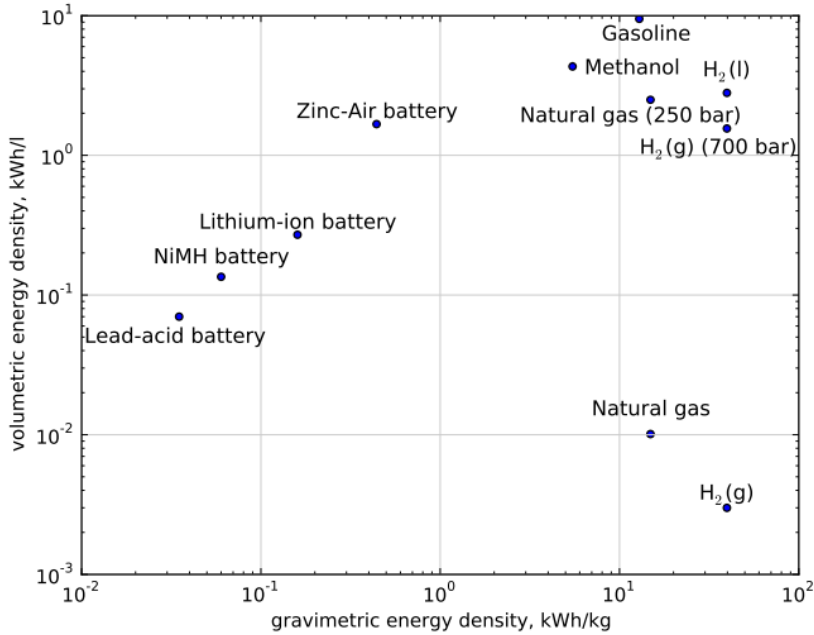


Figure 1. Energy Density of Various Energy Storage Systems [33]

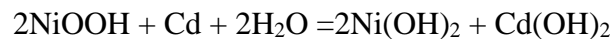
In the present scenario, investment in exploiting the renewable energy resources such as solar, wind and battery power systems has been increased manifold. The focus has been given on fuel cell, Li-ion batteries and nickel containing metal hydride batteries. Among them, batteries have many advantages compared to conventional energy storage systems. Nowadays, Li-ion battery technology is becoming the forerunner among the different battery systems. Lead-acid and nickel cadmium battery technologies, which are considered to be as conventional battery technologies, are slowly being replaced by Li-ion battery technology.

2.1.1 Lead Acid Battery

Lead acid battery is a rechargeable secondary battery. The first prototype lead acid battery was produced by Gaston Plante during 1854-1859 and soon this battery substituted its other contemporary batteries technologies [34, 35]. Till mid-80s, almost 40% of the battery market was dominated by lead acid battery [34]. The minimal voltage of a single cell of lead acid battery is described as 2 V and energy density is 32 mWhg⁻¹. The major drawback of this type of batteries is its weight due to extremely high density of lead. Therefore, for higher voltage applications, the device weight becomes very high [36, 37]. Due to its higher weight, lead acid batteries are not suitable for consumer electronics market and are still used in automobiles. However, lead acid batteries are still preferred for large scale energy storage [29, 30].

2.1.2 Nickel-Cadmium Battery

The Ni-Cd battery is also a secondary battery and falls in the category of alkaline battery family. This battery dominated the consumer electronics market in 1990s. The full-cell reaction for this battery is given below.



The cell voltage of this battery is 1.2 V and its average energy density is ~50 mAhg⁻¹. However, the major drawbacks of this battery are the toxicity of cadmium and rapid capacity fading if charged often without making it fully discharged. Therefore, Li-ion battery having similar cost of production soon replaced this nickel cadmium battery [35].

2.1.3 Lithium-Ion Battery

The main motivation for Li-ion battery technology is its higher energy density because of metallic lithium, which is the most electropositive metallic element having lowest electrochemical potential (-3.04 V vs. SHE) and is lightest in weight (0.534 g cm^{-3}) which makes it favourable in electrochemical energy storage system of higher energy density [7] (**Figure 2**). There are other merits of lithium-ion battery such as size and dimensional flexibility and easy maintenance along with better cyclability over 500 cycles compare to other battery technologies. Many research activities are going on to augment the electrochemical performance of this battery technology such as cycling life, safety as well as cost. This technology is mostly in use in the area of high-end electronic market such as laptop, mobile camera etc. However, recently this technology has been introduced in power tool and hybrid electric automobile market.

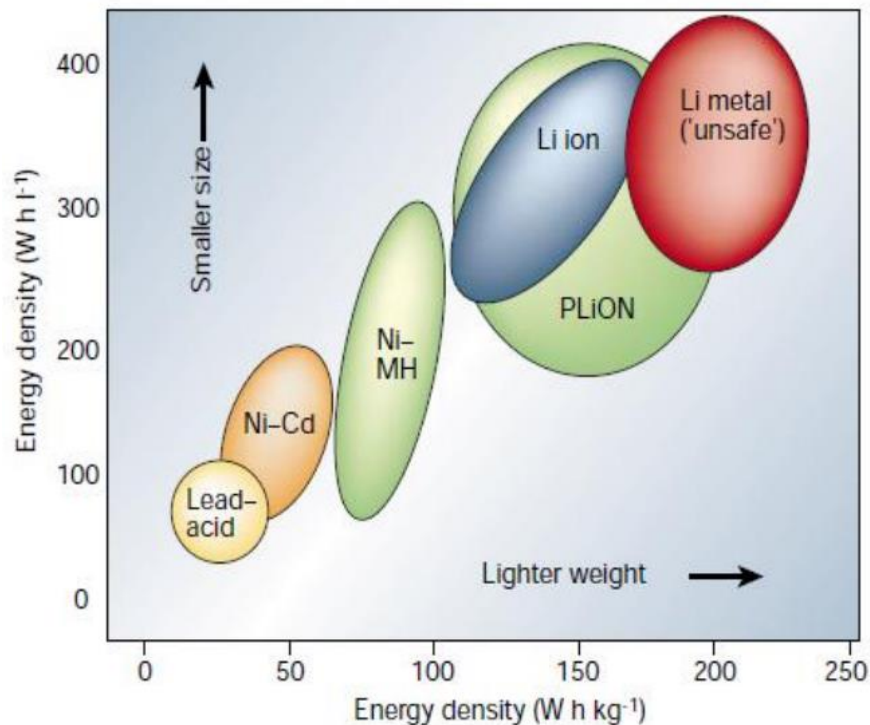


Figure 2. Energy Density of Various Battery Technologies [7]

Globally the CO₂ emission can largely be reduced with the use of electric vehicles and renewable energy sources. The International Energy Agency (IEA) explained that for a sustainable future the CO₂ emission needs to get reduced at least 21% and 42% from transportation and power generation sector respectively by 2050. This can be achieved by introducing three-fourth of all on-road vehicles with electric power source and introducing at least 310 GW for grid storage by electrical power [40, 41]. The new battery technology having higher energy density with lower cost can fulfil both the demands in the respective areas. The energy density of battery requires to be improved to enhance the driving range of electric vehicles with comparable efficiency. The electrode materials are primarily responsible for lowering the cost of batteries. Basic changes in positive and negative electrode materials are needed to increase the specific energy and also to reduce the cost. Developing high energy density electrode materials are mainly responsible to reduce the cost of battery.

The graphite anode and lithium containing transition metal oxide cathodes are generally used in Li-ion batteries and can produce maximum ~ 250 Wh/kg energy density [42-44]. However, the higher price and low energy density Li-ion battery (**Table 1**) restricts its use in electric vehicle which otherwise cannot produce similar or near driving range to that of ICE.

Table 1: Goals Set for Commercial Advanced Batteries for EVs till CY 2020: United States

Advanced Battery Consortium (USABC) (2014)

Parameter (Unit)	System level	Cell level	Current Technology at cell level
Specific energy @C/3 (Wh/kg)	235	350	~250
Energy density @ C/3 (Wh/L)	500	750	~500
Specific discharge power, 30 s Pulse (W/kg)	470	700	-
Cycle life	1000	1000	>1000
Calendar life	15	15	~10
Operating temperature (o C)	-30 to +52	-30 to +52	-
Selling price @ 1000k units (\$/kWh)	125	100	~400 – 500

For large scale use of non-conventional renewable energy systems such as wind as well as solar, an intermittent energy storage is required which must be reliable as well as inexpensive. **Figure 3** shows the significant differences in installation cost (per kWh of energy) between the DOE targets for specified viable grid storage and modern energy storage technologies. The compressed air and hydraulic pump are excluded from this list as this are usually bounded by specific geographical border. Electrochemical energy storage system has the potential to reduce this gap. However, reduction in cost by ten-fold or more is challenging and require new battery chemistry.

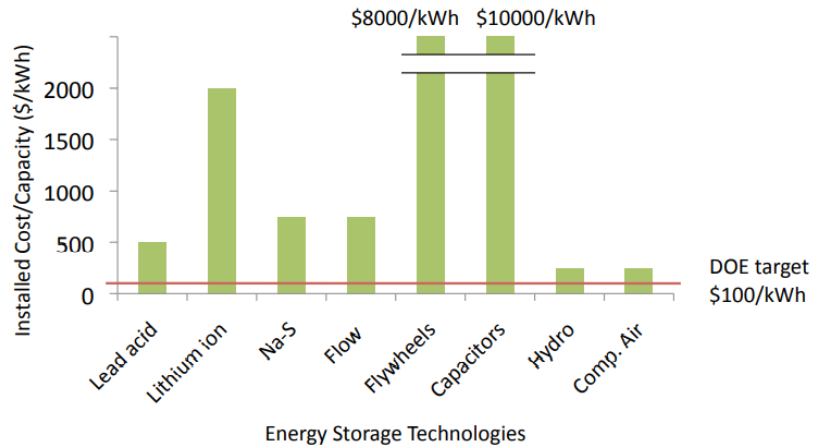


Figure 3. Cost of Current Technologies Compared to DOE Targets [46]

2.2 Approaches to and Challenges for Li-Ion Batteries

Non-conventional and renewable electrochemical energy storage as well as conversion systems are demonstrated to have the full potential to successfully address the issues related to clean energy supply and to fulfil its ever-increasing demand and thus drawn extensive research attraction. **Figure 2** above shows general Ragone plots (gravimetric vs. volumetric energy density) of major energy storage systems [47].

Among the various battery systems Li-ion battery is shown to have the highest energy density. Extensive research has been done on Li-ion battery for last two decades and as a consequence this has taken a shape of a technology and also been commercialized and in use in a wide spectrum of high-end consumer electronics market. The future of Li-ion battery is very much promising. However, this battery system also includes some major challenges as:

A) Improving the energy density can be considered as the foremost challenge of LIB. The higher energy density is required to fulfil the demand particularly, for electric vehicles and for large scale

energy storage applications. The cathode materials are mainly responsible for improving the energy density. The modern day cathode materials are LiCoO_2 , LiNiMnCoO_2 and LiFePO_4 etc. while carbon based anode material such as graphite is used as anode. The theoretical capacities are 140 mAhg^{-1} in the operating voltage range of 3-4.2 V for LiCoO_2 , 150 mAhg^{-1} in the operating voltage range of 3.5-5V for LiNiMnCoO_2 and 170 mAhg^{-1} in the operating voltage range of 2.5-4.2V for LiFePO_4 [46, 47]. However, this capacity values are still too low to fulfil the requirement of high-end applications. Therefore, some alternative materials having higher theoretical capacity is urgently required. **Figure 4** shows the theoretical capacities of various electrode materials. Sn, Si and Si-C composite materials can have very high electrochemical capacities, more than 1000 mAhg^{-1} compare to conventional cathode materials which is having the limited capacity of $<200 \text{ mAhg}^{-1}$. However, there are still chances to improve the electrode potentials to have better energy quality.

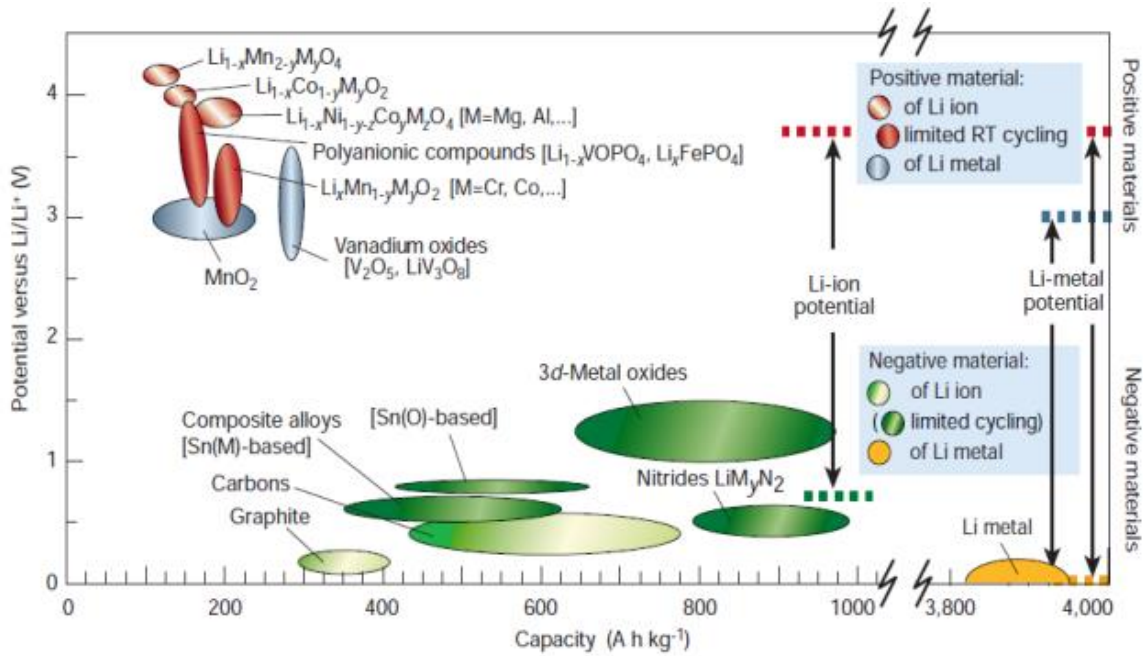


Figure 4. Voltage Vs. Capacity for Various Cathode and Anode Materials [46]

B) The next big challenge of Li-ion battery is to enhance its lifespan without significantly losing the electrochemical performance. It's true that Li-ion battery starts degrading since it leaves the factory. Although, the life of a Li-ion battery largely depends on its internal charge capacity and the temperature of its application but in true sense Li-ion battery loses 20% of its theoretical capacity on every passing year. The one of the solutions to increase the life of a Li-ion battery is to understand and control the electrochemistry of the cell, development of potential electrode materials and the design of the battery.

C) Reduction in cost of LIB particularly, the cost of production of electrode materials would also promote this battery system in many other applications. Many researches are going on various aspects of LIB to reduce the cost. The standard LIB cost as on today is \$680 per kWh. However, this is still four times higher than that of Lead Acid battery. Therefore, reducing the cost of LIB is also a challenge [48, 49].

D) Development of non-toxic and comparatively inexpensive electrode materials, particularly the cathode materials are also a challenge as the cobalt and nickel which are the essential elements for cathode active material till date are expensive and environmentally not benign.

The future research based on the above challenges should primarily focus on the following areas of LIB.

I) The battery chemistry and design as well as engineering aspects of battery are need to be researched on in detail. As for example, the conventional electrolyte solutions often decompose and become unstable at higher voltage and thus restricts the use of high voltage cathode materials.

Selective combination of cathode-electrolyte-anode are required to be optimized to eliminate the detrimental side reactions in electrode-electrolyte interphase. This would consequently enhance the electrochemical performance as well as lifespan of LIB.

II) Understanding and improving the performance of the existing electrode materials along with exploring the new electrode materials is another area to be focussed on. Unlike the intercalation mechanism, conversion mechanism between Li and Si or Sn based anode materials can produce very high capacity. The conversion reaction is mainly an alloying process. In this reaction two or more Li ions can be accommodated by a single transition element thus produce very high capacity. However, the major drawback of this type of mechanism is large volume change (Sn-260% and Si-360%) associated during alloying and dealloying process during charge/discharge which leads to disintegration of the anode material thus decreasing the electronic and ionic conductivity within the negative electrode material. **Table 2** shows some characteristics of the anode materials [50-52].

Moreover, for Sn based anode materials, insulating Li_2O is generated during the conversion reaction within the material which reduces the electronic transfer between the particles. This problem can be minimised by reducing the anode active material particle size from micron level to nano level. Another important change that happens during conversion reaction is the complete structural reorganization of the anode materials, which creates large polarization loss and significantly reduce the rate capability. This problem can also be addressed by decreasing the particle size; thus, decreasing the associated volume change and thereby reducing the particle

disintegration. To this effect, using materials having particles of nano dimension can be a possible solution.

Table 2: Properties of Various Anode Materials (Capacity Values are based on Delithiated State of Material except Lithium Metal [50])

Materials	Li	C	Li ₄ Ti ₅ O ₁₂	Si	Sn	Sb	Mg	Al
Density (gcm ⁻³)	0.53	2.25	3.5	2.3	7.3	6.7	1.3	2.7
<u>Lithiated phase</u>	Li	LiC ₆	Li ₇ Ti ₅ O ₁₂	Li _{4.4} Si	Li _{4.4} Sn	Li ₃ Sb	Li ₃ Mg	<u>LiAl</u>
Theoretical Sp. Capacity (mAhg ⁻¹)	3862	372	175	4200	994	660	3350	993
Volume change (%)	100	12	1	420	260	200	100	96
Potential vs. Li (V)	0	0.05	1.6	0.4	0.6	0.9	0.1	0.3

III) The more sophisticated and in-situ characterization tools are indeed required to study in depth the reaction mechanism of LIB. The computational modelling and simulation are also required to anticipate some critical properties and process mechanisms, which otherwise cannot be approached through experimental procedures [53].

2.2.1 Advantages of Nanomaterials

The usage of nanoparticles having various morphology in positive and negative electrode materials of LIB is a fastest growing area of research. The materials having at least one dimension in nano range, i.e., 1-100 nm is called nanomaterials. Accordingly, nanomaterials can be categorized in three groups, viz., zero dimension (0D) like nanoparticles, nano crystal or nanograin etc. then one dimension (1D) like nanotubes, nanofibers etc. and two dimension (2D) like nanocoating,

graphene etc. The interesting characteristic of nanomaterials is its distinct property unlike single atom (or molecule) or bulk material of same composition. The application of nanomaterials in different components of LIB produces various advantages as summarised below [54].

a) With nanosized particles some reactions proceed effectively which otherwise do not take place in micron scale or above, however, some adversely affected reactions can also take place and thus need to be taken care of.

b) The nanosized particles provides shorter path for Li ion movement from one particle to another within the cathode and anode materials resulting increase in Li ion conductivity and thus improving the rate of Li ion diffusion during intercalation/deintercalation mechanism.

c) The nanosized particles also facilitate faster electron transportation, which improves the rate capability particularly at higher C-rate.

d) The nanostructured electrodes provide better contact between cathode, anode and electrolyte causing higher Li ion flux in electrode-electrolyte interphase. However, caution must be taken against some negative side reactions which may also increase simultaneously.

e) Going down to nano range may change the chemical potentials of Li ions and electrons; thus, modifying the electrode potential.

f) Nanoparticles enhance the reactivity thus forming more solid state composition. However, the strain associated with these solid particles are better accommodated in nano range during charge/discharge.

2.3 History of Li-Ion Batteries

The energy can be stored electrochemically was first discovered in 18th century by Luigi Galvani when he observed a movement in a frog's leg when connected with wires of two different metals. However, he mistakenly explained it as short of vital energy of a living being. After a short time, Alessandro Volta was able to demonstrate the generation of electricity by stacking intercalated zinc and silver metallic plates separated by pieces of cloth soaked with brine solutions without using any living organisms [11, 35]. These two observations motivated the researchers to focus on Volta's pile which eventually led to the generation of present day electrochemical energy storage systems gradually, where energy is stored in different Li containing material by the Li ion intercalation mechanism [34, 35, 55].

Li-ion battery has three major components, viz., cathode (a positive electrode material), anode (a negative electrode material) and separator. The separator is soaked in liquid electrolyte. The working principal of Li-ion battery is based upon the mechanism of Li ion exchange between cathode and anode followed by the redox reaction in the electrode material ('rocking chair' mechanism) [56]. The Li-ion battery research is now on an advanced stage. The main focus is given on to exploit to maximum potential of the existing electrode materials, exploring the new electrode materials, nanoscale production of the cathode as well as anode active materials and also to modify the crystal structure of the electrode materials [57, 58]. Researchers are also going on to

identify the different salt-solvent system of electrolyte solution so as to ensure its higher Li ion conductivity as well as stability at higher voltage along with existing electrolyte solution of LiPF_6 dissolved in carbonate solvents. Understanding the solid electrolyte interphase (SEI) which is an integral part of Li-ion battery is required to be investigated thoroughly [59]. Significant researches have been started on separator material also along with solid-state electrolytes (polymeric, inorganic, glass, glass-ceramic etc.) to solve the issues related to safety of Li-ion batteries [60, 61].

G.N. Lewis initiated the research on exploiting the highest capability of Li-ion battery in 1912 [62]. However, the first commercial Li-ion battery was made available only on early 1970's. M.S. Whittingham first proposed this commercial battery [63]. This initial day battery was composed of TiS_2 as positive electrode material and Li metal as negative electrode material. The cathode of this battery performed well but anode deteriorated due to uneven dendritic growth of Li metal as shown in (Figure 5).

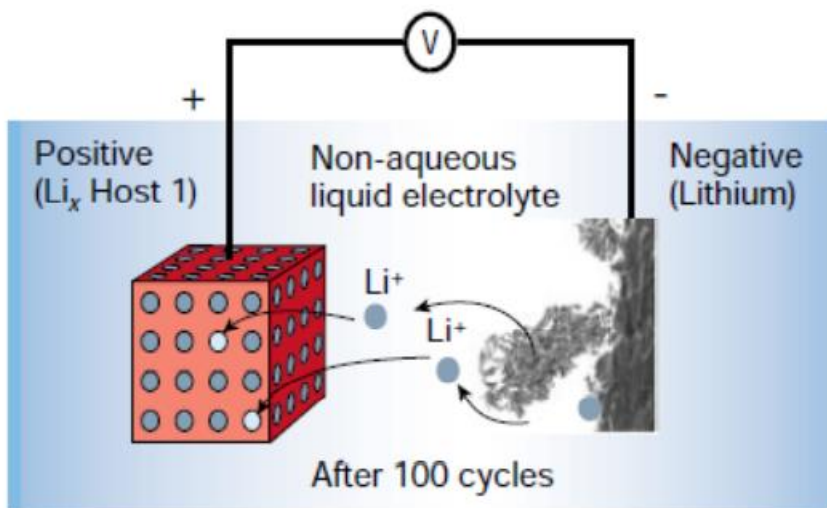


Figure 5. Dendrite Formation on Lithium Anode [7]

The battery research took its impetus on 1980's with rechargeable lithium batteries with lithium metal as anode and was capable of providing higher voltage and improved capacity which consequently resulted in higher energy density. However, this battery did not come up owing to mainly safety problem due to vigorous reactions happening inside the battery at relatively higher temperature. Then the focus on battery shifted to Li-ion battery from Li metal battery due to comparatively better safety. The significant discovery of Li-ion battery came up with the advent of intercalation electrode materials of Li-ion battery. The graphite lithium interaction in lithium-graphite half-cell was first demonstrated by Touzain et al. in 1986 [64].

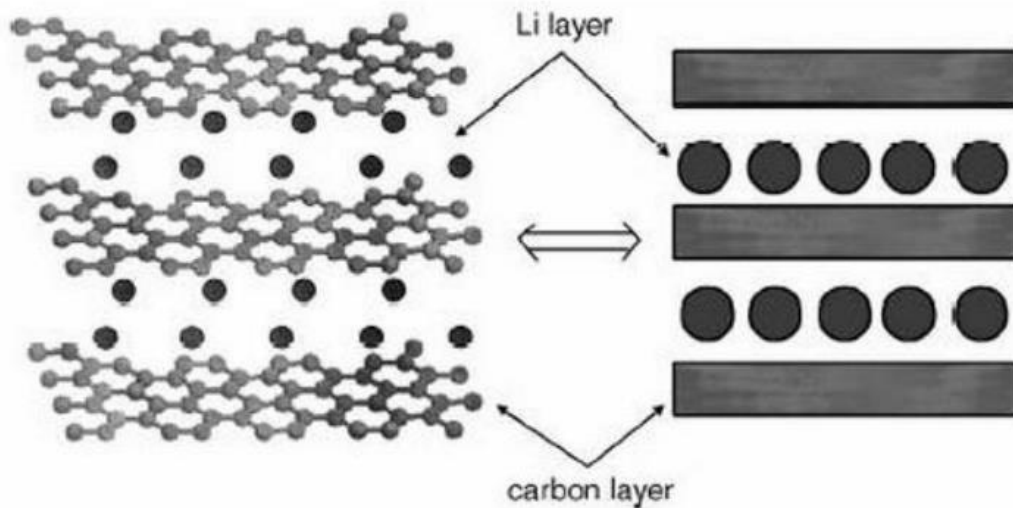


Figure 6. Structure of Graphite Lithium Intercalation [65]

During intercalation mechanism, Li ions are suitably inserted and removed from the electrode materials without making much change to the host structure. However, the first intercalated cathode material in the family of Li_xMO_2 ($\text{M} = \text{Co}, \text{Mn}$ or Ni) was proposed by Dr. J. Goodenough few years later [66]. Following that Sony Corporation commercially first released the Li-ion battery in 1991 [67, 68].

2.4 Working Principal of Li-Ion Battery

A battery is consisting of a single cell or number of cells depending upon its application. This cells actually converts the stored chemical energy into electrical energy following a certain mechanism. Based on its rechargeability, the batteries can be classified into two major categories: primary and secondary. Primary batteries are not rechargeable battery because the reactions responsible for transformation of chemical energy into electrical energy is not reversible. This type of battery must be discarded once its charge is exhausted after one time use. The secondary batteries can be used multiple times by charging every time after it got discharged as it is a rechargeable battery. This is because of the reversible transportation of Li ions (intercalation/deintercalation), back and forth (Rocking Chair) between positive and negative electrodes during charging and discharging while maintaining the host structure and charge neutrality by redox reactions in the electrode materials [69, 70]. The Li-ion battery is mainly composed of mainly four components: positive electrode, i.e., cathode, negative electrode, i.e., anode electrolyte and separator. Cathode and anode periodically get reduced and oxidised during discharging and charging. Electrolyte mainly acts as a vehicle for Li ion movement and separator basically acts as a barrier to insulate the cathode and anode electronically while provide the pathway for Li ion movement. **Figure 7 and 8** graphically represent the working mechanism of Li-ion battery.

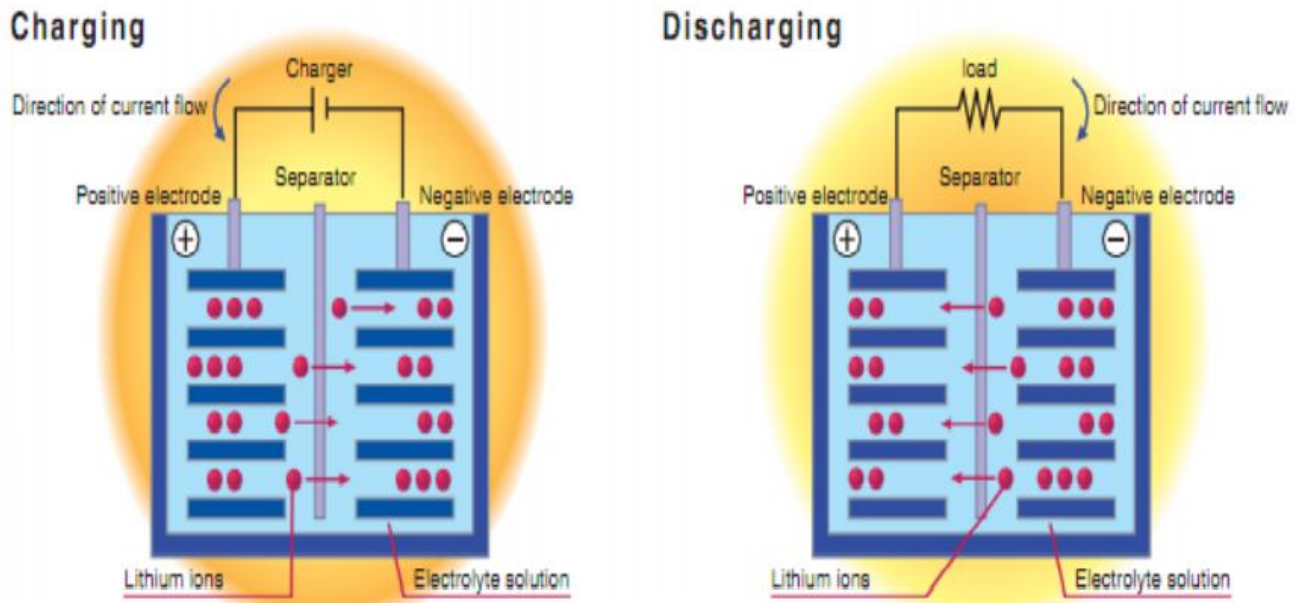


Figure 7. Schematic of Charging and Discharging of Li-Ion Cell [65]

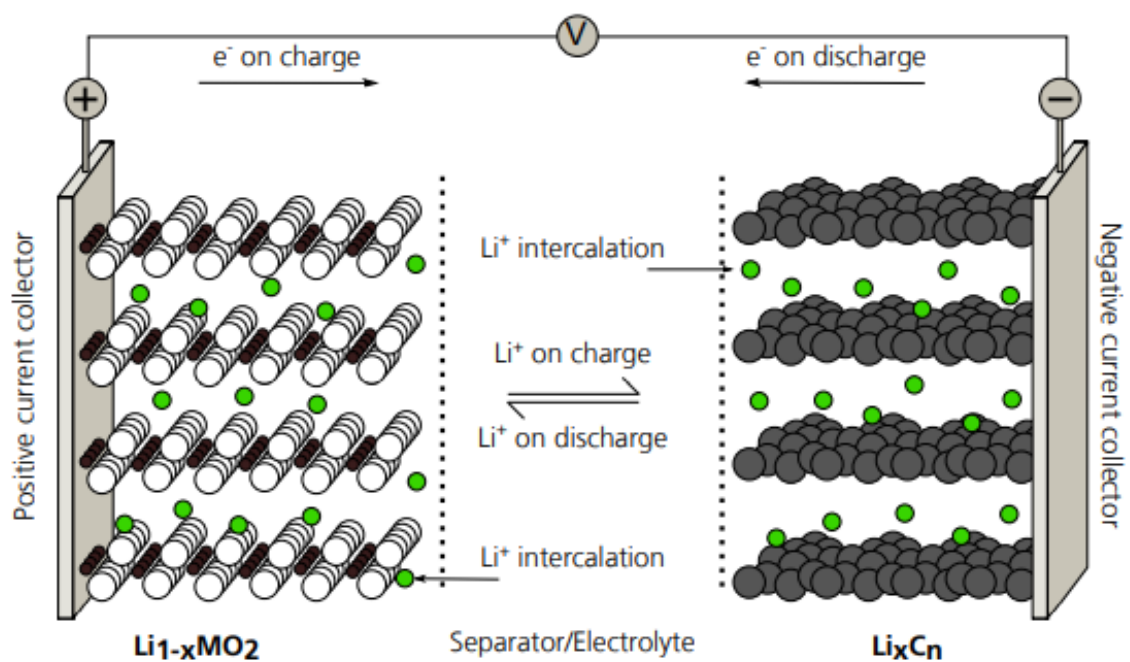
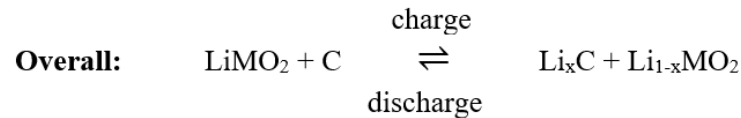
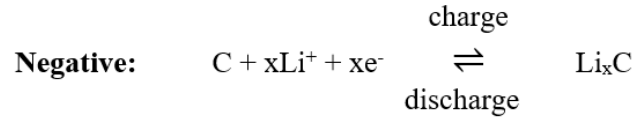
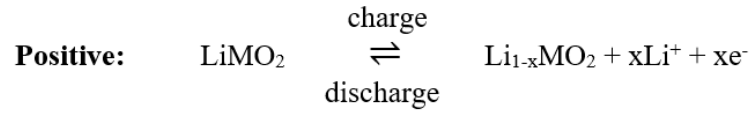


Figure 8. Schematic Representation of Charge/Discharge Mechanism in Li-Ion Battery [71]

The mechanism as shown in the above figures can be explained as follow. During charging Li ions moves from positive to negative electrode through the electrolyte while at the same time electrons

move through external circuit. Similarly, during discharge reverse reactions occur. This red-ox reaction is shown below.



2.5 Design of Cell and Various Configurations

Basically, the design of a Li-ion battery includes four major parts. Part 1: The aluminium foil coated cathode material usually LiCoO_2 ; Part 2: Copper foil coated anode material usually layered meso carbon micro beads (MCMB)carbon; Part 3: A liquid electrolyte connecting cathode and anode ionically and basically composed of a solution of inorganic salt (LiPF_6) in organic solvents generally carbonates; and Part 4: The separator generally composed of layered structure of polyethylene and polypropylene, acts as an electronic insulation between cathode and anode to avoid short circuiting [72].

Nowadays, the most common and available Li-ion battery configurations are like cylindrical or flat polymer type, or coin type or like prismatic shape configurations as shown in **Figure 9**.

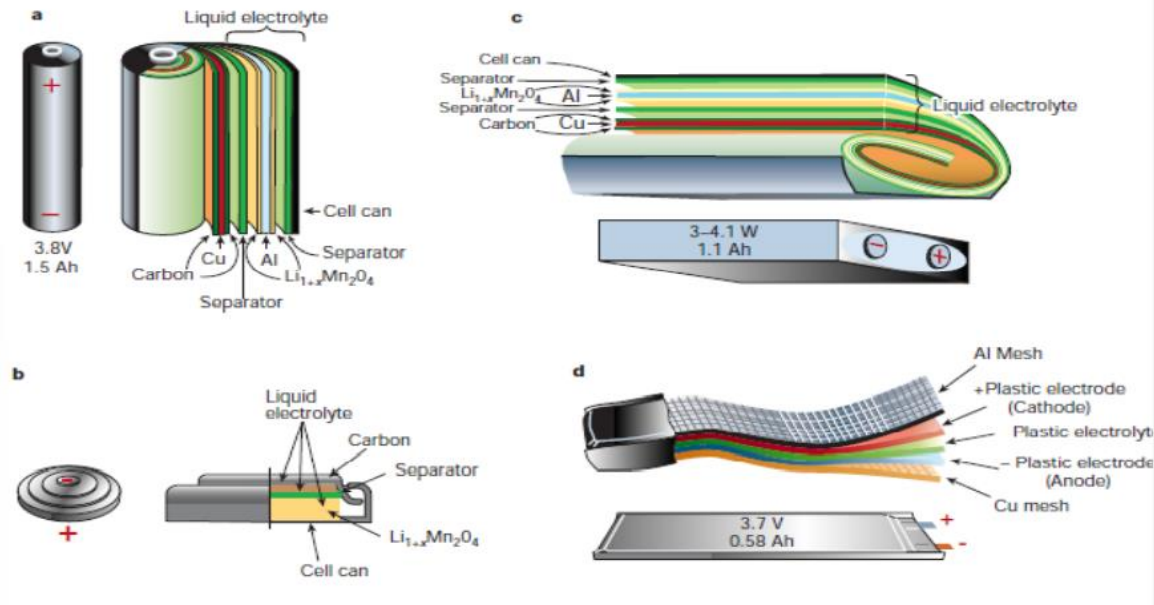


Figure 9. Various Configurations of Battery a) Cylindrical type b) Coin type c) Prismatic type and d) Thin and Flat Polymer type [7]

The cylindrical type 18650 i.e. (18 x 65 mm) is the most common type of Li-ion battery, mostly used in laptops and electric cars. 18650 Li-ion battery from Sony corporation shows the electrodes inside the battery (**Figure 9**). The cell phones are mostly using the prismatic type battery. The coating slurry for positive electrode is prepared by mixing the active cathode material (LiCoO_2) with conducting acetylene black using PVDF (polyvinylidene fluoride) as binder. This slurry is then coated on both side of aluminium substrate. Coating slurry for the negative electrode is prepared by mixing active carbon (MCMB) with polymer binder. This slurry is then coated on to the both surfaces of copper substrate (**Figure 10**).

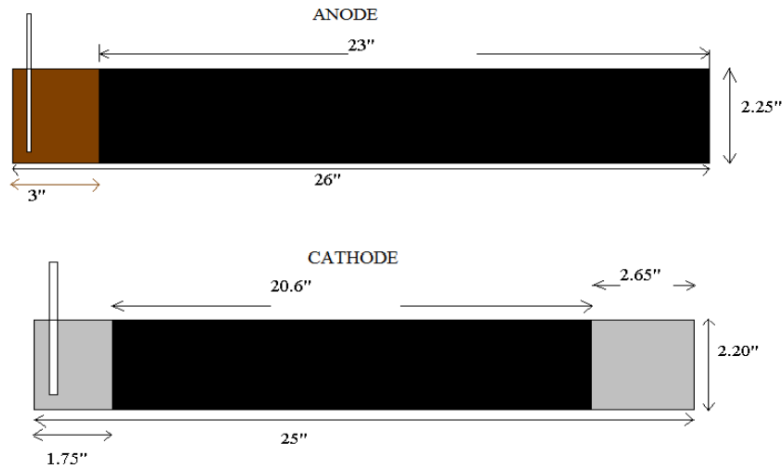


Figure 10. Coated Cathode and Anode for Sony 18650 LiCoO₂ Battery [65]

The cathode and anode slurries are prepared separately by uniformly mixing the respective ingredients and also a certain and uniform thickness is maintained during coating. After drying the coating, the foils are cut into required dimensions and subjected to calendaring for several times to have uniform coating thickness and also to ensure the coating sticks to the foil effectively. Finally, the cathode and anode coated foils are subjected to rolling with the separator in-between them. A winding machine is used to roll the battery component together and after rolling, the whole thing is put it in a cylinder having 18 mm in diameter and 65.0 mm in length.

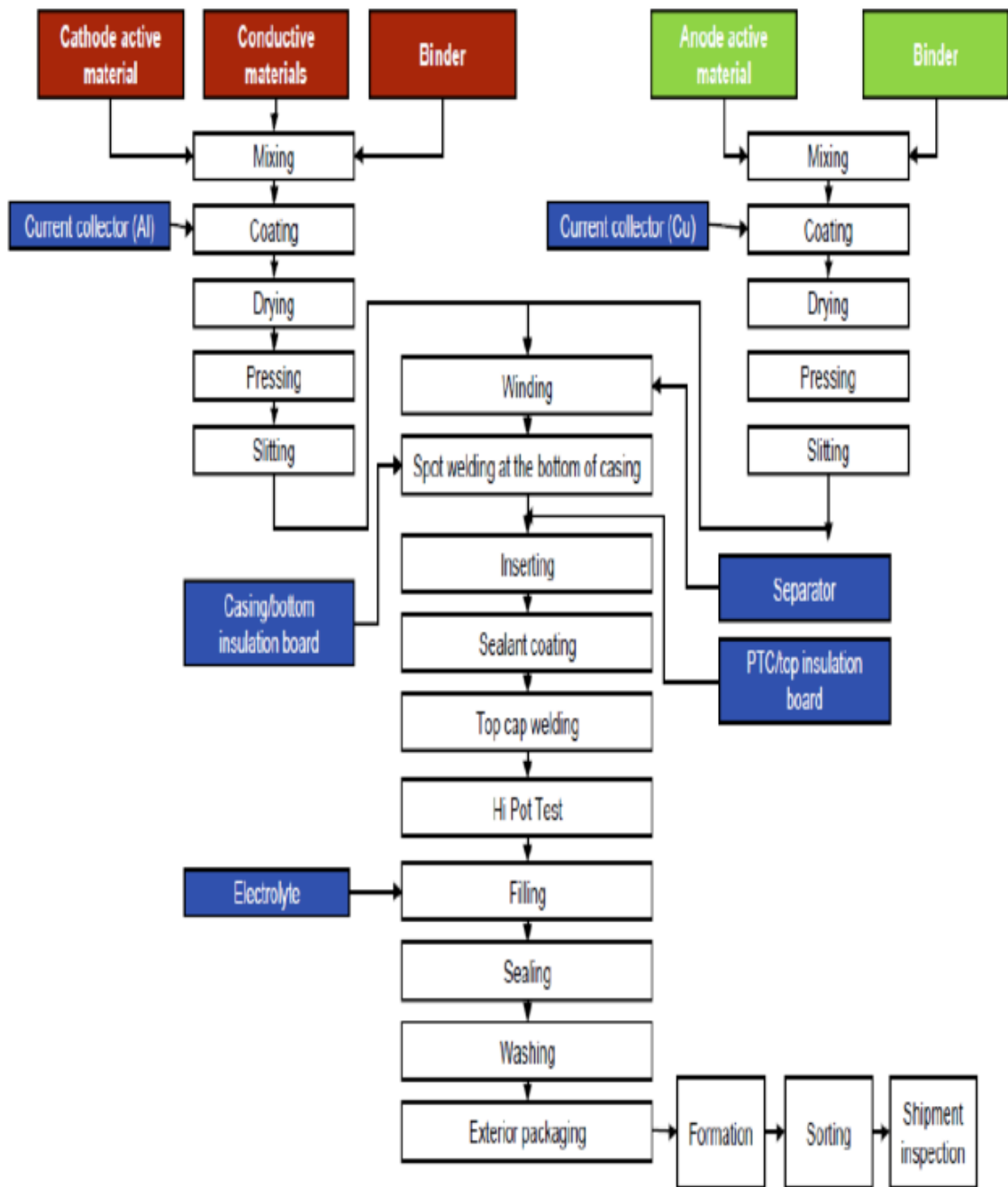


Figure 11. Battery Manufacturing Flow Chart [73]

2.6 Battery Specifications

The electrochemical performance of a Li-ion battery is directly dependent on its major three components, i.e., positive electrode cathode, negative electrode anode and electrolyte. The performance is indirectly dependent on separator also. There is an ample scope of research in the area of cathode materials. This material is having higher free energy of reaction while reacting with lithium and is primarily responsible in determining the cell voltage and capacity of the battery [69, 74]. On the other hand, the research in the area of anode materials is almost saturated. Generally, MCMB is used as negative electrode material in commercial Li-ion battery. This material has the electrochemical capacity almost double the capacity of cathode material (LiCoO_2) and is comparatively safe and inexpensive.

The material design for the cathode component is primarily based on its structural stability, ionic diffusivity and electronic conductivity. As these materials need to accommodate large amount of Li insertion and removal during charge and discharge, therefore it should be structurally stable. The higher ionic diffusivity and electronic conductivity eventually increase the power density as well as rate capability of the cell. The cathode material should be inexpensive also. The selection of anode materials is also dependent on the same factors that of cathode. The electrolyte should be ionically conducting and electronically insulating. It should be stable; thus, should not oxidise or reduce at different voltage range and finally it should be inert and should not react with electrodes or other battery components. The performance of the battery is determined by several parameters such as specific capacity, voltage, cyclability, power density, rate capability etc. along with safety, cost.

2.7 Practical Parameters in Evaluating Battery Performance

In evaluating the battery performance and to compare between various battery systems, following properties are need to be analysed carefully before concluding any battery system.

2.7.1 Capacity and Rate Capability

The specific capacity of a battery system is determined by the electrode materials and is expressed as the amount of energy stored per unit mass or volume of electrode materials. The specific capacity of Li-ion battery electrode materials can be defined as:

$$C_g = \frac{F \times z}{M \times 3.6} \text{ mAh / g}$$

Where, F = Faraday Constant; z = number of charge transfer per mole of material; M = molar mass of materials. The full cell specific capacity is defined as:

$$C_{\text{cell}} = \frac{C_{g(\text{anode})} \times C_{g(\text{cathode})}}{C_{g(\text{anode})} + C_{g(\text{cathode})}}$$

The Coulombic efficiency is another important parameter which literally signify the reversibility of electrode reactions. This parameter is mathematically measured as the ratio between delithiation capacity and lithiation capacity. This Coulombic efficiency accounted all the reactions, positive as well as negative reactions (side reactions), between battery components, in particular electrode and electrolyte and this substantially affect the battery capacity with increasing cycle number especially when the quantity of lithium and amount of electrolyte is limited. **Figure 12** shows the typical capacity fading with increasing number of cycles when Coulombic efficiencies are different and lithium supply is limited. 0.1% decrease in Coulombic efficiency results 10%

reduction in capacity over 100 cycles. And 1% decrease in Coulombic efficiency can reduce the battery capacity to 64% over 100 cycles.

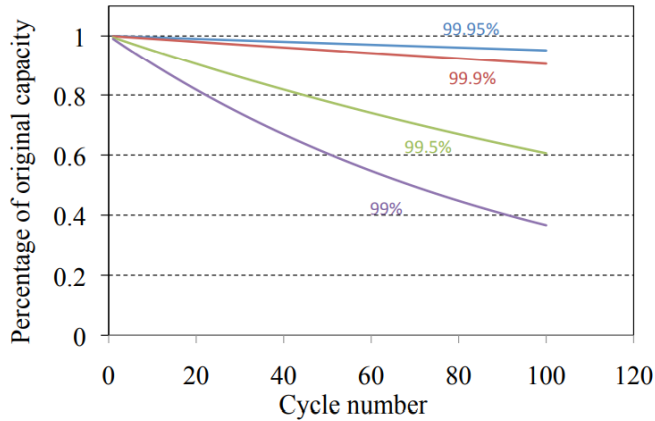


Figure 12. Effect of Coulombic Efficiency on Cyclability [75]

The rate capability for a battery system is defined as the rate of current required to completely charge the battery during galvanostatic cycling and is expressed in terms of ‘C’. The 1C means the current needed to fully charge/discharge the battery to its nominal capacity in 1h. The other current densities are demonstrated as C/R, where R is the time (in hours) needed to fully charge/discharge the battery to its nominal capacity. For example, when a battery having 4 Ah capacity is charged at 2A current then the charging rate is said to be C/2. The capacity as well as rate capability of a battery depends on the electrode materials and design of the cell. The reaction kinetics can be best understood by subjecting the system at different C-rate. The following figure shows the typical discharge capacity profile for C/LiCoO₂ (18650-type) Sony battery.

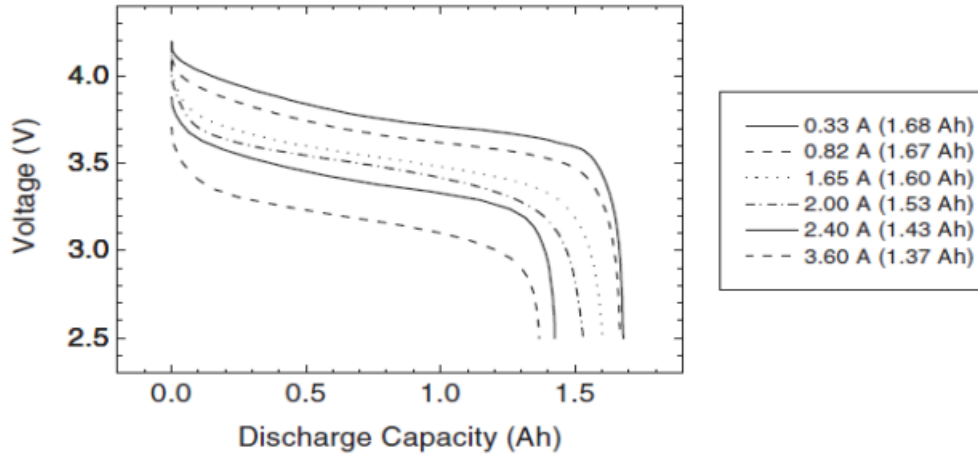


Figure 13. Capacity Plots with Voltage [69]

Typical rate capability graphs for C/LiCoO₂ cell (18650 type) are depicted in the figure below (Figure 14).

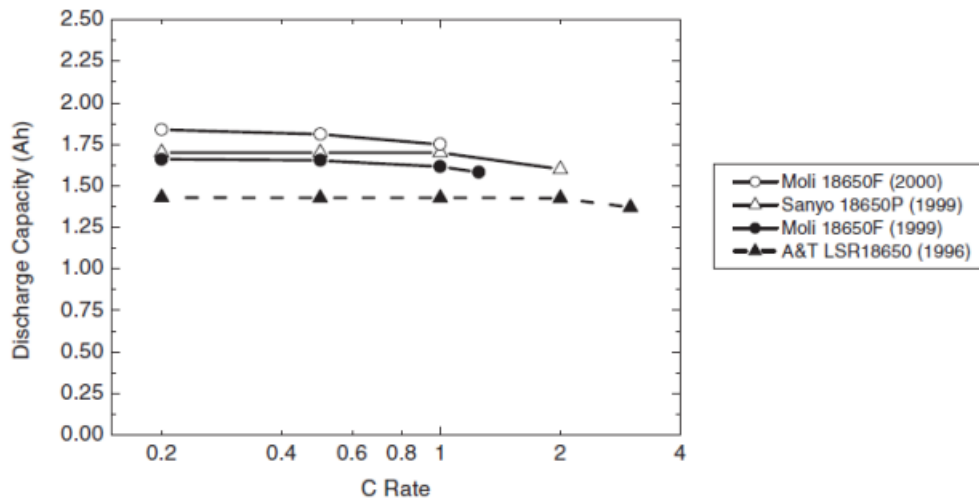


Figure 14. C/LiCoO₂ (18650 type) Batteries Show Rate Capability at Constant Current [69]

2.7.2 Cyclability

In literal sense, cyclability defines the lifespan of a battery. Compare to other battery systems, Li-ion battery can hold its stability without significantly decreasing its capacity and rate capability

even after 500 cycles and that too in a short range of varying temperatures. Mathematically, cyclability is defined as the number of charging cycle, which an electrochemical cell can undergo during its lifespan.

In a lithium-ion battery, the capacity, rate capability and cyclability are inter-related to each other. The cyclability of a battery is directly affected by its rate capability. Generally, cyclability decreases at higher C-rate. Similarly, discharge capacity decrease with increasing cycle numbers. From the structural point of view, this can be explained as all the Li that goes from cathode to anode side during charging does not make it to come back to cathode during discharging. Along with that as the cycles goes on increasing, due to other side reactions cell impedance also increases which eventually lower down the voltage and thus deliver lower energy density.

2.7.3 Voltage

The voltage of a cell is determined by the thermodynamic reactions that are happening in the electrodes during charging and discharging. The cathode and anode in any battery system has different electrochemical potentials. The electrochemical potential is defined as the relative tendency to lose electrons during reactions. Now, when two electrodes are connected in charged state, then anode loses electrons to the external circuit produces current while the Li ions move from negative to positive electrode through the electrolyte. The driving force for losing the electrons from anode and accepting to the cathode is expressed by the Gibbs free energy of reaction (ΔG_r^0):

$$\Delta G_r^0 = \sum \Delta G_f^0 (\text{product}) - \sum \Delta G_f^0 (\text{reactant})$$

Where, ΔG_f^0 is the Gibbs free energy during formation.

Then voltage of electrochemical reaction is defined as:

$$E_{\text{cell}} = \frac{\Delta G_r^0}{-zF}$$

Here, E_{cell} = voltage of the cell, F = Faraday constant and z = number of charges.

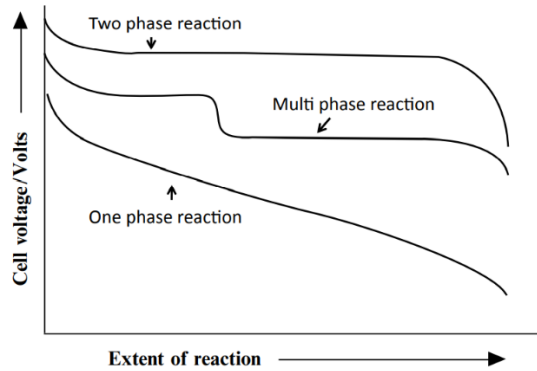
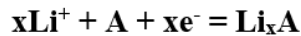


Figure 15. Different types of Discharge Curves Represented Schematically [76]

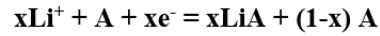
The voltage of a specific battery system is primarily determined by the cathode materials and this may include number of phases depending upon the composition used for cathode material. The voltage profile actually expresses these phases resulting from different stages of electrode reactions.

For a single-phase reaction such as:



If Li and A produces a solid solution, then as the reaction progresses, the composition of Li_xA changes continuously, thus the Gibbs free energy for the reaction between Li and Li_xA also changes accordingly. Consequently, the voltage varies with the magnitude of reaction.

Whereas, if the reaction between Li and A forms a new phase (LiA), then reaction can be expressed as:



The Gibbs free energy of reaction (ΔG_r°) and the Gibbs free energy of formation of LiA, [ΔG_f° (LiA)] are equal to each other, therefore, the electrode potential remains constant. In case of a multi-phase reaction, the Gibbs free energy of reaction (ΔG_r°) at any given stage of the reaction can be expressed as the combination of above reaction mechanisms.

From electrodes point of view, the voltage of the cathode should be as high as possible whereas the voltage of anode should be very low so that the overall cell voltage would be high. Having the lowest potential -3.04 V (vs. SHE), Li metal can be considered as a favoured choice for anode material to get the higher voltage and thus higher energy density. Conventionally, low quality energy system is said to have voltage between 0-1.5 V while a cell is considered to be high quality energy system when its voltage ranges between 3.5-5.5V [77].

2.7.4 Energy Density

The Li-ion battery energy density is generally the product of voltage and capacity. The specific energy is the integration of capacities across the voltage range of a battery system. The gravimetric energy density is expressed in terms of Wh/kg.

$$\text{Energy} = \int \text{E}d\text{C}$$

Specific energy is the parameter directly indicate the amount of useful work that can be obtained from a cell for practical applications.

2.7.5 Power Density

From application point of view, the power density indicates the amount of energy that can be drawn instantaneously from a battery system. This is particularly applicable for electric vehicle, where momentary energy requirement is more to start the vehicle. The power density is actually the product of current and voltage.

2.7.6 Safety

The safety of a battery is a major concern particularly to secure the future of Li-ion battery. Overcharging and overheating of a Li-ion battery may cause thermal runaway and thus disintegration the battery components. Compared to other battery systems, this has been the main drawback for Li-ion battery [17]. In the recent past, the major thrust in the area of research has been focussed on safety issues of Li-ion batteries related to internal short circuiting, overcharging and thermal safety [17].

2.7.7 Cost

Cost is always a major factor for commercialization of any technology. Compare to other battery systems, Li-ion battery is most cost effective. However, for electric vehicle applications, the cost is still much higher. In other ways reducing cost of Li-ion battery system can be done by replacing the Cobalt element of conventional cathode material (LiCoO_2) with other elements having +3 oxidation state, which include manganese, iron, nickel or vanadium or chromium. Another way to reduce the cost is to lowering the amount of cobalt as this element is expensive and rare. Many researches are going on in this area.

2.8 Details of Battery Components

The driving force of research for Li-ion battery advancement is the development and growth in consumer electronic market and electric vehicle. Ever since, the first commercial Li-ion battery for consumer electronics market was brought by Sony Corporation in 1991, researchers are constantly searching for a new combination of cathode-electrolyte-anode to improve the battery performance in terms of energy density, power density, safety and cost along with materials availability and its environment benignity. However, whatever the battery technology, the primary parameters, to evaluate a battery such as capacity, rate capability, energy density, power density and safety, depends on the electrodes and electrolyte materials.

In the area of positive electrode materials, initially the research was focussed on layered structured materials such as LiCoO_2 , LiFeO_2 , LiNiO_2 and LiMnO_2 . Out of these materials only LiCoO_2 established itself as a commercial cathode material. However, Co is expensive and toxic. On the other hand, LiFeO_2 is not easy to prepare while LiNiO_2 and LiMnO_2 inherently possess structural instability along with some safety issues for LiNiO_2 . Moreover, LiMnO_2 converted to spinel structured LiMn_2O_4 with increasing cycles. However, recent studies show that cationic substitution with chromium can significantly decrease this conversion from LiMnO_2 to LiMn_2O_4 [69]. Therefore, research on cathode materials shifted to some other materials having different structures such as olivine, spinel and NaSICON (family of Na super-ionic conductors) type of materials [7]. The olivine structured LiFePO_4 has a great potential to be used as positive electrode material for future Li-ion battery. Almost 90% (165 mAhg^{-1}) of its theoretical capacity can be exploited when used this material in suitable condition in Li-ion battery.

2.8.1 Cathode Materials

The cathode is the positive electrode in Li-ion battery. This material is required to have the following criteria [77]:

- a) This material should have high redox potential to have high cell voltage
- b) The material should have the low molar mass with higher amount of intercalated to lithium which gives rise to higher electrochemical capacity
- c) The material should be structurally stable with minimum volume change/ structural modification so that it can accommodate large volume of lithium intercalation and deintercalation reversibly
- d) The chemical diffusion coefficient of the material should be high so that faster redox reaction can take place
- e) The material should have good electronic conductivity as well as better lithium-ion diffusivity simultaneously so as to minimize the addition of conducting additives externally and to reduce the polarization loss respectively.
- f) Lastly the material should be abundantly available, non-toxic and environmentally benign

2.8.1.1 Requirements for Cathode Materials [78]

Higher working voltage with high capacity gives rise to higher energy density. Long cycle life indicates the better structural stability both in terms of Li intercalation/deintercalation and electrode-electrolyte interaction. These are the basic requirements for a high performance cathode materials. Therefore, some basic aspects are required to be taken into consideration while designing a new cathode material.

a) Open Structure

The structure of the material should be open enough to reversibly accommodate a large volume of lithium in the lattice without any structural disintegration/modification

b) No Electrode and Electrolyte Interaction

There should not be any chemical reaction at the interphase between electrode-electrolyte. Moreover, electrodes should not induce any oxidation or reduction in the electrolyte. This would give rise to higher cycle life.

c) Higher Energy Density

The specific energy density is the product of voltage and capacity. The voltage depends on the redox potential of transition metal element in the composition while capacity depends on the number of Li ions that can be accommodated reversibly. Therefore, to have higher specific energy density both these components should have higher values.

d) Higher Electronic and Ionic Conductivity

The both lithium insertion and extraction to and from the cathode material involves the Li ion diffusion within the particles along with transfer of electrons from bulk to surface and vice versa. Both this process is interrelated and happens simultaneously within the material. The higher Li ion diffusivity and higher electronic conductivity essentially increase the rate capability and reduces the polarization loss.

e) Inexpensive and Environment Friendly

The lower cost and environmental benignity (non-toxic/or less toxic) are always the prerequisite as well as challenge while developing of a new cathode material. The minimum working voltage required for a material to perform as a cathode material is 3 V. They include lithium containing transition metal oxides of different structures like layered structure, spinel structure, olivine structure etc. [7].

The cathode materials can be broadly categorized in three major groups: layered structure (LiCoO_2 , LiNiO_2 etc.); spinel structure (LiMn_2O_4 , LiFe_2O_4 etc.) and olivine structure (LiFePO_4 , LiNiPO_4 etc.). However, in recent times, many new materials have come up which are not falling in these categories. The more open structure like V_2O_5 , tunnel structure like MnO_2 and olivine structure like LiFePO_4 are the most promising cathode materials at present [66, 79].

Layered Li_xCoO_2 [66, 80, 81], Li_xNiO_2 [79, 82, 83] and Li_xMnO_2 [84-86], spinel $\text{Li}_x\text{Mn}_2\text{O}_4$ [87-89] and olivine structured Li_xFePO_4 [90] are the most investigated cathode materials in the last two decades [66]. The above materials will be studied in detail in the subsequent sections.

2.8.1.1.1 Layered Oxides

Lithium cobalt oxide (LiCoO_2):

Still today LiCoO_2 is the most commonly used commercial positive electrode material for Li-ion battery. Structurally LiCoO_2 is having $\alpha\text{-NaFeO}_2$ structure with R-3m space group representing a Rock salt structure. The oxygens are positioned as a cubic close packed order and the alternate Li^+ and Co^{3+} containing planes (111) are located in octahedral sites. LiCoO_2 as a Li-ion battery cathode

material was first reported by Goodenough and his team 1980 [66]. LiCoO_2 is a stable compound and does not undergo any significant structural changes even after several Li-ion intercalation/deintercalation reactions, have theoretical capacity of 248 mAhg^{-1} and flat voltage plateau at 3.6 V vs. Li^+/Li . However, in spite of possessing higher theoretical capacity, only 120-180 mAhg^{-1} can be exploited for practical applications. In spite of having the above advantages, LiCoO_2 also possesses several drawbacks, like environmental issues as the Cobalt is toxic in nature, thermal issue as the Co^{4+} is thermally unstable, safety issues as the Co^{4+} reacts with electrolyte and finally expensive and not abundant on earth. Furthermore, larger ratio of $\text{Co}^{4+}/\text{Co}^{3+}$ destabilize the structure of the material resulting loss in cell reversibility [81]. Therefore, delithiation is restricted to only half of the lithium available in the material; thus, the capacity is not achieved up to the theoretical level. These drawbacks, however, motivated the researchers to explore the new materials having same structure with improved properties, which includes LiNiO_2 and LiMnO_2 and many substitutional materials.

$\text{Li}(\text{Ni},\text{Mn})\text{O}_2$:

The other layered oxides, LiNiO_2 and LiMnO_2 are structurally identical with LiCoO_2 and their crystal structures are also same as $\alpha\text{-NaFeO}_2$ [91]. The phase pure LiNiO_2 is difficult to obtain because of the volatilization loss of lithium from the structure [92]. Although, the discharge capacity of LiNiO_2 can be as high as 195- 210 mAhg^{-1} [93], but due to rapid loss of lithium, the cyclability of the system becomes low [94]. To mitigate these problems several efforts have been attempted to improve the structural stability, thus, improving the capacity as well as cyclability by coating the material with metal oxides or substituting nickel with other metallic elements such as Al, Mg, or Co.

The phase pure LiMnO_2 is prepared in various ways such as ion exchange reaction from $\alpha\text{-NaMnO}_2$, hydrothermal reaction, synthesis at high temperature in air atmosphere etc. This material is non-toxic, comparatively inexpensive and have high theoretical capacity. Bruce et al first reported the capacity of LiMnO_2 as high as 230 mAhg^{-1} on the first cycle. However, capacity drops drastically to 130 mAhg^{-1} on subsequent cycle. The major drawback of this material is its thermodynamic instability at higher temperature [84, 95, 96].

2.8.1.1.2 Spinel Structure

The spinel structured LiMn_2O_4 is another potential material to be used as Li-ion battery cathode material. The major advantage of this type of structure or material is the 3D diffusion of Li ions in the structure during intercalation/deintercalation process and this has been possible due to the interconnected structure of empty 8c octahedral sites and empty tetrahedral sites. Along with this, LiMn_2O_4 has several other merits such as it is non-toxic, stable at higher temperature, comparatively less costly having theoretical capacity 148 mAhg^{-1} and almost flat voltage plateau between 3.95 - 4.1 V. However, the capacity fading during cycling is the major drawback of this material [88].

2.8.1.1.3 Olivine Structure

Goodenough and his team reported a new structure (olivine) of a material which is phosphate based rather than oxide based in 1997. The family of such materials can be expressed as LiMPO_4 (where $\text{M} = \text{Fe, Mn, Co and Ni}$). Out of these four compositions, LiFePO_4 shows many advantages such as environmentally non-hazardous, having low cost, thermal stability, resistance to overcharge etc. The theoretical capacity of this material is 170 mAhg^{-1} and it has also a flat voltage plateau which

is at 3.40 V vs. Li+/Li and this eventually give rise to higher energy density [81]. Moreover, this material is open enough to accommodate large volume of Li insertion/de-insertion during charging/discharging without undergoing any structural changes, thus having excellent cyclability with no obvious capacity degradation over cycling even after 100 cycles [90]. LiFePO₄ although possesses many advantages still have some demerits such as low electronic conductivity ($< 10^{-9}$ Scm⁻¹) and comparatively lower Li ion diffusivity. Conductive additives such as carbon may be added to increase the electronic conductivity. Substituting Li with higher super valent elements may also increase the electronic conductivity. On the other hand, Li ion diffusivity can be enhanced by decreasing the particle size from micron level to nano level [97, 98].

Depending upon the structure, the Li ion diffusion is 1D in olivine based material, 2D in layered structure and 3D in spinel structure. The respective structures are shown in **Figure 16**. The important parameters related to electrochemical performance for these three types of materials are also tabulated in **Table 3** [99].

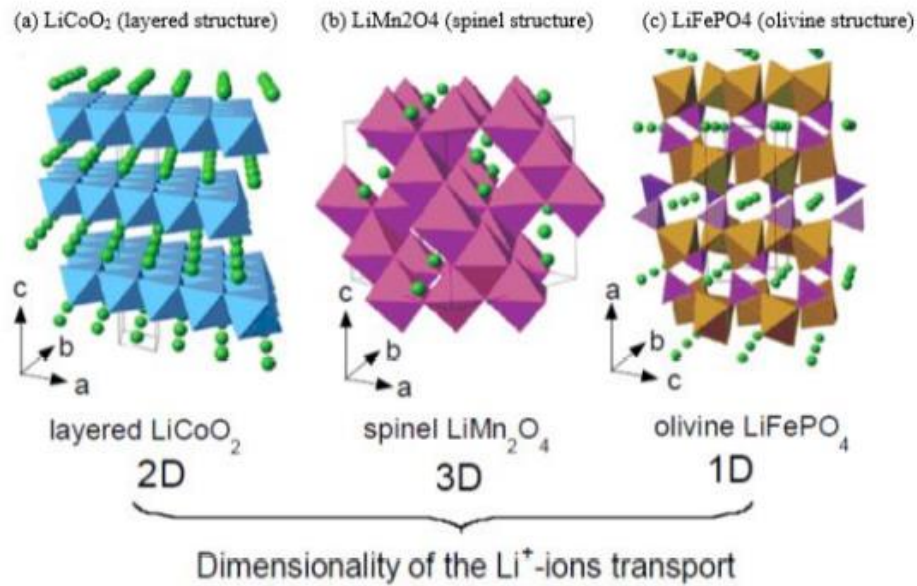


Figure 16. Schematic Representation of Three Major types of Positive Electrode Materials [100]

Table 3: Characteristics of Three Major Types of Positive Electrode Materials [100, 101]

Characteristics	LiCoO ₂	LiNiO ₂	LiMn ₂ O ₄	LiFePO ₄
Framework	Layered rock salt	Layered rock salt	Spinel	Olivine
Redox couple	Co ⁴⁺ /Co ³⁺	Ni ⁴⁺ /Ni ³⁺	Mn ⁴⁺ /Mn ³⁺	Fe ³⁺ /Fe ²⁺
Average potential (V vs. Li/Li ⁺)	4.2	4.0	4.1	3.45
*Sp. Capacity (mAhg ⁻¹)	272	274	148	170
**Discharge capacity (mAhg ⁻¹)	140	160	120	160
Safety	Fair	Poor	Good	Good
Environmental	Poor	Fair	Good	Good
Cost	High	Fair	Low	Low
* Theoretical ** Practical				

2.8.1.2 Brief Detail of Cathode

The materials having properties Li ions intercalation and de-intercalation without much changes in the structure are the favourable choice for Li-ion battery and the lithium containing metal oxides having such properties were first discovered by Goodenough et al. in 1980. Soon after, Sony corporation released the first commercial battery having LiCoO₂ (LCO) as cathode material [88]. The LCO dominated the market for more than 15 years after its discovery. But the inherent disadvantages possessed by LCO such as its toxicity, scarcity and unable to exploit its full theoretical capacity due to structural instability pushed the researchers to think over some new materials [9, 102-105].

Another potential material came up in the market to compensate the demerits of LCO is the spinel type LiMn₂O₄ (LMO) which is comparatively inexpensive having higher operating voltage but ultimately this material was unable to replace LCO. The most serious problem of this material was

leaking of Mn^{2+} in the electrolyte solution during deintercalation, which gradually makes the structure unstable over a number of cycles. Moreover, this free Mn^{2+} ultimately moved to the anode and deposited on it; thus, reducing the electrochemical performance of anode resulting severe capacity fading [106]. A comparative study of important electrochemical parameters of commonly used cathode materials are shown in **Table 4**.

Table 4: Properties of Commercially Available Cathode Materials [107]

Crystal structure	Compound	Sp. Capacity (mAhg ⁻¹) (Theoretical/Experimental)	Volumetric capacity (mAh cm ⁻³) (Theoretical/Experimental)	Average voltage
Layered	LiCoO ₂	274/148	1363/550	3.8
Layered	LiNi _{0.33} Mn _{0.33} Co _{0.33} O ₂	280/160	1333/600	3.7
Layered	LiNi _{0.8} Co _{0.15} Al _{0.05} O ₂	279/199	1284/700	3.7
Spinel	LiMn ₂ O ₄	148/120	596	4.1
Olivine	LiFePO ₄	170/165	589	3.4

Instead of using pure LCO, hybrid materials such as LiCoNiO₂ is used now a days for several applications including electric vehicles. Substitution of a suitable transition metal by some other metals ions such as aluminium can results in accessing more lithium from the material, thus, eventually increase the capacity with sacrificing a minimum voltage drop.

The olivine structure LiFePO₄ are composed of FeO⁶⁻ octahedra and PO⁴⁻ tetrahedra layers and in-between Li atoms are located in interstitial position. The octahedra and tetrahedra are connected through oxygen atoms in b-c plane and also this octahedra and tetrahedra are shared by one edge. This makes an infinite chain of lithium atoms in alternate a-c planes.

The equation for calculating maximum theoretical specific capacity (MTSC) at constant current condition for an electrode material is demonstrated below [76].

For an example, if the electrode reaction is: $x\text{A} + \text{R} = \text{A}_x\text{R}$

$$\text{MTSC} = (xE/W_t) F$$

Here, x is expressed in equivalent per mole, E is expressed in volts, W_t is expressed in g mol^{-1} and F is Faraday constant. For an example, the charge-discharge profile of a graphene based anode material is shown in **Figure 17**.

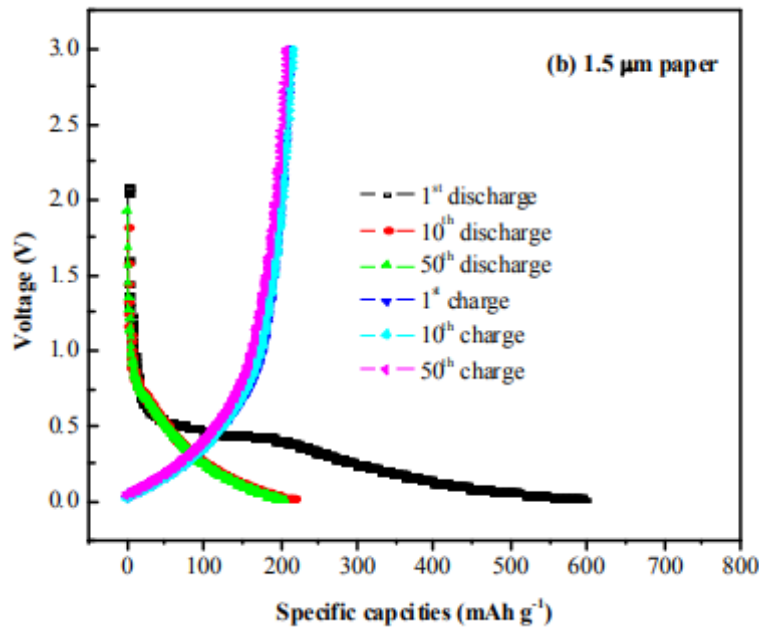


Figure 17. Graphene based anode material showing Typical charge-discharge profile [108]

Another important evaluating parameter for a Li-ion battery performance is the operating voltage and based on the output voltage Li-ion battery can be classified in to three categories [76]; High voltage battery (3.5-5.5 V), then Medium voltage battery (1.5-3.5 V) and Low voltage battery (0-1.5 V).

2.8.1.3 Recent Developments in Cathode Materials

The layered structure cathode materials in the family of LiMO_2 (where $M = \text{Co}, \text{Ni}, \text{Mn}$ and Fe) are isomorphic of $\alpha\text{-NaFeO}_2$ structure. This is also called distorted type rock-salt structure. The cations in this structure are arranged in alternate (1 1 1) planes. This type of structures also forms a trigonal structure of $R3m$ space group [109]. LiMO_2 type of structure supports the Li insertion/de-insertion as Li atoms situated between the oxygen layers. The oxygen forms a face centred cubic closed pack order. The transition metal resides within the oxygen octahedral [110].

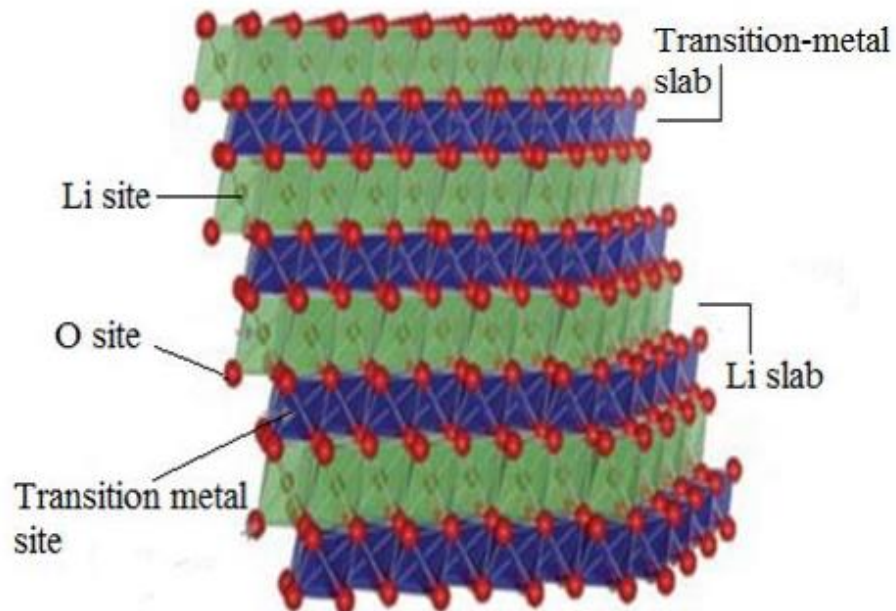


Figure 18. Layered Structured LiMO_2 [65]

LiCoO_2 is the most suitable and first commercial cathode material for Li-ion cell and dominated the battery market for a long period. As described above LiCoO_2 is identical to that of $\alpha\text{-NaFeO}_2$ structure where oxygen atoms form an FCC closed pack arrangement. Now upon de-lithiation, the oxygen atoms rearrange themselves to form hexagonal closed pack structure of CoO_2 .

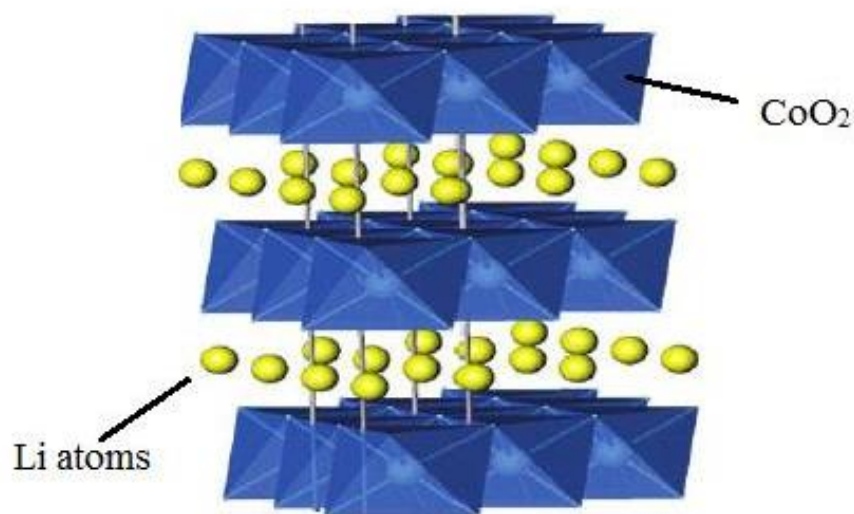


Figure 19. Layered Structure of LiCoO₂ [111]

The electrochemical performance evaluating parameters for LiCoO₂ are as capacity 140 mAh⁻¹, operating voltage 3.7 V. However, the capacity of this material can be significantly increased by coating the material by oxide and or phosphate based compounds. The capacity of the material can also be improved up to 170 mAh⁻¹ when operated between 2.75 and 4.4 V with enhanced cyclability. However, the major two disadvantages of the material like its toxicity and higher cost have motivated the researchers to venture in to the other family members of this material, viz., LiNiO₂, LiFeO₂ and LiMnO₂ as these materials are not toxic and abundantly available. Moreover, research have been continued in the area of solid solutions of LiCoO₂ where part of Co can be substituted by other transition metal elements such as Ni, Fe, Mn etc. e.g., LiNiO₂-Li₂MnO₃-LiCoO₂ [111], LiCoO₂-Li₂MnO₃ [112], LiNi_{1/2}Mn_{1/2}O₂-Li₂MnO₃-LiCoO₂ [113, 114], LiNiO₂-LiCoO₂ [115].

2.8.1.3.1 $\text{LiNi}_{1-y}\text{Mn}_y\text{O}_2$

Dahn et al. reported a contemporary potential cathode material, $\text{LiNi}_{1-y}\text{Mn}_y\text{O}_2$ in 1992 [114, 116-118].

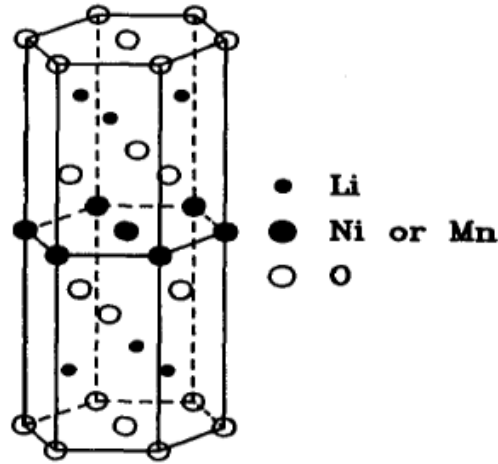


Figure 20. Unit Cell of $\text{LiMn}_y\text{Ni}_{1-y}\text{O}_2$ Showing Li Layer and Ni, Mn Layers [118]

After experimenting the different ratios of Mn:Ni in this composition, it has been concluded that $\text{LiNi}_{1/2}\text{Mn}_{1/2}\text{O}_2$ is the most suitable material. Moreover, this material is not toxic and not expensive and could be a possible alternative for LiCoO_2 . Saphr et al also showed the maximum solubility of Mn in Ni is 0.5 to form a stable compound [119]. In their work, they proved that Ni and Mn present in the material in +2 and +4 state and the oxidation-reduction potential of Ni in between +2 and +4 state is only responsible for output voltage while oxidation state of Mn remained constant at +4 state; thus, Jahn-Teller effect due to Mn^{+3} ion is not apparent here. At initial cycle, the discharge capacity of this material is 150 mAhg^{-1} , which after 25 cycles come down to 125 mAhg^{-1} and 75 mAhg^{-1} after 50 cycles, if prepared at 700°C . Commercially this composition is called as “550” material (0.5Ni, 0.5 Mn, 0 Co) [120]. Ohzuku and Makimura showed that the cyclability of the material can be improved to 30 cycles with capacity 150 mAhg^{-1} at operating

voltage 4.3 V, if prepared at 1000°C. The capacity can be improved as high as 200 mAhg⁻¹ for 30cycles if operated between 2.5-4.5V [117].

2.8.1.3.2 LiNi_{1/3}Mn_{1/3}Co_{1/3}O₂

Another potential material LiNi_{1/3}Mn_{1/3}Co_{1/3}O₂ in the family of LiNi_{1-y-z}Mn_yCo_zO₂ was first demonstrated by Liu et al in 1999 and Yoshio et al in 2000. This material can provide the benefit of all the three elements (Mn, Co and Ni) if mixed in this equal ratio. Otherwise, more Co would decrease the capacity whereas more Ni may lead to cation mixing and more Mn results to the transformation to spinel structure. The addition of Co in LiMn_{1-y}Ni_yO₂ stabilizes the material in layered 2D structure by blocking the Ni atom entering in to the Li layer, while Ni and Mn increase the capacity and stability of the material respectively [121-123].

This LiNi_{1/3}Mn_{1/3}Co_{1/3}O₂ is thermally stable having very good rate capability with 200 mAhg⁻¹ discharge capacity in the voltage range of 2.5– 4.6 V [109, 122, 124]. In commercial market this material is called as “333” material. The oxidation state of all three elements is kept at +3 state for maintaining the stoichiometry. Thus, Ni is maintained at +2 state, Co is maintained at +3 state and Mn is maintained at +4 state. Here the active material is Co^{3+/4+} and Ni^{2+/4+} [125-128]. The rate capability of the material is higher than LiNi_{1/2}Mn_{1/2}O₂ but lower than LiCoO₂ and the material becomes unstable when operate more than 4.6 V [129].

2.8.1.3.3 LiMnO₂ (Layered)/LiMn₂O₄ (Spinel)

LiMnO₂ is nontoxic and inexpensive and belongs to the same family of LiCoO₂. Lot of researches have been done on this material in past two decades [84, 130]. The main disadvantage of this

material is that its thermal stability at higher temperature. Moreover, this material cannot be easily prepared like NaMnO_2 . Low temperature hydrothermal synthesis and ion exchange methods are successfully adopted to prepare this material [84, 130]. However, the synthesized LiMnO_2 has always a tendency to transform itself to the spinel structure of LiMn_2O_4 .

LiMn_2O_4 can be demonstrated as a viable positive electrode material for Li-ion battery mainly because of its structure. The three dimensionally open structure of LiMn_2O_4 allows Li ion insertion and de-insertion during discharge/charge in more effective and faster way resulting higher rate capability without destabilizing/modifying the structure. The discharge capacity of this material is 150 mAhg^{-1} . Moreover, this material is much more inert in terms of reacting with liquid electrolyte which provides better safety.

A comparison between LiMnO_2 and LiMn_2O_4 structures is depicted in the figure below.

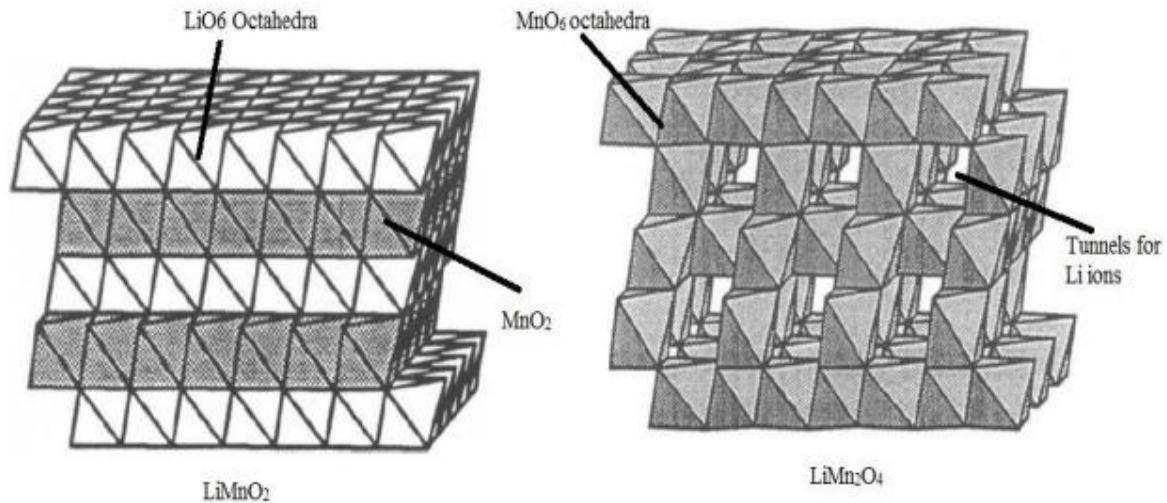


Figure 21. Layered LiMnO_2 and Spinel LiMn_2O_4 Structure [131]

The main disadvantage of this material is its two discharge voltage plateau, one at 4 V and another at 3 V. Therefore, even after discharging at 4 V, there may be chances of remaining few Li ions at +3 state in the host cathode material, which eventually leads to the Jahn-Teller distortion and modify the structure from cubic to tetragonal. Another disadvantage of this material is that this material slowly loses its charge at elevated temperature even when not in use [132].

Several attempts have already been made to mitigate these disadvantages to improve the structural stability; thus, reducing the capacity fading and also to reduce the self-discharging by cationic substitution or coating the material with other oxide materials after necessary surface treatment etc. [133-135].

2.8.1.3.4 Li_2MnO_3

In recent past, this material has gained a significant interest because of its higher capacity due to higher Li content and better safety as Mn is more inert compare to other transition metal elements. This material produces better electrochemical performance when used in association with other layered structured materials such as LiCoO_2 or LiNiO_2 etc as a composite material [113, 136, 137].

The structure of Li_2MnO_3 material is similar to that of Rock salt structure having R3m space group. Li and Mn layers are alternatively arranged in 2:1 ratio and in-between these layers cubic closed packed oxygen layers are situated [138].

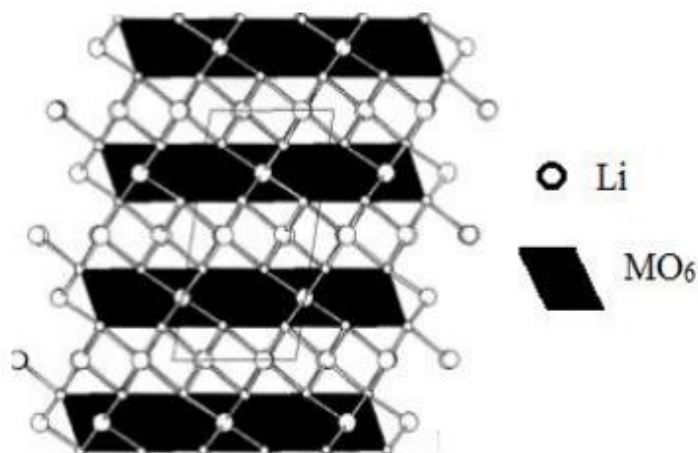


Figure 22. The Rock Salt Structure of Li_2MnO_3 [139]

Electrochemically Li_2MnO_3 is not active as Mn is in +4 state and there is no further chance to oxidize this material at lower voltage. However, at higher voltage (> 4.5 V), Li tends to come out as Li_2O keeping the host structure as MnO_2 . But this process is not both ways. Upon coming back during discharging Li ions form LiMnO_2 instead of forming Li_2MnO_3 . Thus, the researches thought to use this Li_2MnO_3 with addition of other layered structured materials (LiMO_2) as a composite material. This composite structure facilitates Li intercalation/deintercalation without modifying the structure [116, 138].

2.8.1.3.5 Binary and Ternary Solid Solutions of Li_2MnO_3

The solid solution of Li_2MnO_3 with other layered structured materials has primarily two major advantages: the more Li atoms in Li_2MnO_3 gives rise to higher capacity when charge at > 4.5 V as well as structural stability after delithiation as MnO_2 is more stable than other Mn compounds. The concept of solid solution of Li_2MnO_3 with other LiMO_2 materials came into consideration to take advantage of higher capacity of Li_2MnO_3 material at the same time to preserve the structural

stability upon lithiation/ delithiation during discharge/charge respectively. Therefore, the solid solution of this materials shows better electrochemical performance like higher capacity, better cyclability, improved stability along with lower cost as Mn is abundantly available.

Recently, researchers have investigated many such solid solutions such as $\text{LiNiO}_2\text{-Li}_2\text{MnO}_3\text{-LiCoO}_2$ [111, 140], $\text{LiNiO}_2\text{-Li}_2\text{MnO}_3$ [141-144], $\text{LiCoO}_2\text{-Li}_2\text{MnO}_3$ [112, 145], $\text{LiNi}_{1/2}\text{Mn}_{1/2}\text{O}_2\text{-Li}_2\text{MnO}_3$ [116], $\text{LiNi}_{1/2}\text{Mn}_{1/2}\text{O}_2\text{-Li}_2\text{TiO}_3$ [146, 147], $\text{LiCrO}_2\text{-Li}_2\text{TiO}_3$ [148, 149], $\text{LiNiO}_2\text{-Li}_2\text{TiO}_3$ [150, 151], $\text{LiFeO}_2\text{-Li}_2\text{MnO}_3$ [152, 153].

2.8.2 Anode Materials

The next main component of a Li-ion battery is anode which is the negative electrode material. Broadly, the anode materials are put into three major categories. Insertion type, conversion type and alloying type. Many researches have been done and still going on in the area of these three types of materials. Insertion type materials are like carbon materials, $\text{Li}_4\text{Ti}_5\text{O}_{12}$, TiO_2 ; then conversion type of materials like cobalt oxides and iron oxides and alloying type materials like Sn, Si and SnO_2 are generally used in Li-ion battery technology. However, the materials to be used as negative electrode materials for Li-ion battery are required to fulfil the following requirements.

- a) Operating voltage should be as low as possible ($\leq 1\text{V}$ vs. Li^+/Li) close to metallic lithium
- b) High capacity so that it can produce high energy density
- c) Better structural stability upon lithiation/delithiation which gives better cyclability
- d) Ability to accommodate faster Li ion insertion/deinsertion to have better rate capability
- e) It should be non-toxic thus environmentally benign and abundantly available thus having lower cost

2.8.2.1 Lithium Metal

Since the Li-ion battery came up in market the lithium metal as anode material is being used. It has many merits to be used as Li-ion battery anode material. This metal is having high gravimetric (3.86 Ahg^{-1}) as well as high volumetric (7.23 Ahcc^{-1}) specific capacity, then lowest electrochemical potential ($E_0 = - 3.04 \text{ V vs, SHE}$) and finally lightest weight metal ($M = 6.94 \text{ g mol}^{-1}$) in the periodic table. These three major properties have made this material most suitable for Li-ion battery [7]. Along with these primary positive characteristics, Li metal has many other advantages such as flat voltage plateau on discharge, stability in wide temperature range, long self-life and ability to form solid electrolyte interphase (SEI) which prevent the Li metal to directly interact with liquid electrolyte; thus, no side reactions [71]. However, the main disadvantage of using Li metal as anode is the plating of Li metal on anode during charging which significantly reduce the energy density of anode material. Moreover, slowly this lithium plating starts growing in dendritic fashion which is called lithium dendritic growth. These dendrites slowly grow and penetrate the separator through electrolyte destroy the insulation and causes short circuiting which poses significant safety issues may even results in explosion. This particular problem has restricted the Li metal as anode materials in Li-ion battery and motivated the researchers to find out some possible alternative materials [35, 154].

2.8.2.2 Carbon-based Materials

The materials based on carbon find their application as negative electrode materials in Li-ion battery after Li metal. There are two types of carbon based materials, so far reported, to be used as anode materials. They are soft carbon and hard carbon. In soft carbon all the crystals are oriented

in the same direction like graphitic carbon while in hard carbon the crystal orientation is random. This classification also includes the degree of crystallinity as well [155-158].

2.8.2.2.1 Graphite

Mostly the Li-ion battery uses graphitic carbon as anode material. Several forms of graphitic carbon so far reported to have excellent properties that are required for a anode material. These are mesocarbon microbead (MCMB), mesophasepitch based carbon fibre (MCF). Other forms of graphite are vapour grown carbon fibre (VGCF) and also massive artificial graphite (MAG).

Generally, Graphite is having a planer structure making stacks together. Mainly two types of symmetries are there for graphite material, i.e., hexagonal and rhombohedral. The stacking sequence of the hexagonal graphite is repeated in every after two layers. On the other hand, the stacking sequence for rhombohedral graphite repeats itself after three layers. That is why the stability of rhombohedral graphite is lower than that of hexagonal graphite [159]. **Figure 23** shows the hexagonal and rhombohedral forms of graphite.

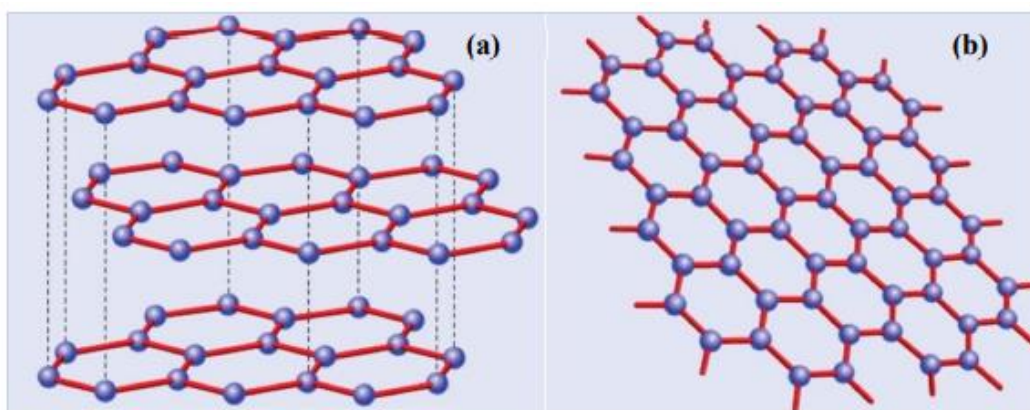


Figure 23. Hexagonal Graphite as (A) Graphene Layers Stack Together and (B) Single Layer Graphene [160]

The graphite electrode has many advantages as well as disadvantages. The advantages are as high capacity (initial capacity of 372 mAhg^{-1}) leads to larger number of Li ion insertion/deinsertion (nominally form LiC_6 when charged) at low flat voltage ($< 0.1 \text{ V}$ vs. Li^+/Li) plateau to generate overall cell voltage high. The major disadvantages are low operating voltage, which tends to oxidation of carbon thus poses high risk or safety issues, tendency to form solid electrolyte interphase (SEI) during initial cycle that significantly reduces the capacity, graphite is fragile therefore structurally not stable [7, 161].

Recently another potential graphite material has been reported by Bao et al. This graphite has interconnected graphene like structure having 3D porous network with larger pore volume and very high surface area. This type of graphite is called hierarchically porous graphite (HPG). This type of graphite fulfils almost all the critical requirements of an anode material and can produce excellent electrochemical performance [162].

2.8.2.2.2. Graphene

Essentially a single layer of graphite is called graphene. The sp^2 hybridized carbons are bonded in a hexagonal structure in a layer of nanometre thickness [160]. **Figure 23(b)** This graphene material possesses excellent properties that are required for an anode material such as higher electrical conductivity, improved mechanical stability and higher surface area [163, 164]. But the lithium storage mechanism is not well understood for this material. Some researches claimed it as adsorption mechanism on both sides of the graphene sheet, which may give rise to capacity value of ($< 372 \text{ mAhg}^{-1}$) while others said that lithium may be trapped within the covalently bonded benzene ring. This may give rise to very high capacity value of ~ 780 to 1115 mAhg^{-1} .

Many researches have put their effort to understand the interaction of Li-ion with graphene. Pan et al. reported that distorted structured graphene can produce the capacity as high as 790-1050 mAhg⁻¹ but this structure failed due to its poor electronic conductivity [165]. A group of researchers showed using high quality graphene, the initial capacity can be attained up to 1200 mAhg⁻¹ and then dropped to 848 mAhg⁻¹ at 40th cycle [166]. Improving the existing graphene structure is a major area of focus for researchers in recent times. This includes doped hierarchically porous graphene (DHPG) [167], nano-ribbons from MWCNTs [168], or hybrid systems of graphene and metals or graphene and metal oxides or metal phosphides [169-171] and nanorod/graphene [172].

Materials for negative electrode in Li-ion battery:

Up to a certain time, Li metal was considered as the most favoured anode material. This was because of its low electrochemical potential (-3.04 V vs. SHE) in addition to high specific capacity (3.86 Ahg⁻¹). But the major safety concern due to dendritic growth of Li metal over cycling pushed the researchers to think over carbonaceous material as possible alternative [173, 174]. Broadly carbonaceous material for anode material can be divided into three categories namely graphite, soft carbon and hard carbon where graphite sometimes come under the soft carbon. From structural point of view graphite is very regular, soft carbon is little bit irregular and hard carbon is randomly oriented. **Figure 24** The capacity of graphite is 372 mAhg⁻¹ but this graphite cannot be used as anode where PC (propylene carbonate) or EC (ethylene carbonate) based electrolytes are used because both this type of electrolytes decomposes on graphite surface. The capacity of the soft carbon is 372 mAhg⁻¹ which is similar to graphite and this can be used in association with EC based electrolyte. The structure of hard carbon is randomly oriented having much higher porosity. This type of carbon can have the capacity more than 372 mAhg⁻¹ because of more active sites.



Figure 24. Three Types of Carbon used in Li-Ion Battery [175]

This graphitic anode was first used by Sony corporation in Li-ion battery and in today's commercial battery this graphitic anode is still being used at large. The main advantages of this material are its abundance on earth which made it inexpensive, low electrochemical potential and high capacity [102, 176]. Silicon is another potential anode material, can accommodate large number of lithium; thus, producing very high capacity. However, the volume expansion after lithiation is ~ 300% and this is the major drawback of this material. The faster lithiation/delithiation eventually destabilize the structure completely [103-105, 107, 176, 177].

2.8.2.3 Li- Metal Alloys/ Intermetallic Alloys

The alloys of lithium metal have proved to solve many disadvantages of lithium metal anode material and can be considered as potential substitute for carbonaceous anode materials. Li-Al alloy are able to solve the dendrite problem to a large extent [178]. Alloy of Li with other low melting metals, e.g., Bi, Pb, Sn and Cd was first introduced as anode materials in Li-ion battery by Matsushita in 1980 [7]. The alloy of lithium metal shows very high specific capacity such as 993 mAhg⁻¹ for Li_{4.4}Sn and 4200 mAhg⁻¹ for Li_{4.4}Si [54]. However, the major drawback of this metallic alloys is their large volume expansion (> 200%) which ultimately disintegrate the particles thus,

destabilize the material during operation [6]. Reducing the alloy particle size from micron level to nano level can mitigate the problems of particle disintegration but overall volume expansion remains unchanged [5, 54, 76, 179].

To solve the problem of volume expansion a composite electrode material is prepared, where two different metals having different electrochemical potential are used and the active metal is distributed in the matrix of non-electrochemically active material. This includes Sn-C, Sony Nexelion battery uses Co-Sn-C as anode material [7, 180, 181]. An approach based on displacement reaction can also be utilized to solve this volume expansion problem. Li_xM type of Intermetallic alloys such as Copper-Tin (Cu_6Sn_5), Indium-Antimony (InSb), and (Copper-Antimony) Cu_2Sb results much lower volume change (46%) upon lithiation/delithiation compared to binary alloy system such as Li-Al which results the volume expansion more than 200%. However, these intermetallic alloys show poor cyclic stability [7, 54, 182].

2.8.2.4 Tin-based Compounds

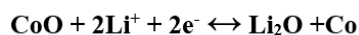
Tin oxide based anode materials have very good potential to be used as negative electrode materials for the application in Li-ion battery. These materials are abundantly available on earth and also non-toxic. This material has higher specific capacity compared to Li metal and also have high Li ion diffusivity ($\sim 10^{-8} \text{ cm}^2\text{s}^{-1}$). The tin oxide based material was first introduced in the commercial market by Fujifilm in 1997, where they used the composition SnM_xO_y (where M = B, P or, Al). Commercially this material is termed as TCO, i.e., Tin-based composite oxides [179, 183]. The Li intercalation with this material can be explained as forming $\text{Li}_{4.4}\text{Sn}$ alloy which theoretically gives rise to very high capacity value of 993 mAhg^{-1} . However, during initial cycle

the capacity loss is also very high, i.e., 300 – 600 mAhg⁻¹. However, during alloying dealloying the volume change is ~ 260%, which makes this material unstable; thus, difficult to retain the initial capacity. This large amount of volume change can be solved to some extent by using tin oxide instead of using metallic tin. However, after initial cycles tin oxide converted to metallic tin [184]. The reaction between lithium and tin oxide based material can be explained as during initial cycles tin oxide reacts with lithium and forms metallic tin and lithium oxide. Structurally it appears that metallic tin is distributed in lithium oxide matrix. Here lithium oxide acts as a stabilizer for metallic tin. During subsequent cycles this metallic tin acts as the active anode material by forming Li-Sn alloying/dealloying in lithium insertion/deinsertion reaction [184].

Various attempts have been made to solve the problems of this volume expansion thus to increase the stability such as doping molybdenum [185], using mesotubes of tin dioxide [186], using tin oxides carbon nanotubes composite [187], tin oxides-silicon oxides composite [188] and tin oxide-cobalt oxide composite [189], controlling the particle size [190] and using thin film materials [191].

2.8.2.5 Transition Metal Oxides

The transition metal oxide (MO, where M= Co, Cu, Ni, Fe, Mn) is another potential alternative for anode material [192, 193]. The lithium insertion/deinsertion mechanism for this transition metal oxide can be explained as shown in the following equation.



One of the disadvantages of this material is decomposition of electrolyte material on anode surface and SEI formation which eventually decrease the capacity [194, 195]. Much improvement in

electrochemical performance can be achieved with this material having the capacity as high as 600–700 mAhg⁻¹ [192, 193, 196]. The size and morphology of the particles played a crucial role in determining and improving the electrochemical performance of the of the cell. So far various particle morphologies such as sheets, cubes, wires, tubes etc in nano dimension. have been investigated by the researchers [155]. The theoretical capacity of CoO and Co₃O₄ are 715 and 890 mAhg⁻¹ respectively [197, 198]. Even if the operating voltage for such material is quite high (~2 V) still it produces high capacity [155].

The most commonly used transition metal containing oxide is iron oxide. Both Fe₂O₃ and Fe₃O₄ have the theoretical capacity as high as 900-1000 mAhg⁻¹ [197]. This iron based oxide have some major disadvantages also such as large volume expansion, segregation of iron particles during charge/discharge and poor ionic and electronic conductivity. Researchers showed that these problems can be solved by decreasing the particle size and modifying the particle morphology. Moreover, applying carbon coating and forming carbon based composite with Fe₂O₃ and Fe₃O₄ can also improve the performance of Li-ion battery such as improved stability, rate capability and retaining higher capacity 900 mAhg⁻¹ over cycling [199-201]. Some other transition metal compounds (general formula MX_y where M = Fe, Mo, Sn, Sb, Ni, co etc. and X =S, N, P etc.) have also been investigated and found very good results in terms of structural stability and capacity [155, 202].

2.8.2.6 Titanium Oxides based Anode Materials

Anode materials based on titanium oxide (TiO₂ and spinel Li₄Ti₅O₁₂) have many advantages and can be a strong alternative for carbonaceous materials. The major advantages of this material

include moderately high theoretical capacity (335 mAhg^{-1}), higher thermal stability, improved chemical stability in terms of interacting with electrolyte, low or negligible volume change ($\sim 3\%$) during lithium intercalation/deintercalation process and less toxic. Moreover, lower operating voltage $\sim 1.5 \text{ V vs. Li}^+/\text{Li}$ for this material can avoid electrolyte decomposition and SEI formation thus provide higher safety [203-208].

2.8.2.7 Solid-Electrolyte Interphase

The solid electrolyte interphase (SEI) is an interphase between electrolyte and anode in particular. Actually, at higher operating voltage liquid electrolyte decomposes in presence of anodic materials and the decomposed product deposited on the anode surface and acts as a protector for a further decomposition of electrolyte material while reducing the capacity [209]. This SEI layer composed of both organic phases (carbonates and polyethylene oxide) as well as inorganic phases (Lithium oxides and lithium ethylene decarbonate) [102, 177, 210-215]. SEI formation is a common issue for almost all the battery type. However, extensive research is going onto reduce or eliminate the formation of SEI layer or to reduce the negative effects of this layer.

2.8.3 Separators

Separator is another essential component of Li-ion battery. The function of separator is to prevent the electronic conduction while providing the Li ion pathways between cathode and anode. The commonly used separator materials are cellulose, organic fibres, polyolefin and nylon [11]. Among all this type of separators, polyolefin based separator (**Figure 25**) found the maximum application in commercial Li-ion battery since 1990 [11].

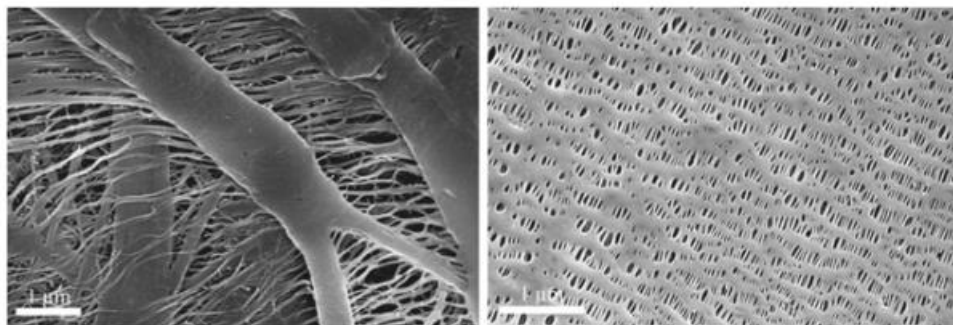


Figure 25. Typical Polyolefin Separators Prepared by Wet Process (Solupor 8P01E) (left) and Dry Process (Celgard 2325) (right) [216]

In recent times, focus has been given on to improve the wettability and thermal stability of the separator materials. The existing polyolefin separator after surface modification and produced in different methods with additional treatments shows better performance in Li-ion battery [11, 13, 14, 217]. The modified separators can resolve various issues of Li-ion battery like polysulfide shuttling [15] and Li dendrite growth [16]. Many advanced separators with improved physicochemical properties have been developed since 2010 and the performance of Li-ion battery, with respect to electrochemical properties, with the application of those separators has improved a lot.

2.8.3.1 Fundamental Requirements of Separators

a) Thickness

The separators being an insulator and have no direct electrochemical properties should be as thin as it is possible to fulfil the requirements of Li-ion battery. For consumer applications such as mobile, laptop, camera the separator thickness should be below 25 μm while for electric vehicle

application the separator is bit thicker, i.e., $\sim 40 \mu\text{m}$. Reducing separator thickness would also decrease the internal cell resistance.

b) Permeability and Gurley value (Air permeability)

Being an insulator, separator increases the electrolyte resistivity by a factor of 6-7 compared to resistivity of electrolyte alone. The ratio of resistivities between separator filled with electrolyte to electrolyte alone is called the McMullin number. The desired value of McMullin number for commercial cell is 10 – 12.

Being a porous material, the separator can also be evaluated by measuring the Gurley value, i.e., extent of air permeability. The Gurley value and electrical resistivity of separator are proportional to each other. Once the relation between electrical resistance and Gurley value is settled then by measuring the Gurley value, we can say the value of electrical resistance. The Gurley value of separator should be kept at low.

c) Porosity, wettability and electrolyte absorption retention

The porosity of the separator determines the amount of electrolyte uptake. The more the electrolyte uptake better would be the Li ion diffusivity during charge/discharge.

The faster and improved wettability of liquid electrolyte to separator is a significant factor to determine the Li ion movement through the electrolyte. More the wettability of the separator material to electrolyte the more will be the electrolyte uptake.

The separator should have capacity to absorb and retain the electrolyte without swelling or changing its structure.

d) Chemical stability

The separator should be chemically inert in liquid electrolyte and should not undergo any oxidation or reduction at higher operating voltage during charge/discharge up to the temperature of 75°C. Better the oxidation resistance of the separator more would be the chemical stability.

e) Thermal stability

The stability of a separator at elevated temperature is a crucial issue from the perspective of safety concern. If the separator is not stable at higher temperature eventually short circuiting would result and that may lead to explosion of the battery.

f) Puncture strength

The separator should have high puncture strength so as to prevent any particulate movement across the separator. The separator having high puncture strength are able to resist the movement of Li dendrite from anode to cathode.

I. Basic functions

The fundamental functions of a separator in Li-ion battery are to prevent electronic contact between the electrodes while allowing Li ion transport through it. These two basic functions demand the following properties of a separator material which include high dielectric constant, thermal stability, mechanical and chemical stability, wettability and porosity. (**Table 5**) [10, 12].

Table 5: General Requirements for LIB Separators [11, 13]

Parameter	Requirement
Thickness	20 – 25 μm
Porosity	40 – 60%
Pore size	< 1 μm
Wettability	Wet quickly/ completely with common electrolyte
Dimensional stability	Lay flat and no curl up outside/ inside battery
Thermal stability	< 5% shrinkage after 60 min at 90 °C
Tensile strength	> 1000 kg cm ⁻² (98.06 MPa)
Air permeability	< 0.025 s μm^{-1}
Chemical stability	Stable in battery for a long period
Electrochemical stability	Stable in battery for a long period
Thermal shutdown	Shutdown of the battery at ~ 130°C

II. Electronic insulation

The separator material should be electronically insulating. It should have high dielectric constant. However, to maintain this electronic insulation between cathode and anode, the separator should have the other required properties such as mechanical as well as thermal stability and also porosity. A separator generally needs small size pores but small pores increase the electrolyte resistivity, on the other hand large pores decreases the mechanical stability. Therefore, an optimized pore size with required tortuosity is desired. Repeated charge discharge in Li-ion battery increases the cell temperature along with the effect of external temperature. Thermal stability is therefore, also an important factor as with decrease in thermal stability would increase the shrinkage in separator material resulting contact between cathode and anode; thus, destroying electronic insulation. In commercial Li-ion battery the separator size is kept little bit more than what is required so that even if it shrinks at higher temperature still it dimensionally covers the interfacial area between

cathode and anode and maintain the electronic insulation. Conventional separators are usually made of polyolefin materials viz. polyethylene and polypropylene. The melting point of polyethylene and polypropylene are 120 and 160°C. However, both the separators start shrinking much below their respective melting point. Sufficiently mechanical strength is also required so that any particulate growth on electrode surface or dendrite formation cannot puncture the separator. Therefore, separator should have high puncture strength but at the same time it should be as thin as possible so that resistance resulting from separator is reduced while active material in cathode and anode can be increased. In advanced Li-ion battery the separator thickness is 10 μm [11, 218, 219]. However, smaller thickness of the separator requires higher mechanical strength. The porosity and pore size distribution largely determine the mechanical strength of a separator [11, 13]. Another strategy that is thermal shut down by blocking the pores during overheating can prevent the short circuiting but inhomogeneous current distribution across the separator can generate localised heating thus increasing the chances of short circuiting. Therefore, separator materials having high shrinking and melting temperatures are preferred. The separator should be electrochemically inactive also otherwise irreversible electrochemical reaction may consume the separator material thus increase the risk of short circuiting.

III. Ionic conduction

The ionic conduction of a battery separator depends on its porosity, interconnectivity of pores, i.e., tortuosity, electrolyte uptake percentage in separator pores and wettability and Li ion conductivity of electrolyte through separator. Maintaining the required mechanical stability an optimum porosity with narrow and uniform pore size distribution is required to have better electrolyte uptake. The tortuosity is another important factor to prevent particulate or dendrite

penetration while maintaining higher Li ion conductivity. McMullin number (N_m) determines the electrolyte resistance in presence and absence of separator and is very much dependent on porosity and pore structure. The McMullin number, porosity and tortuosity are related according to the following equation:

$$N_m = \frac{\rho_s}{\rho_e} = \frac{\tau}{\epsilon}$$

where ρ_s = electrolyte resistances in the presence of separator, ρ_e = electrolyte resistances in absence of a separator, τ = tortuosity and ϵ = porosity of the separator. From the equation, it can be said that higher porosity and lower tortuosity yield a low N_m and a high ionic conductivity.

The separator material should have high affinity to the liquid electrolyte. The electrolyte should completely wet the inner surface of the pores and fill the void space of pores completely [220]. However, as the polymeric separator materials are non-polar and electrolyte solvents are polar, so there is always a wettability problem between separator and electrolyte. Many researches are going on to improve the wettability of the separator material [11, 221-223].

The present day demand for higher energy density along with high power output have motivated researchers to improve the chemistry of Li-ion battery. But with increase in energy and power density several other problems associated with stability and safety have also been increased. Much efforts have been put together to solve these problems in recent times [34, 224-226].

IV. Homogenizing current distribution

Li-ion battery separator plays a salient role in distributing the current homogeneously across the electrodes. This is especially needed for the battery operating at high current rate. Inhomogeneous

distribution of current increase the localized current density on the electrode. This is particularly detrimental in anode side where this localized inhomogeneity enhances the Li dendrite formation resulting safety issues [11, 13].

V. Dendrite suppression

Lithium dendrite is a standard problem for Li-ion battery. This problem is more severe when Li metal is utilized as anode material and this has prevented the use of metallic lithium as anode material in commercial Li-metal battery. This problem is also prevalent for carbonaceous anode materials when operating at high current rate, high state of charge and lower temperature. This dendrite formation significantly reduces the capacity and poses the threat for short-circuiting when these dendrites grow enough to penetrate the separator [227-229]. In recent days research has again been started on Li anode material as this material largely contribute to high energy density battery [230]. The researches on Li metal anode are focussed on to decrease or eliminate the chances of dendrite formation or its growth [231].

VI. Facilitating Li-ion transport

The Li ion movement through the separator largely depends on the pore structure, i.e., overall porosity, pore shape and size, pore size distribution and tortuosity. Along with that the polarity and surface charge are also important to have better contact between electrolyte and pore surface. This would also increase the electrolyte uptake. The commonly used organic solvent based electrolyte is polar while the polymer based separators are nonpolar or having lower polarity. This has eventually reduced the interaction between separator and electrolyte, lowering Li ion movements through the pores of separator and this is the main reason for poor wettability. To

mitigate these problems, researchers proposed the modified separators with surface charge or attached with polar functional groups [232-234].

VII. Separator for special applications

The ion selective separator is needed for some special cases. This is particularly important for Li-S battery as well as for some other advanced batteries where polysulphide diffusion and moisture/O₂ penetration are highly detrimental in lowering electrochemical performance of the battery in terms of the cyclability, coulombic efficiency and self-discharging tendency [21]. Different working mechanisms have been proposed for this type of ion selective separators [235-237]. The spinel type cathode materials in Li-ion battery can cause transition metal dissolution in electrolyte solution and HF generation when operating at high voltage and at comparatively higher temperature resulting capacity loss. Many functional separators have been investigated to address these issues and proved to be successful to some extent to scavenge the dissolved transition metals (particularly Mn^{x+}) and also the HF molecules resulting increase in stability of Li-ion battery using such cathode materials [238-242]. In Li-ion battery, separator is an insulating material so that it should not conduct electrons but only Li ions. But in some cases, particularly in Li-S battery during poly-sulphides dissolution, it is advantageous to apply a conductive coating on the separator. so that it can provide an extra stage of electron transfer to the external circuit thus increase the stability of the battery [243-245].

VIII. Heat management

The operating temperature of Li-ion battery has a considerable effect on its electrochemical performance, stability as well as safety of Li-ion battery. Moreover, the battery mechanisms such

as Li ion movement, intercalation/deintercalation etc. also generates significant heat inside the battery particularly when operating at high rate. Another major factor is separator, which due to its low thermal conductivity limiting the heat dissipation or equal heat distribution within the battery. Thermal shutdown, which is an inbuilt function of the separator can mitigate this problem to an extent by blocking the pores of the separator at higher temperature (close to its melting point) thus preventing short circuiting. However, many advanced technologies have come up to address this heat management issues of Li-ion battery, particularly for electric vehicle application [246, 247]. Many advanced researches have been performed on separator materials to solve these thermal problems using various strategies such as thermal shutdown, flame retarding [248, 249], fire extinguishing [250] and heat dissipating [247, 251], etc.

IX. Some other issues

In recent times, mechanically flexible Li-ion battery is of great importance for various applications where it can be used suitably in any complicated electronic devices. The research towards achieving this has suggested to eliminate the metallic electrode substrates (current collectors) and instead using a 3D flexible freestanding matrix for electrode active species for the both the electrodes or using separator as the substrate for both cathode and anode with an added electron transfer layer [252-257].

X. Redox-active separator

Although the separator is an insulating material, however, some redox active separator materials have also been investigated in recent times to increase the usage of active materials and to enhance the energy density. But attention to be given to the three dimensionally open porous redox active

part of the separator material so that it cannot block ionic movement while maintaining its insulating properties as well [258]. Many separators with some other functional properties along with its basic functions are also being researched on at present and this includes catalytic separators [259] and separators with short-circuit detection [260, 261] as well as overcharge protection capabilities [262-264].

2.8.4 Electrolyte

The electrolyte in Li-ion battery cell acts as a vehicle for Li ion movements between the electrodes while resisting electronic conduction between cathode and anode.

A typical electrolyte of a Li-ion battery should fulfil the following major requirements [35, 91]:

- a) The ionic conductivity of the electrolyte should be high ($\sigma_i > 10^{-3} \text{ Scm}^{-1}$) so as to minimize the cell impedance
- b) The electronic conductivity should be low or negligible so as to avoid electrical short circuiting and to maintain the fundamental purpose of the battery
- c) The electrolyte should be stable at cell operating voltage and also at higher temperature
- d) Chemically the electrolyte should be unreactive to other cell components, particularly cathode, anode and separator so as to avoid any side reactions while at the same time electrolyte should be compatible to all the cell components.

In broader perspective, electrolyte can be put into three major groups. This includes liquid electrolyte (all liquid state), solid electrolyte (all solid state) and polymer electrolyte [265]. The solution of inorganic salts in organic solvents produces the liquid electrolyte. A variety of inorganic lithium salt and organic solvent combination has been investigated over the past two decades. One

of the lithium salts is LiClO₄ which possess higher ionic conductivity with broader electrochemical stability (up to 5.1V) while keeping the interfacial resistance at low [266, 267]. However, LiClO₄ has some disadvantages too. The perchlorate anion is a strong oxidant and thus have tendency to react with electrolyte at higher operating voltage and or at higher temperature [268]. Another lithium salt LiBF₄ possesses moderate ionic conductivity and also comparatively safer than LiClO₄ but lack in cycling efficiency [269]. LiPF₆ is the most suitable lithium salt having all the prerequisite to be used as solvent for electrolyte produces higher ionic conductivity (10⁻³ Scm⁻¹), higher transference number (~ 0.35) for Li ions movement and also safe. However, the only disadvantage of LiPF₆ is that it breaks down to LiF and PF₅ at higher temperature [71, 270, 271]. A new lithium salt, lithium bis(oxalate) borate (LiBOB) has been investigated and found to have required potentials such as higher conductivity, resistant to hydrolysis and also inexpensive [272-274]. **Table 6** shows the Li based inorganic salts used in electrolyte of Li-ion battery.

Table 6: Common Lithium Salts and Their Properties [270]

Conducting salt	E_{ox} V vs. Li/Li ⁺	Advantage	Disadvantage
LiPF ₆	6.8	Standard conducting salt Most balanced properties	Thermally unstable Form highly toxic HF with moisture
LiClO ₄	6.1	Economical High ionic stability	Explosive Impractical for industry purpose
LiBF ₄	6.6	Less toxic Good electrochemical properties	Hydrolysis Moderate ion conductivity Thermally unstable

The liquid solvents for the above discussed lithium salts are required to ensure some major prerequisites to be able to act as a solvent. This organic liquid first of all must be inert as well as compatible to all cell components which comes in contact with it, high dielectric constant, low viscosity, low melting temperature, high vapour pressure thus high boiling point, high solubility

to lithium salts. Finally, the solvent should be safe and inexpensive. Although, many organic carbonate based solvents such as ethylene and diethylene carbonate (EC and DEC), propylene carbonate (PC) and dimethyl carbonate (DMC) can satisfy many of the properties as stated above still they have their own shortcomings too. Therefore, a mixture of different solvents maintaining a proper ratio is considered to be the ideal. Although liquid electrolyte is the most favoured choice for Li-ion battery but still it has a major safety issue as it is flammable at higher temperature and outside its operating voltage range.

Another group of electrolytes is polymer electrolyte. The various types of Polymer electrolytes include Classical liquid electrolytes, Dry single-ion-conducting polymer electrolytes, Gel electrolytes and Dry polymer electrolytes [275]. The major advantage of such type of electrolyte is that it can be designed at any shape size and pattern along with these electrolytes are comparatively less flammable and inexpensive.

The major advantages of solid electrolytes are all solid state material thus possesses higher safety and also not toxic. There are two types of solid electrolytes so far reported, which includes crystal based electrolytes and non-crystalline electrolytes [276]. Lithium superionic conductor (LiSICON) having general composition $\text{Li}_{16-2x}\text{D}_x(\text{TO}_4)_4$ (where D is bi-valent cation and T is a tetra-valent cation) is one of the crystalline electrolytes used in Li-ion battery. $\text{Li}_{14}\text{ZnGe}_4\text{O}_{16}$ in this family shows the ionic conductivity of $1.0 \times 10^{-7} \text{ Scm}^{-1}$ at room temperature [277]. Another crystalline electrolyte is $\text{Li}_7\text{La}_3\text{Zr}_2\text{O}_{12}$. This has a Garnet-type structure which possesses a Li ion conductivity of $\sim 2.1 \times 10^{-4} \text{ Scm}^{-1}$ at ambient temperature [278]. Sodium superionic conductor (NaSICON) having general composition $\text{A}_x\text{M}_2(\text{XO}_4)_3$, and $\text{Li}_{1+x}\text{Al}_x\text{Ti}_{2-x}(\text{PO}_4)_3$ ($x = 0.3$) is another crystalline

electrolyte used in Li-ion battery shows the ionic conductivity of $7 \times 10^{-4} \text{ Scm}^{-1}$ at ambient temperature [279].

So far used non-crystalline electrolytes is $50\text{Li}_2\text{S}-17\text{P}_2\text{S}_5-33\text{LiBH}$ [280] and composite glass-ceramic based electrolyte is $70\text{Li}_2\text{S} \cdot 30\text{P}_2\text{S}_5$ [281]. The lower Li ion conductivity at ambient temperature and higher electrode-electrolyte interface resistance resulting higher cell impedance are the major challenges for these types of solid electrolytes.

The conventional liquid electrolytes used in Li-ion battery demands high dissolution of lithium salts in the solvent while still maintaining the low viscosity. As these two requirements simultaneously are seemingly contradicting so combination of various electrolytes is used for practical applications to obtain the positive effect of different electrolyte materials [25]. The electrolyte used in Li-S battery provide a medium for various activities during discharge such as polysulphide dissolution, oxidation-reduction and crystallization. Some researchers have shown tetrahydrofuran based electrolytes to address all these issues [282], cyclic ethers are also commonly used, usually employing the lithium bis(trifluoromethanesulfonyl)imide (LiTFSI) salt [283].

Some ionic liquids have also proved themselves as potential electrolytes for Li-ion batteries. These liquids exhibit lower vapour pressure, higher ionic conductivity and thermal stability. However, they show lower solubility of polysulphide in Li-S battery resulting reduction in polysulfide redox shuttle [284]. In Li-S battery the cation structure is modified from the standpoint of design aspects, while anions typically remain unchanged as in Li^+ salts [285]. The most common

ionic liquid is [TFSI]. This as electrolyte facilitates the formation of an effective and stable SEI on the negative electrode material [286]. Ionic liquid can be used alone or in combination with other liquid electrolytes to adjust the desired properties [287].

2.9 Future Batteries

The developments of future batteries are based on to simultaneously improve the energy density as well as power density for the application in the area of electric vehicle. **Table 7** depicts the next generation batteries with their theoretical capacities.

The future research has been focussed on to improve mainly the cathode materials. Sulphur is found to be one of the potential positive electrode materials and can have the capacity to increase the energy density as high as 10 times more than that of usual Li-ion batteries. The other merits of sulphur are as it is inexpensive, abundantly available and also environment friendly [288, 289]. However, the sulphur based batteries have some challenging disadvantages lower Coulombic efficiency, poor cyclability and chances of utilising lower active material [290], lithium sulphide cathode fabricated with poly-(vinylpyrrolidone) binder is proved to be a better option as cathode material for improved cycling stability [291].

Table 7: Performance Comparison of Future Battery Systems [292]

Battery type	Voltage (V)	Theoretical capacity (mAh g ⁻¹)	Theoretical specific energy (Wh kg ⁻¹)
Conventional Li-ion	3.80	155	387
Li-S	2.20	1672	2567
Li-Air (Non-aqueous)	3.00	3862	11248
Al-Air	2.70	2980	8100
Zn-Air	1.65	820	1086

On the other side, silicon as anode material has emerged as a strong contender for carbon based anode material in Li-ion battery. However, the problems related to larger volume change and an unstable material growth on silicon-electrolyte interface is required to be overcome for this Si based material [293, 294]. Another recent advancement is to use polymer hydrogel as a conducting material with porous silicon-based negative electrode active material to improve its electronic conductivity [295]. With very high theoretical capacity, Li-Air battery is having high potential to be used as future generation battery. This type of battery was first reported in 1996. Li-Air battery is almost comparable to that of gasoline [296]. However, this type of batteries has many challenges, like reversible Li insertion and deinsertion, that are required to overcome [297]. Along with the development of new cathode and anode materials for battery technology another major area of research is nano-technology to improve the materials performance. Using nano-materials battery performance can be improved a lot in various ways thus increasing the interfacial surface area between cathode-electrolyte, electrolyte-anode and electrolyte-separator. The nanomaterials also decrease the Li ion diffusion path [192]. The only issues with nanomaterial are low packing density and lower energy efficiency. However, these issues are need to be addressed before making it a commercially viable option.

CHAPTER 3

MATERIAL AND METHODS

CHAPTER 3

MATERIAL AND METHODS

3.1 Objective of This Thesis Work

In this thesis work we have primarily investigated two major areas of Lithium-ion batteries, namely cathode materials and separator. In last two decades, major research has been focussed on these two components.

3.1.1 Cathode Material

Importance of cathode materials: Cathode materials determine the operating voltage and specific capacity of the Li-ion battery. Capacity is dependent on the number of extractable lithium from cathode during charge. Voltage is dependent on the reduction-oxidation potential of transition metal element. The combined effect of voltage and capacity determines the energy density and power density of the cell. The relevance of these two areas is explained below.

Requirements of cathode materials: Cathode materials should contain at least one transition metal ion (readily reducible/oxidizable) which determines the cell voltage. It should interact with lithium containing material in a reversible manner. The host structure should not change during addition/removal of lithium and should react with lithium during insertion/deinsertion with a high free energy of reaction thus producing high capacity. This leads to high energy storage. It should also react with lithium very rapidly both during insertion and removal which leads to high power density. Along with that cathode materials should be a good electronic conductor and should be stable structurally otherwise it will degrade during over discharge /over overcharge. It should be low in cost and environmentally benign.

Challenges and approaches to develop cathode materials: In Li-ion battery, the negative electrode material is well developed and little advancement can be made in terms of design aspects. The cathode, however shows a great prospect for further enhancement. Battery research is therefore concentrating on the cathode materials. For utilization in hybrid electric vehicle (HEV) system, Li-ion battery needs to overcome major two challenges, i.e., high energy density at the same time high power density. A high energy density can be obtained by choosing a high voltage cathode material with high capacity. Olivine structured based cathode material LiMPO_4 is having high operating voltage around (4.1 - 5.1 V) and a maximum theoretical capacity ($\sim 170 \text{ mAhg}^{-1}$). Compared to many commercialized compounds, this material can provide higher specific energy, which is $> 850 \text{ Whkg}^{-1}$.

Motivation (Why LiMPO_4 ?): Development of advanced Lithium-ion battery to meet the emerging high performance demand mainly requires cathodes containing transition elements with higher redox potentials. In this work a high energy LIB with high voltage cathode material is prepared based on olivine structured cathode material having general formula LiMPO_4 ($M = \text{Fe, Mn, Co \& Ni}$). Phosphates can provide higher voltages than oxides of same transition metal with similar thermal stability. In (PO_4^{3-}) polyanion, the strong P–O covalent bond stabilize the oxygen in fully charged MPO_4 state thus making LiMPO_4 electrochemically excellent, thermodynamically stable, and electrically safe material. The strong covalent bond in polyanion making $M^{2+/3+}$ redox energy lower and V_{oc} vs. lithium higher for that couple. The theoretical redox potential of LiFePO_4 , LiMnPO_4 , LiCoPO_4 and LiNiPO_4 are 3.5 V, 4.1 V, 4.8 V, and 5.1 V respectively and the corresponding specific energies are 578, 697, 816 and 867 Whkg^{-1} respectively.

Key challenges of the materials: The key challenges of LiMnPO_4 material are low ionic diffusivity, Low electronic conductivity, anisotropic movement of Li ions within the materials [010] direction, instability of the fully de-lithiated phase (i.e., MPO_4 & MVO_4), Jahn Teller effect (LiMnPO_4) and large volume mismatch between the phases with (lithiated) and without (delithiated).

Approaches to meet the challenges: To overcome the above challenges the following strategies have been thought to be followed. (1) The growth of nano-sized material with desired morphology to decrease the Li^+ ion migration path and increase the Li^+ ion diffusivity. (2) Increasing ionic diffusivity and electronic conductivity by suitable addition of dopants in cation as well as anion sites. (3) Increasing inter-particle conductivity of the cathode materials by increasing the ratio of graphitic vs. amorphous carbon with suitable synthesis procedure. (4) Synthesis of $\text{Li}_y\text{MPO}_4\text{X}$ [$\text{X} = \text{S, F, N}$ etc., $y > 1$] to increase the specific capacity and also to make isotropic Li^+ ion diffusivity. (5) Increasing capacity by increasing the ratio of Mn^{2+} vs. Mn^{3+} with suitable synthesis procedure and (6) Increasing energy density of Lithium-ion battery either by improving voltage or increasing capacity (or both).

3.1.2 Separator

Improving the electrochemical performance of the separator is another important issue. Various strategies have been followed to improve the performance of separator. A simpler strategy is to coat the polyolefin membranes with suitable nanostructure ceramic oxides [298-300]. The coated ceramic layers composed of close-packed nanoparticles with a well-developed interconnected porous structure may significantly affect the separator properties by playing a substantial role in

enhancing the mechanical and thermal stability along with improving electrical properties of the separator without directly taking part in lithium-ion conductivity or diffusivity.

In this respect, boehmite (γ -AlO.OH), which is a light weight, non-toxic and low-cost material, could be a suitable coating material. It has a favourable layered structure composed of AlO₆ octahedra and more importantly, it possesses a large number of -OH functional groups on the surface [301-303]. Besides, it is a well-known flame retarding material [304-306]. In fact, boehmite is widely used in several industrial applications such as catalysis, adsorbent, filler in plastic etc. Additionally, this material is having other advantages which include its better dispersity in aqueous slurries which would facilitate uniform coating on the polymer membrane.

However, till now, there is only a handful of reported work on boehmite coated polyolefin separators [307-310]. Yang et al. have reported improvement in both wettability and thermal stability of polyethylene (PE) membranes coated with boehmite [309]. Zhong et al. have used electrospinning technique to coat boehmite on polyimide (PI) membrane and observed an improvement in electrochemical stability as well as in Li-ion conductivity [310]. The effect of boehmite particle size on dimensional stability of coated polypropylene separator and its electrochemical performance are investigated by Xu et al. [308]. In the present work, we have synthesized boehmite (γ -AlO.OH) nanofibers (length 90-140 nm; dia. ~15 nm) by a simple low-temperature (180 °C) hydrothermal method and coated onto both sides of surface modified polypropylene (Celgard). The prepared composite separator has been tested in LiFePO₄//Li half cells as well as in LiFePO₄//MCMB full cells in coin cell configuration for understanding the influence of this separator on electrochemical performance.

3.2 Cathode Materials Synthesis and Characterization

3.2.1 Synthesis of Lanthanum doped Lithium Manganese Phosphate Cathode Materials:

Solvothermal method was used for preparing the cathode materials. The stoichiometric ratios of Lithium sulphate ($\text{Li}_2\text{SO}_4 \cdot \text{H}_2\text{O}$), Ammonium dihydrogen phosphate ($\text{NH}_4\text{H}_2\text{PO}_4$), Manganese sulphate ($\text{MnSO}_4 \cdot \text{H}_2\text{O}$) and lanthanum nitrate ($\text{La}(\text{NO}_3)_3 \cdot 6\text{H}_2\text{O}$) are the major raw materials used along with Sucrose ($\text{C}_{12}\text{H}_{22}\text{O}_{11}$) for in-situ carbon deposition. The solvent used is Glycerol : Water (2:1) ratio. The pH is maintained by adding required amount of NH_4OH in the solution. The solution is kept in the Autoclave at 180°C for 24h. After taking out from the autoclave the solution is centrifuged and washed till it becomes neutral with water and IPA. Then the neutral solution kept for drying initially under IR lamp and finally in an oven for overnight at 80°C . The slurry for casting cathode materials on aluminium foil is prepared by maintaining the Active material: Active carbon: PvdF in 80:10:10 ratios in NMP solvent and then casting using Doctor's blade and drying it in oven at 110°C and finally calendaring at 80°C .

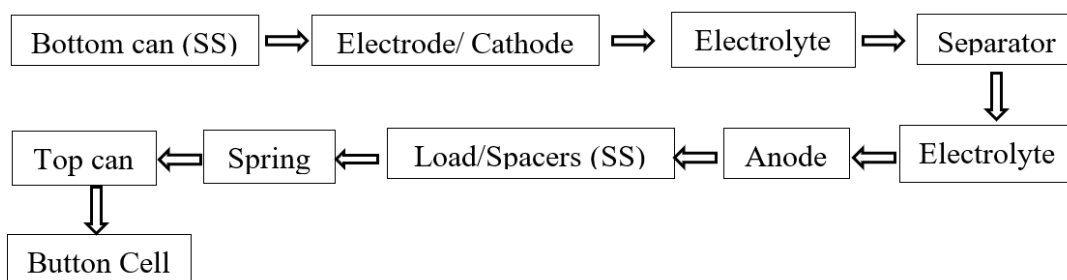
3.2.2 Structural Characterization: The properties of the materials related to the structure is measured by X-ray Powder Diffraction (XRD) followed by Rietveld refinement, Fourier Transform Infra-Red Spectroscopy (FTIR), Raman Spectroscopy etc.

3.2.3 Microstructure and Morphology: The microstructural information as well as morphology of the as synthesized materials is investigated by Scanning Electron Microscopy (SEM) and Field Emission Scanning Electron Microscopy (FESEM) as well as Transmission Electron Microscopy (TEM) along with surface area measurement.

3.2.4 Fabrication of LIB Coin Cell and Electrochemical Tests

3.2.4.1 Cell Fabrication: For studying the electrochemical properties, 2032 type coin cells are fabricated using lithium metal disc as the counter electrode, LiPF_6 dissolved in EC:DMC (1:2 by vol.) as electrolyte and commercial Celgard 2300 as the separator. (EC – Ethylene carbonate; DMC – Dimethyl carbonate) The cell is assembled in the globe box where the gaseous atmosphere can be precisely controlled.

The button cell fabrication is done in Argon filled Glove box following the steps:



3.2.4.2 Electrochemical Measurements: Cyclic voltametry, galvanostatic charge discharge and AC impedance spectroscopy is carried out to study the electrochemical performance of the cells. The energy as well as power density of the lithium-ion single cell are also evaluated. The detailed electrochemical reaction mechanism is investigated. Finally, the analysis of all the results and their correlation are made for evaluating the suitability of the materials in rechargeable energy storage devices in real condition.

3.3 Separator Materials Synthesis and Characterization

3.3.1 Synthesis of $\gamma\text{-AlO.OH}$

AlO.OH nanofibers were synthesized by hydrothermal method in slightly acidic medium. The precursors, $\text{Al}(\text{NO}_3)_3 \cdot 9\text{H}_2\text{O}$ (99%, Sigma-Aldrich) and citric acid (GR grade, Merck India) were

dissolved in de-ionised water under constant stirring and transferred into a 100 ml Teflon coated stainless steel autoclave. The SS autoclave is heated at 180°C for 24 hours under autogenously developed pressure. After completing the procedure in autoclave, the resulting precipitate was centrifuged, washed repeatedly with de-ionised water and then dried at 80°C for 12 h in vacuum to obtain white powder of γ -AlO.OH.

3.3.2. Preparation of γ -AlO.OH Coated PP (ALO-PP) Separator, LiFePO₄ Cathode and MCMB Anode

γ -AlO.OH powder was thoroughly mixed with PVB (Polyvinyl butyral) as binder in 4:1 (wt/wt) ratio and subjected to ball milling for 12 h in isopropyl alcohol (solvent). The slurry, thus prepared was then applied onto both sides of the polypropylene (PP) film (chemically etched and washed; thickness ~19 μ m) using an Elcometer 3500 [USA] to develop the required coating. Several both side coated γ -AlO.OH/ PP films (named as ALO-PP) were prepared by varying the total thickness from 23 μ m to 45 μ m. Standard slurry casting method was used for preparing the LiFePO₄ cathode and MCMB anode. The mass loading of active electrode material is 2.8 mgcm⁻².

3.3.3. Materials Characterization

X-ray diffractometer (Philips X'Pert, The Netherlands) was used to obtain X-ray powder diffraction patterns of the synthesized material. A Cu-K α radiation at 40 kV and 40 mA was applied in the 2 θ range of 20-80°. The scanning rate was maintained at 1° min⁻¹. FTIR spectra in transmission mode were obtained by a BOMEN infrared spectrophotometer in the range between 4000-400 cm⁻¹. The morphology and microstructure of the prepared powder was investigated by ZEISS Supra35 (Germany) Field Emission Scanning Electron Microscope (FESEM). Operating

Tecnai G² 30ST (FEI) Transmission Electron Microscope at 300 kV, high resolution TEM images and selected area diffraction patterns are obtained. Quantachrome (USA) Autosorb Surface Analyzer was used to perform the nitrogen adsorption-desorption measurements and BET surface area measurements at 77.3K. Brunauer–Emmett–Teller (BET) method and Barret–Joyner–Halenda (BJH) method were used to measure the Specific surface area and pore size distribution respectively.

3.3.4. Electrochemical Characterization

Coin cells of 2032 type were fabricated with ALO-PP as separator in two different configurations using LiPF₆ dissolved in EC:DMC as electrolyte (1:2 by vol%) using an argon filled glove box (M'BRAUN, Germany). The oxygen level and moisture inside the globe box were controlled below 1.0 ppm. Configuration 1: LiFePO₄ cathode against Li/Li⁺ for half-cell configuration and Configuration 2: LiFePO₄ cathode against MCMB as anode for full cell configuration. For comparison, cells with uncoated polypropylene (PP) were also fabricated in all three configurations.

A galvanostat-potentiostat (PGSTAT 302N, Autolab, The Netherlands) was used to carry out cyclic voltammetry of the cells. This cyclic voltammetry was determined in-between 0.05 and 3.0V at a scanning rate of 0.1 mVs⁻¹. The galvanostatic charge-discharge measurement was performed using an automatic battery tester (BT2000, Arbin, USA) in the voltage range of 0.05-3.0 V. During initial formation cycle a constant current density of 0.05 mA cm⁻² was maintained. For subsequent cycle varying current densities in-between 0.05-1.0 mA cm⁻² were used. Constant current density was maintained during charging and discharging of the cells throughout one

experiment. The same galvanostat-potentiostat was used to record the electrochemical impedance spectra in the frequency range 10 mHz to 1 MHz with an AC amplitude of 10 mV.

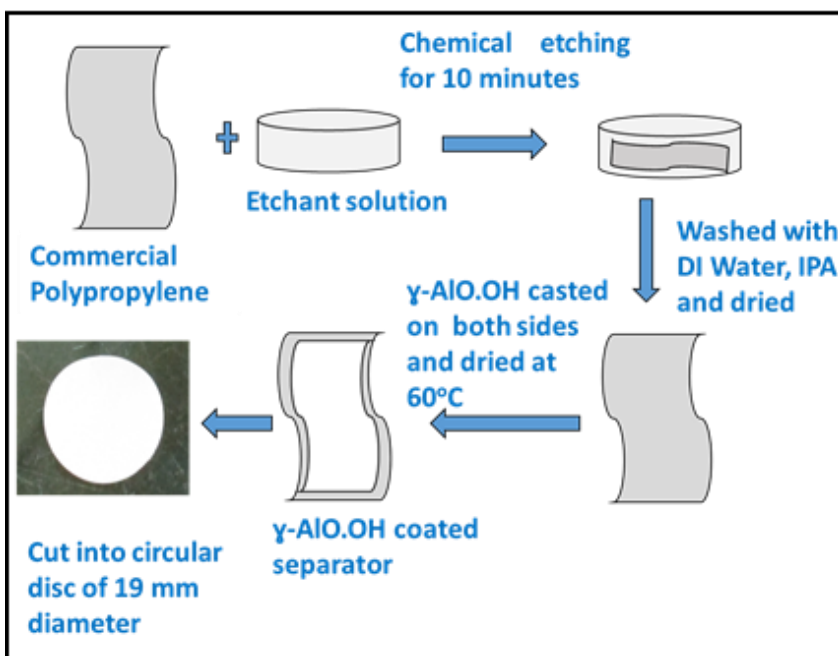


Figure 26. Schematic Representation of γ -AlO.OH Coated Separator Preparation

CHAPTER 4
RESULTS AND DISCUSSION

CHAPTER 4

RESULTS AND DISCUSSION

4.1 Cathode Materials:

The evolution of phases studied through XRD analysis at different pH conditions in the pH range 3.16-9.36 (**Figure 27a**). Optimized condition is found at pH 8.53 to maximize Mn^{2+}/Mn^{3+} ratio and phase pure olivine structure material is obtained. The phase purity is further supported by FTIR of the materials obtained at different pH condition (**Figure 27b**). The bands between $(950 - 1020) \text{ cm}^{-1}$ and between $(1050 - 1150) \text{ cm}^{-1}$ are due to symmetrical and asymmetrical stretching of PO_4^{3-} ions respectively. IR band between $450 - 650 \text{ cm}^{-1}$ are due to asymmetrical bending of O-P-O mode.

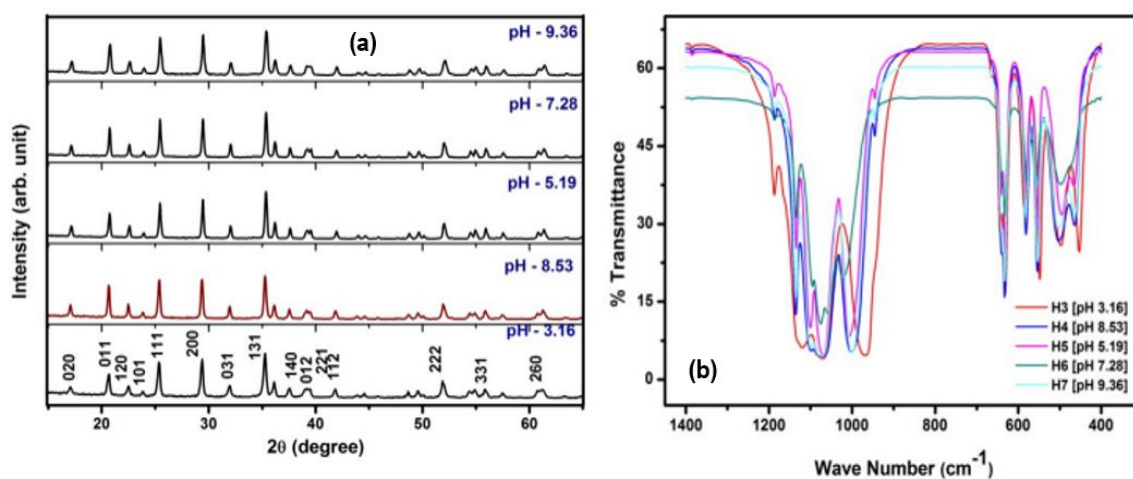


Figure 27. (a) X-ray Diffractogram and (b) FTIR Spectrum of Synthesized $LiMnPO_4$ at Different pH Condition

The optimization of carbon content for improved charge transfer has been obtained. Sucrose (up to 30 wt% of C) has been added for in-situ formation of conducting carbon. The 20% carbon containing sucrose corresponds to 8.77% of actual carbon is optimized (**Figure 28a**) based on the

maximum discharge capacity of LiMnPO_4/C material. The first peak at $\sim 375^\circ\text{C}$ corresponds to residual organics loss. The second peak is due to carbon loss. (**Figure 28b**)

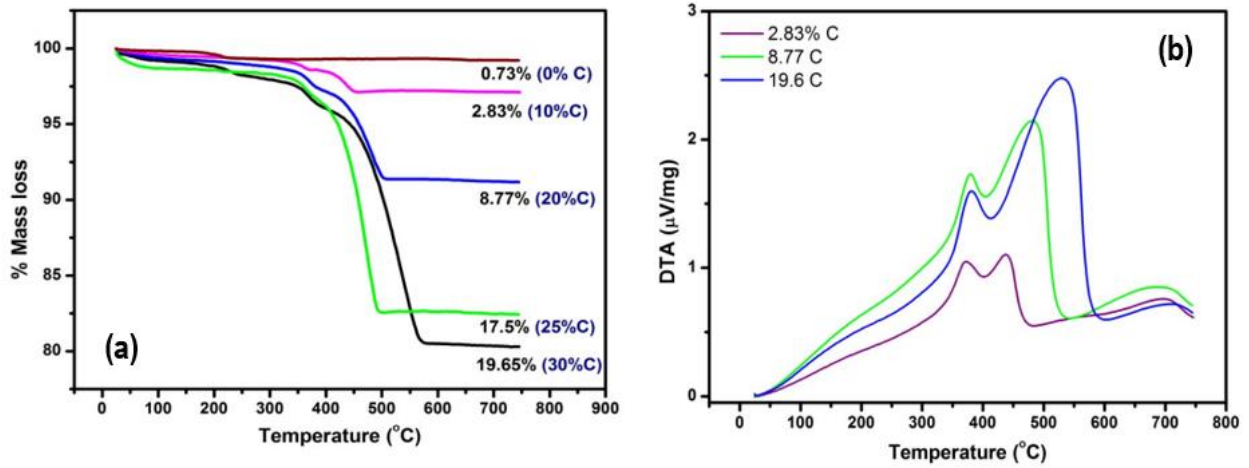


Figure 28. (a) TGA and (b) DTA of Synthesized LiMnPO_4 with Different Carbon Content

The phase purity is also maintained after in-situ carbon deposition on LiMnPO_4 powder particles produced after hydrothermal method. The XRD analysis after carbon deposition is also shown in **Figure 29**.

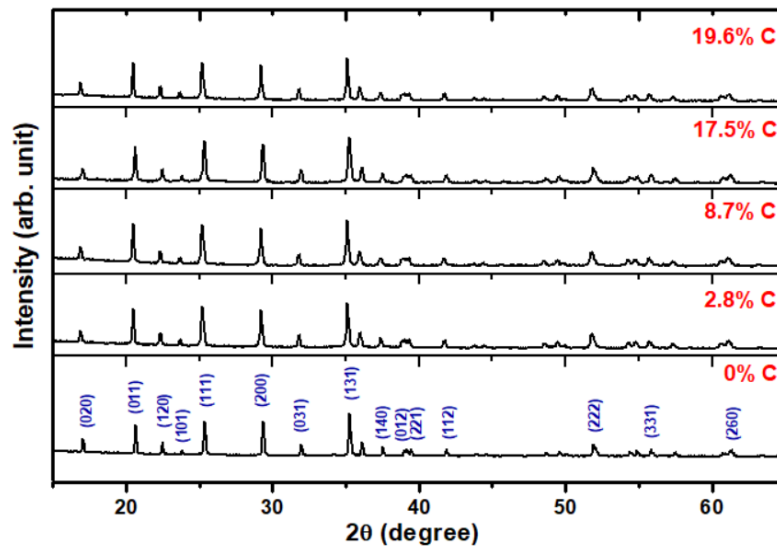


Figure 29. X-ray Diffractogram of LiMnPO_4/C Composite Produced by Hydrothermal Method

The electrochemical performance of LiMnPO_4/C has been studied with different carbon content. All the materials produced at optimized pH condition (8.53).

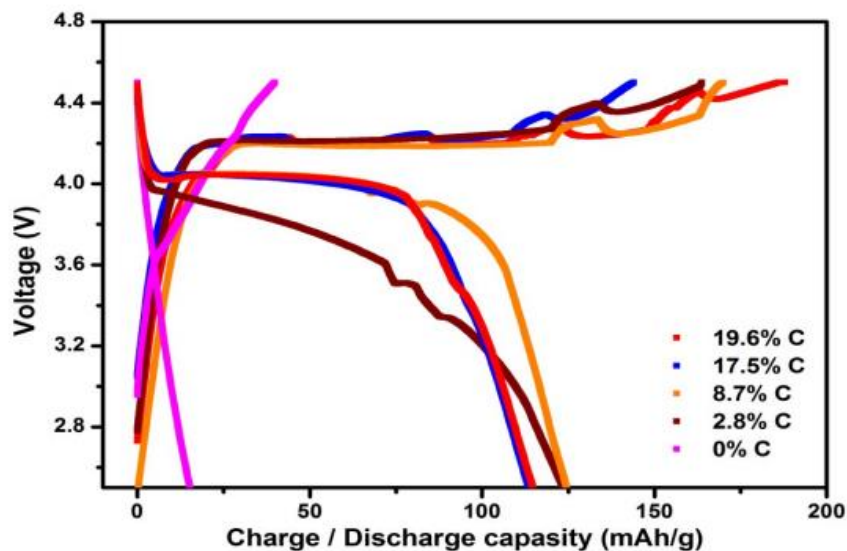


Figure 30. Electrochemical Charge Discharge Capacity of LiMnPO_4/C Composites

LiMnPO_4 without in-situ carbon shows a negligible capacity of $\sim 15 \text{ mAhg}^{-1}$. However, with increasing in-situ carbon content the capacity is increasing and become maximum ($\sim 124 \text{ mAhg}^{-1}$) at 8.7% C. Further increasing carbon decreases the capacity due to unnecessary increase of weight. The charge discharge reversibility is also much better in the material correspond to 8.7% in-situ carbon.

After optimizing the pH condition and in-situ carbon content of LiMnPO_4 , then Lanthanum doping has been done with the aim to enhance the electrochemical performance of the material.

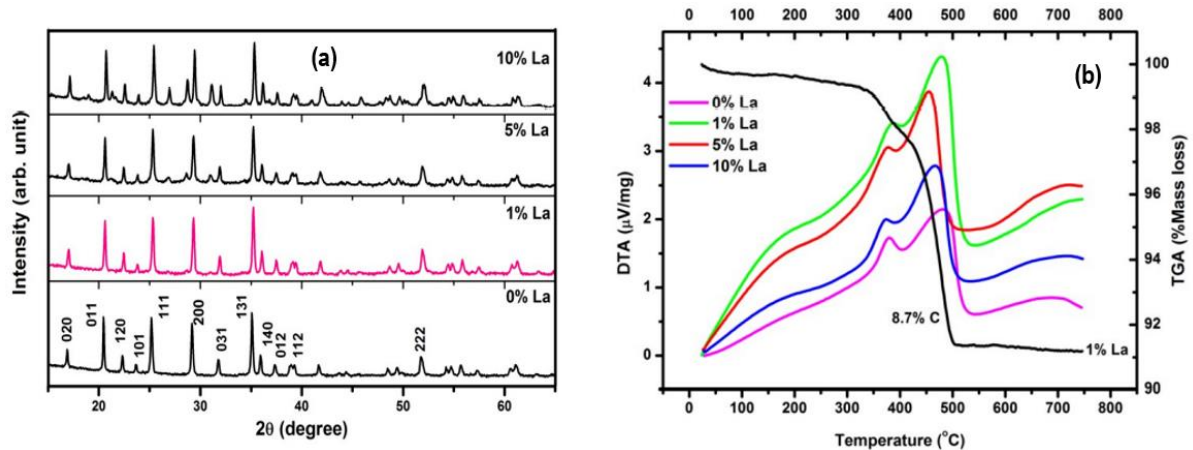


Figure 31. (a) X-ray Diffractogram and (b) DTA/TGA of Synthesized La-doped LiMnPO_4/C Composite

This has been observed that there is no phase change up to 1% doping of La. However, with increasing lanthanum percentage, in 5% and 10% of La doped materials, additional impurity phases appeared (**Figure 31a**). The change in weight loss corresponding to 1% La remains unchanged as without La. The thermal history with La is similar like without La also (**Figure 31b**).

The Structure of LiMnPO_4 after doping 1% La remain unchanged as without La and this has been supported by the Raman spectroscopy of LiMnPO_4 with and without lanthanum. (**Figure 32**)

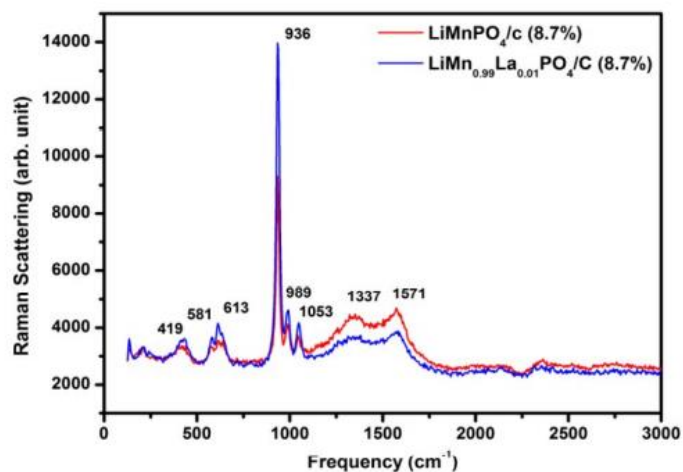


Figure 32. Structure of LiMnPO_4/C With and Without Lanthanum

Sharp peak at 936 cm^{-1} indicates PO_4^{3-} symmetric stretching mode. Raman band between $950 - 1100\text{ cm}^{-1}$ assigned to the PO_4^{3-} anti-symmetric stretching mode. Two sharp bands at 576 and 618 cm^{-1} are attributed to the out of plane bending modes of PO_4^{3-} units. Peak at 419 cm^{-1} assigned to the PO_4^{3-} bending modes. The peaks at 1337 and 1571 cm^{-1} indicates the amorphous and graphitic carbon.

The particle morphology of LiMnPO_4 with and without lanthanum has been studied by FESEM analysis. (**Figure 33**) Average particle size has been found to be $\sim 100\text{ nm}$ in both with and without La in LiMnPO_4 . No major change in particle shape after addition of La in LiMnPO_4/C is observed. Addition of La promotes inter particle diffusion leading to increased agglomeration, which in turn promotes better ionic and electronic conductivity within the cathode material.

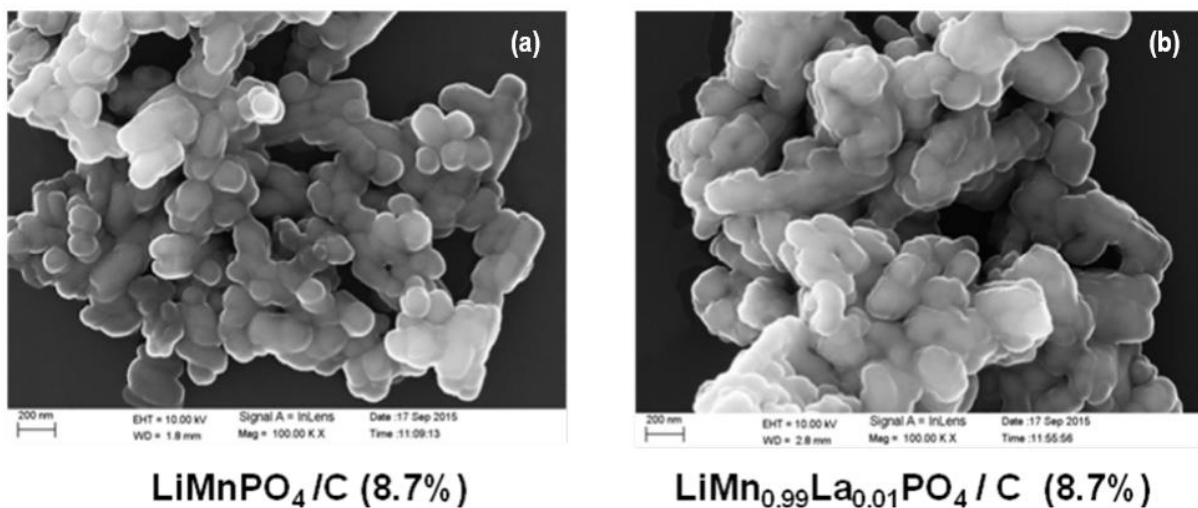


Figure 33. Particle Morphology of LiMnPO_4 (a) Without doping and (b) With 1% La

It has also been observed that after in-situ carbon optimization (8.7%) and after lanthanum doping (1%), there is no significant phase shift and that has been ascertained through X-ray diffractogram.

(Figure 34) This may be indicative of the fact that lanthanum has substituted manganese and does not go to interstitial position.

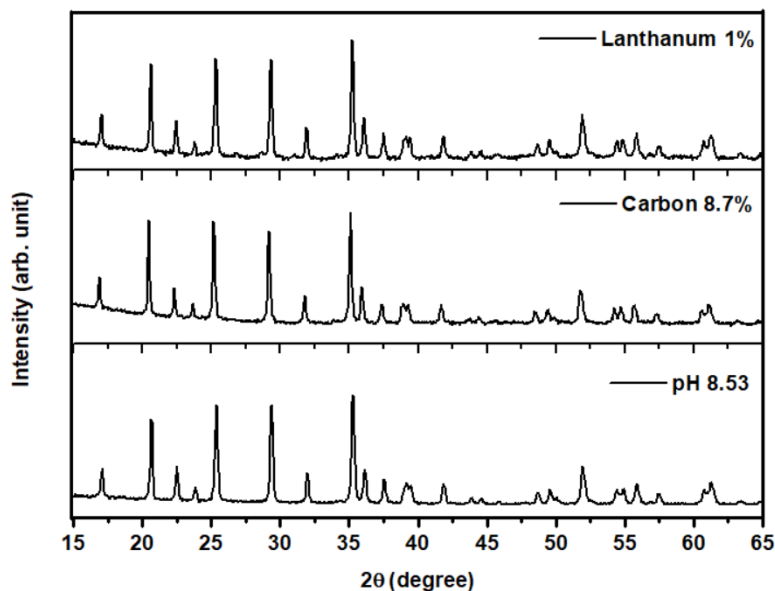


Figure 34. X-ray diffractogram of Synthesized LiMnPO₄ after In-Situ Carbon Deposition and Lanthanum Doping

The electrochemical performance has been studied after lanthanum doping. (Figure 35) It has been observed that lanthanum doping up to 1% increases the capacity to 129 mAhg⁻¹. However, with further increasing lanthanum concentration (5% and 10%) capacity decreases gradually. This may be because of increasing lanthanum content to a higher percentage, lanthanum goes in interstitial position instead of substituting Manganese or remains as free lanthanum oxide in the materials, which in turn reduces the capacity. The charge discharge voltage separation is decreased which improves the reversibility in 1% La in LiMnPO₄.

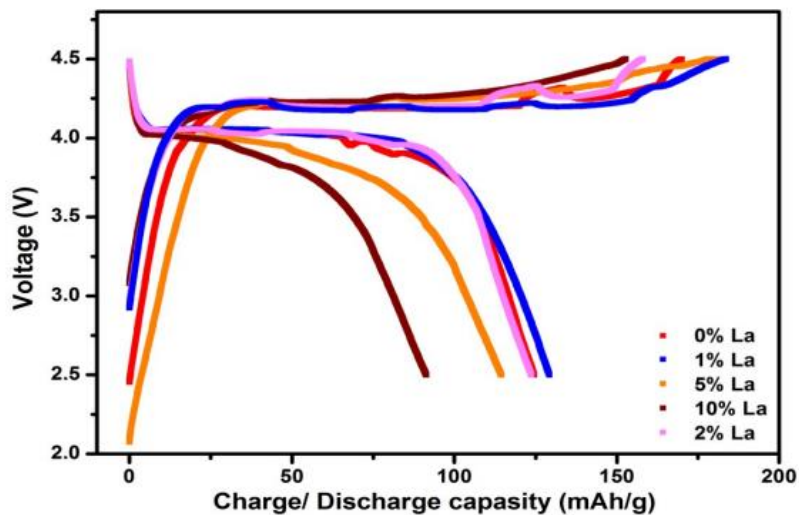


Figure 35. Electrochemical Charge Discharge Capacity of La-doped LiMnPO_4/C Composites

The electrochemical rate performance has been studied with varying C-rate in both with and without lanthanum doping to see the stability of the material (**Figure 36**).

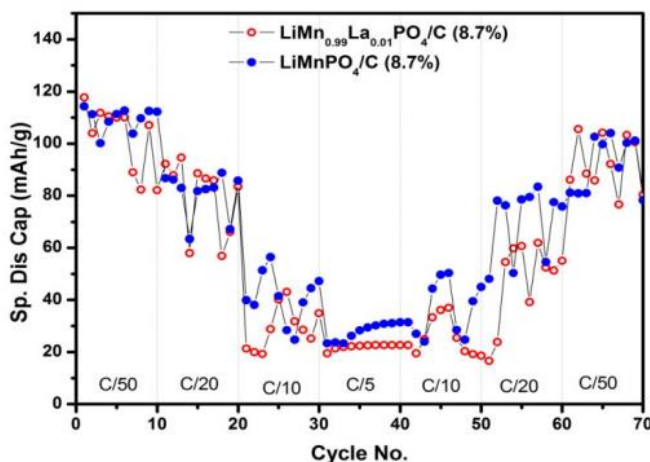


Figure 36. Electrochemical Rate Performance of LiMnPO_4/C Composites With and Without Lanthanum

This has been observed that both the material with and without lanthanum shows noticeable electrochemical stability, which in turn indicates the lithium-ion reversibility of cathode materials.

This has been also shown in studying coulombic efficiency. **(Figure 37b)** Moreover, it has been observed that at higher current (C/5), the capacity of lanthanum doped material is much more stable than that of without lanthanum.

The cyclability and coulombic efficiency have also been studied to see the performance degradation of the materials for both with and without lanthanum doping. **(Figure 37)**

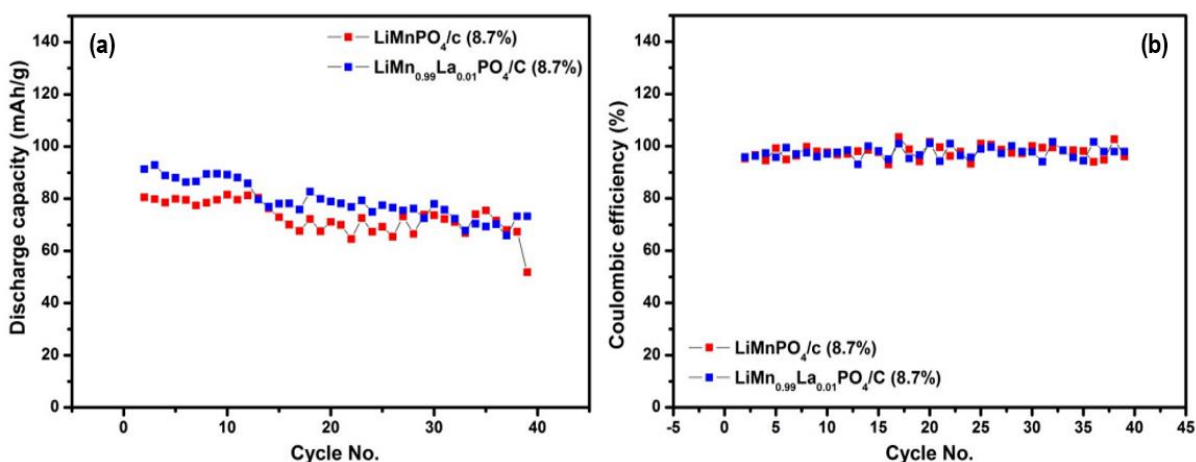


Figure 37. Electrochemical Performance of LiMnPO_4/C Composites (a) Cyclability and (b) Coulombic Efficiency With and Without Lanthanum

This has been observed that capacity degradation is not significant but rather stable in LiMnPO_4 material both in lanthanum doped and without doping materials. Moreover, capacity is better and more stable in lanthanum doped material compared to without lanthanum material with increasing cycle number. This has been also counter supported by coulombic efficiency measurement. It shows, both with and without lanthanum. The Coulombic efficiency is almost comparable between with and without La in LiMnPO_4 and excellent with increasing cycle number.

4.2 Separator

4.2.1 Structure and Morphology of Synthesized AlO.OH Powder

The X-ray diffractogram of the synthesized AlO.OH powder (**Figure 38a**) shows the characteristic peaks of γ -AlO.OH similar to previous reports [311-313] and could be indexed to an orthorhombic boehmite phase (JCPDS 21–1307). The calculated lattice parameters are $a = 2.875 \text{ \AA}$, $b = 12.215 \text{ \AA}$ and $c = 3.691 \text{ \AA}$. The average crystallite size measured by FWHM method of the (020), (120), (150) and (080) diffraction peaks by using the Scherrer equation, is found to be $\sim 13 \text{ nm}$ [314].

Formation of γ -AlO.OH is further supported by the results of FTIR studies. The spectrum, depicted in **Figure 38b**, shows all the characteristic adsorption bands of γ -AlO.OH. In the higher wavenumber region, there are two intense bands at 3300 and 3095 cm^{-1} , originated from ν_{as} AlO-H and ν_{s} (Al)O-H stretching vibrations respectively. In the mid wavenumber region, there appears a weak combination band at 1972 cm^{-1} and an strong band at 1069 cm^{-1} together with a shoulder at 1157 cm^{-1} which can be correlated to the δ_{s} Al-O-H and δ_{as} AlO-H bending vibrations. A weak band at 1635 cm^{-1} reflects the bending mode of adsorbed water. Three strong bands in the lower wavenumber region at 756 , 648 , 478 cm^{-1} are signatures of the vibration mode of AlO_6 . Therefore, FTIR results confirm and support the X-ray analysis of hydrothermally produced γ -AlO.OH powder as a pure-phase material [311, 313].

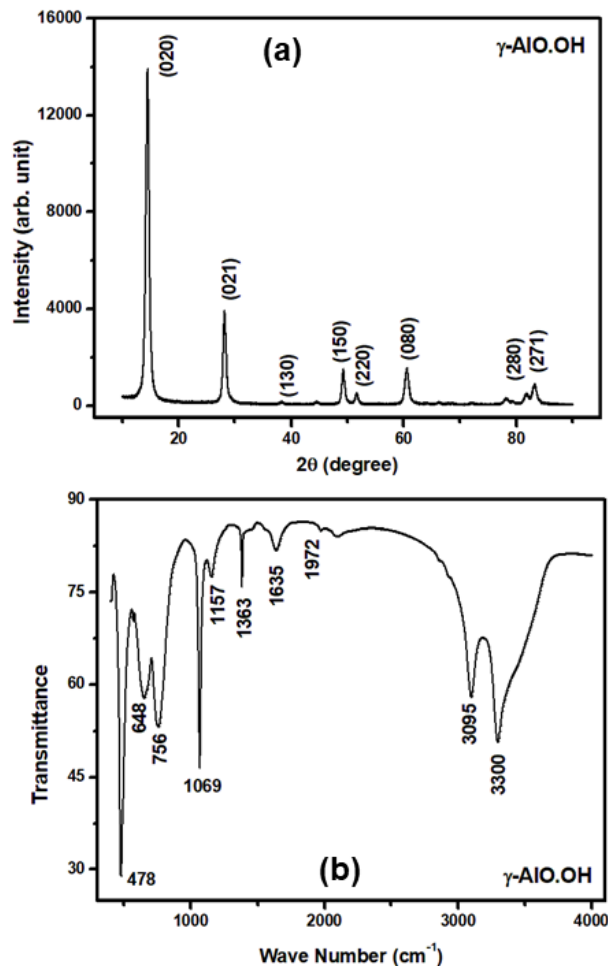


Figure 38. (a) X-ray Diffractogram and (b) FTIR Spectrum of Synthesized γ -AlO.OH Powders

The morphology and structure of the synthesized γ -AlO.OH have been studied by FESEM and TEM. The low magnification and high magnification FESEM images (**Figure 39 a and b**) depict a flaky morphology assembled in a flower like fashion. The constituent flakes are of approximately 2.0 μm in length and 0.15-0.78 μm in diameter. It is well known that the shape and morphology of hydrothermally synthesized AlO.OH may vary with reaction conditions. A somewhat similar morphology was observed by Tang et al. [313]. Rajaram and Kim studied the effect of pH, reaction time and hexadecyl trimethyl ammonium bromide (CTAB) concentration on the morphology of AlO.OH powder produced by hydrothermal method [311].

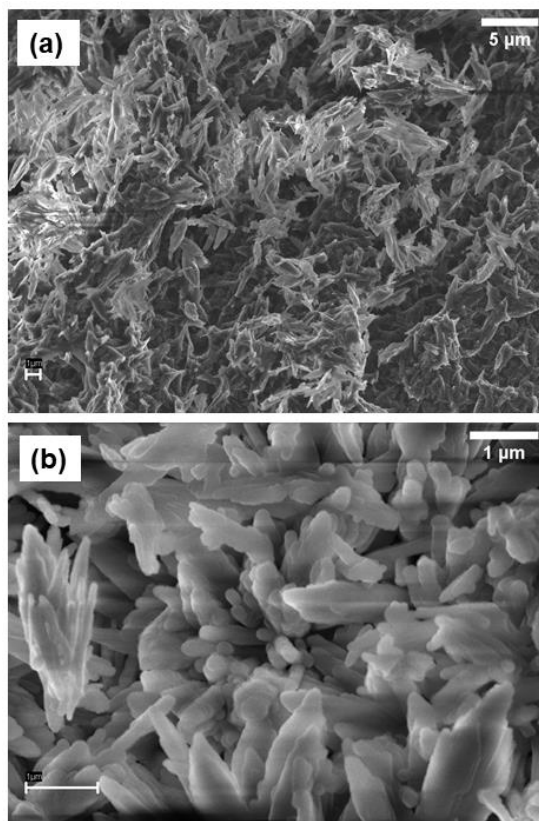


Figure 39. (a, b): FESEM Micrographs of Synthesized γ -AlO.OH Powder at Different Magnifications

To examine the microstructure further, TEM investigations have been undertaken. The bright field images, shown in **Figures 40 a and b**, clearly reveal formation of distinct elongated fibre shaped rods of γ -AlO.OH of 90-140 nm in length and around 15 nm in diameter. The HRTEM image along with appearance of bright diffraction spots in the SAD pattern, which then arranged in circular rings confirm formation of a well crystalline γ -AlO.OH phase (**Figures 40c and d**). The HRTEM image shows a lattice spacing of ~ 0.30 nm, which corresponds to the (120) and 0.152 corresponds to (080) plane of γ -AlO.OH. Santos et al. showed various shape and morphology of AlO.OH powder depending upon several aluminium hydroxide precursor materials using a single temperature for hydrothermal treatment [312].

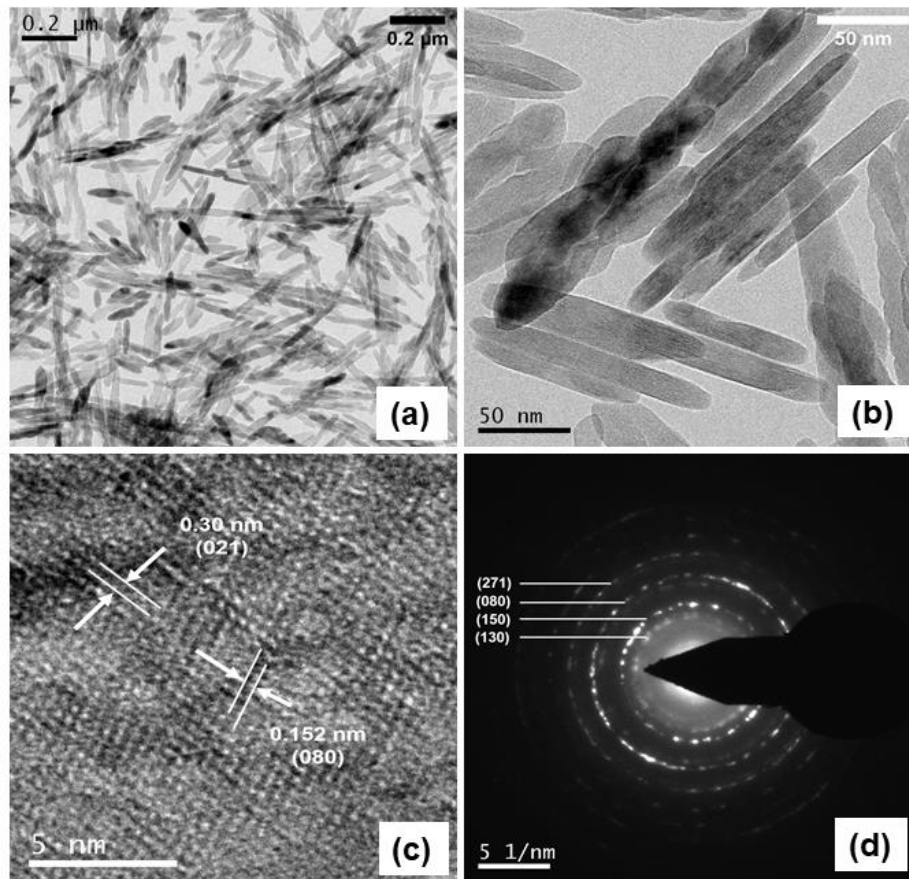


Figure 40. (a, b): Bright Field TEM Images; (c) High resolution TEM Image and (d) SAD Pattern of TEM of AlO.OH Powder

BET nitrogen adsorption-desorption isotherms for the synthesized AlO.OH powder is shown in **Figure 41**. The isotherms can be characterised as type IV with typical convex nature up to $P/P_0 = 1.0$. A prominent hysteresis loop starting from $P/P_0 = 0.8$ indicates mesoporous nature with coexistence of structural pores and inter-particle pores. The surface area is found to be $66.63 \text{ m}^2 \text{ gm}^{-1}$ with a pore volume of $0.319 \text{ cm}^3 \text{ gm}^{-1}$. Furthermore, their pore size distributions (**inset pattern of Figure 41**) show the flower-like architectures possessing a uniform and narrow pore size distribution centred at 3.694 nm for γ -AlO.OH. Tang et al. also shows higher surface area γ -AlO.OH produced by hydrothermal synthesis [313].

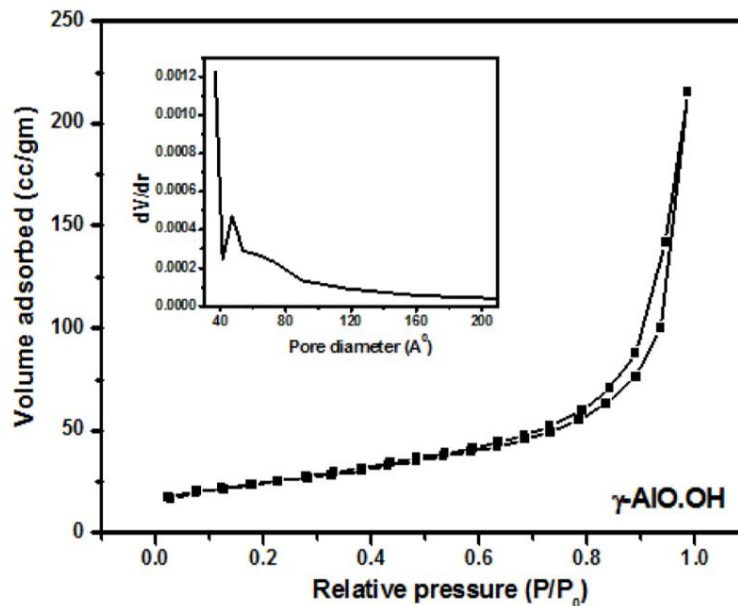


Figure 41. Adsorption-desorption Isotherms of γ -AlO.OH Powder along with its Pore Size Distribution

4.2.2 Structure and Morphology of γ -AlO.OH Coated PP (ALO-PP)

The effect of γ -AlO.OH coating on the surface of the PP is investigated by performing both FESEM and BET studies. A comparison of FESEM micrographs reveals that a homogeneous coating is obtained on top of PP though the original pores of PP appear to be somewhat blocked by the coated γ -AlO.OH layers. However, the BET adsorption-desorption isotherms reveal that both the membranes have a mesoporous character. As expected, the BET surface area of the coated film (ALO-PP) is decreased to $33.77 \text{ m}^2\text{g}^{-1}$ from $42.298 \text{ m}^2\text{g}^{-1}$ of PP. Correspondingly, the pore volume also decreases to $0.348 \text{ cm}^3\text{g}^{-1}$ (ALO-PP) from $0.540 \text{ cm}^3\text{g}^{-1}$ (PP). Interestingly, the mean pore diameter of ALO-PP (59.96 nm) is much higher than that of PP (33.85 nm). Similar reduction in surface area and pore volume is commonly observed for ceramic coated polyolefin membranes. For instance, Yang et al. have observed a lower porosity and narrower pore size distribution in AlO.OH particle coated PE membrane compared to pristine PE membrane [309].

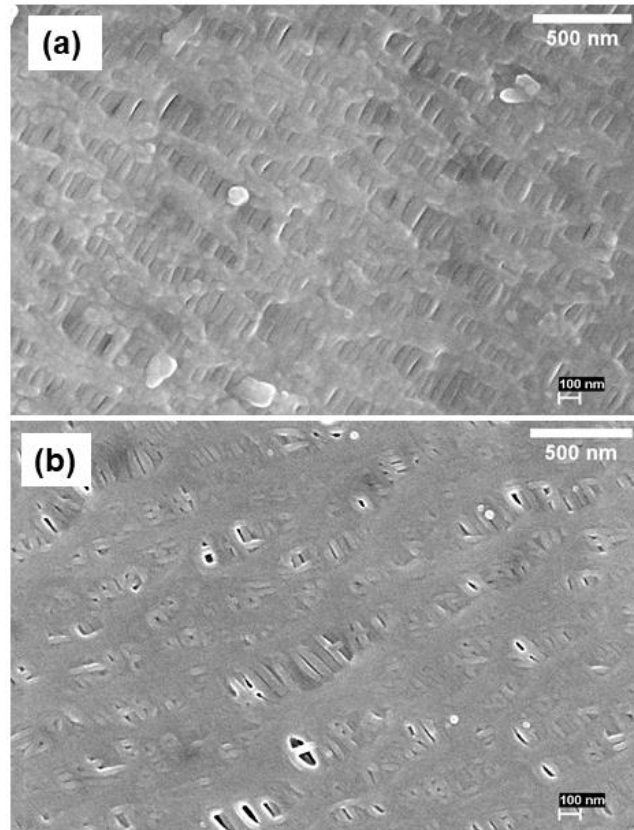


Figure 42. FESEM Micrographs of (a) PP and (b) ALO-PP-35

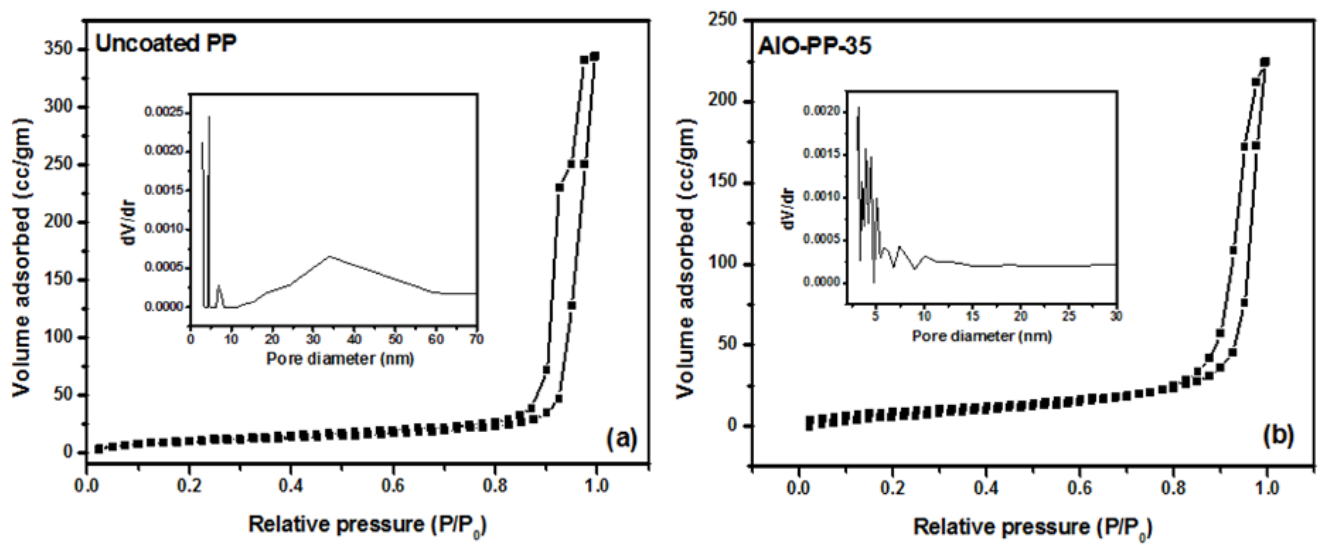


Figure 43. Adsorption-desorption Isotherms with Pore Size Distribution of (a) Uncoated PP and (b) ALO-PP-35

The AlO.OH powder so produced by hydrothermal process in our experiment and coated on the polypropylene sheet shows much lower pore diameter compared to the above referred work resulting increase in volume of electrolyte uptake.

4.2.3 Thermal, Chemical Stability and Electrolyte Up-take of γ -AlO.OH coated PP(AlO-PP)

The thermal stability is mainly important to prevent the thermal runaway of the separator when the internal temperature of the battery increases beyond a certain limit where, the separator starts to shrink and thus results in short circuiting between cathode and anode. The thermal stability studies show that AlO-PP-35 μm is stable at around 145°C, while PP starts degrading slowly from 80°C (**Figure 44a**). However, the substantial degradation of PP occurs only after 120°C. This is primarily due to the refractory nature of AlO.OH having high heat resistivity. The results also support formation of a uniform homogeneous coating. A similar kind of improvement in thermal stability has also been observed by Yang et al. for AlO.OH coated polyethylene membrane [309].

As shown in **Figure 44b**, the thermal stability increases with increasing thickness of coated γ -AlO.OH layer and the maximum stability of ~150°C is reached for a coating thickness of 45 μm . However, the increase is not linear; a coating thickness of ~ 35 μm is found to be optimum. Increasing the coating thickness further does not lead to significant gain in thermal stability; rather, it would be detrimental to the electrochemical performance of the cell due to unnecessary increase in weight of the separator. A similar kind of thermal stability has also been shown by Yang et al. by putting the AlO.OH coating on polyethylene membrane [309].

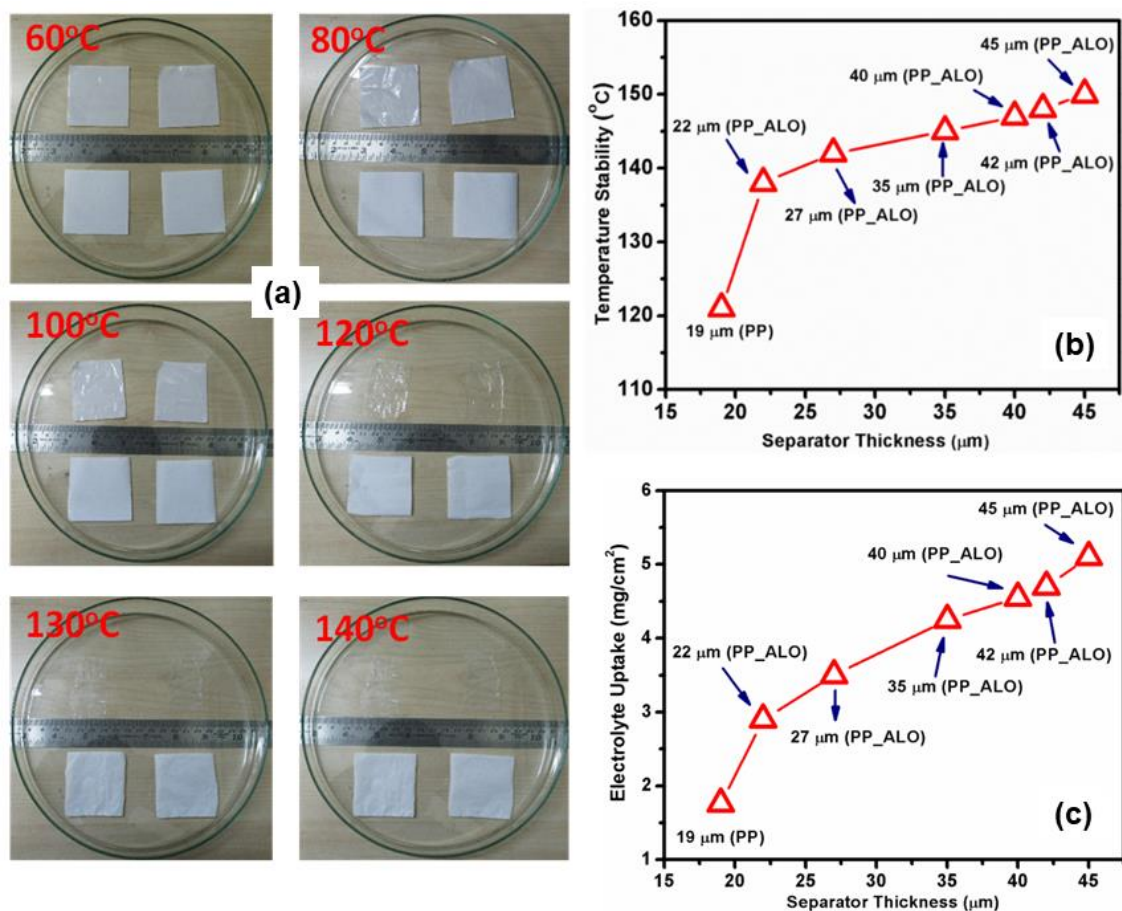


Figure 44. (a) Photograph showing (a) Comparative Thermal Stability of PP and ALO-PP (b) Variation of Thermal Stability and (c) Variation of Electrolyte Uptake of ALO-PP with Coating Thickness

The chemical stability of ALO-PP has been tested in different electrolytes such as 1.0 M LiPF₆ in EC: DMC (1:1 vol.), 1.0 M LiPF₆ in EC: DMC (1:2 vol.), 0.1 M LiClO₄ in DMSO, 1.0 M LiClO₄ in TEGDME, 0.1 M LiClO₄ dissolved in DMSO:TEGDME (1:1 vol.) and 1.0 M Et₄NBF₄ in acetonitrile by dipping for seven days and is found to be stable in each electrolyte. The electrolyte up-take measurements have been carried out in 1.0 M LiPF₆ dissolved in EC:DMC (1:2 vol.) (**Figure 44c**). The up-take of electrolyte in coated film increases with increasing thickness of the

AlO.OH layer. For ALO-PP-35 μm , the electrolyte up-take is 4.25 mg/cm^2 compared to 1.76 mg/cm^2 for PP. This can be attributed to the better wettability of AlO.OH layer compared to pure polypropylene (PP) owing to hydrophilic nature of AlO.OH. A better electrolyte up-take may result in formation of reservoirs for the electrolyte on either side of the separator and act as a buffer source for Li^+ ions, thus improving the cell kinetics. This would ensure that the rate of Li^+ ion diffusion through the electrolyte does not decrease during charging/discharging at higher C-rate.

4.2.4 Mechanical Properties

The properties related to mechanical characteristics of the coated separator have also been tested and compared with the uncoated ones. The deformation characteristics and elasticity of the developed ceramic coated separators have been studied by nanoindentation method. As shown in **Figure 45**, (force vs. indentation depth) the coated separator showed a much superior strength compared to the uncoated PP. In case of coated separator, the permanent deformation (permanent penetration depth) is less than that of uncoated one.

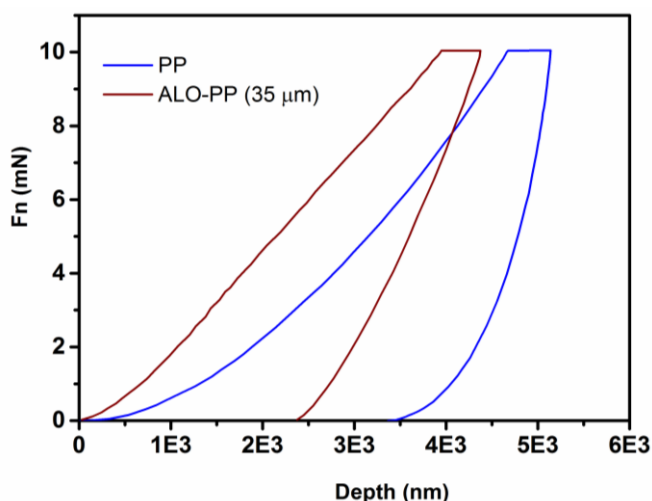


Figure 45. Nanoindentation Profile of PP (19 μm) and AlO.OH Coated PP (35 μm)

[The experimental measurements have been carried out by Anton-Paar at their facility at IIT Bombay as test samples]

For a viscoelastic material, the storage modulus which can be expressed as in **Eq. 1**, increases with decreasing δ , i.e., phase lag between stress and strain and thus material becomes more elastic at constant initial stress strain ratio. The variation of storage modulus with thickness is shown in **Figure 46a**. With increasing coating thickness, the storage modulus is increasing first up to the thickness of 35.6 μm and then again decreases.

$$E = \sigma_0 / \epsilon_0 \cos \delta \dots\dots\dots(1)$$

E – Extensional storage modulus

σ_0 – Initial stress

ϵ_0 – Initial strain

δ – Phase lag between stress and strain

Therefore, it can be attributed that the elastic portion of the material is maximum (~ 2050 MPa) at the optimum coating thickness of 35.6 μm and this is much better than that of uncoated film of thickness 25 μm which is around 970 MPa at room temperature. This storage modulus is decreasing with increasing temperature which is also well in agreement with literature.

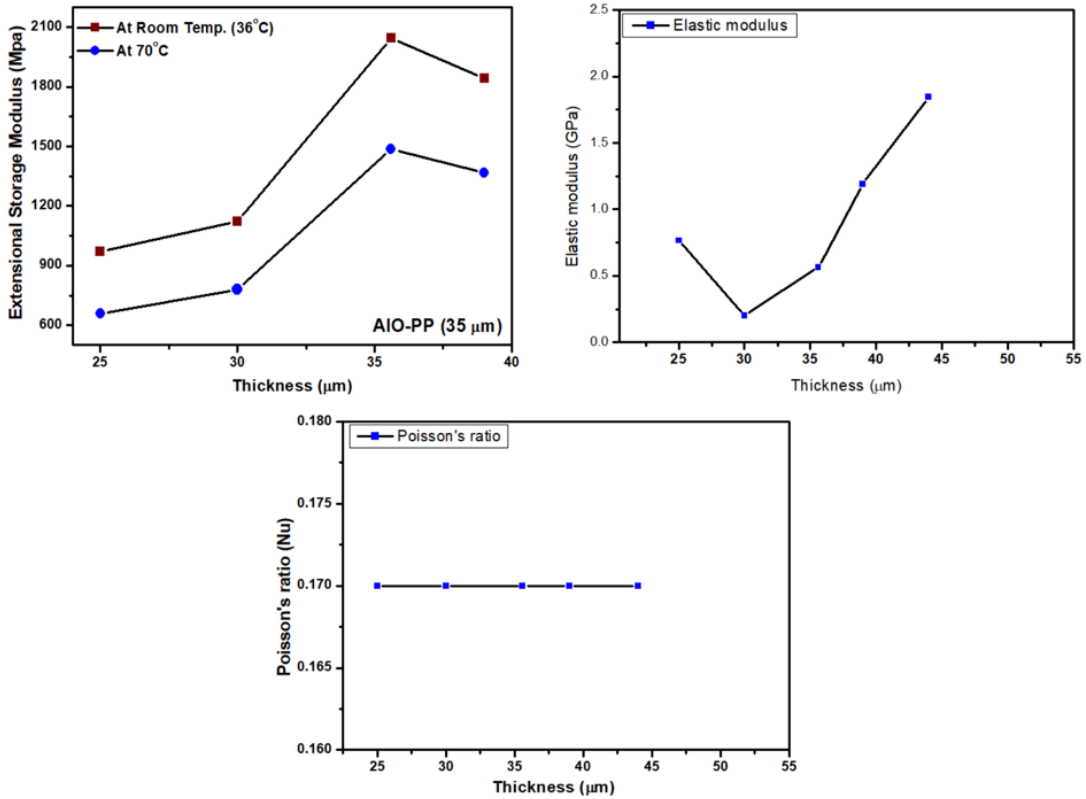


Figure 46. Variation of (a) Extensional Storage Modulus and (b) Elastic Modulus and (c) Poisson's Ratio with Thickness of Coated Separator

[The experimental measurements have been carried out by Anton-Paar at their facility at IIT Bombay as test samples]

For a constant stress, young's modulus (**Eq. 2**) decreases with increasing strain and vice versa. In this study it has been found that the young's modulus is minimum (0.2 GPa) at coating thickness on 30 μm and then with increasing thickness it is increasing (**Figure 46b**).

$$E = \sigma_0 / \epsilon_0 = \sigma / \epsilon \dots\dots\dots(2)$$

The coated sample of thickness of 35.6 μm can accommodate more strain compared to uncoated one for a constant stress which indicates that the rigidity of coated separator is more than uncoated

one. The Poisson's ratio is constant over the entire thickness which indicates the uniform distribution of coating material on the surface of polypropylene film (**Figure 46c**).

While winding the battery components together the separator remained under tension in between electrodes. To sustain this tension, separator should have high tensile strength in the direction of machining (MD). At the same time high puncture force is also required to prevent the penetration of uneven electrode surface through the separator. Pristine separator poses significant safety issues because of its inherently low tensile strength (106.0 MPa) as well as puncture force (2.3619 N). On the other hand, composite separator can accommodate higher tensile strength as well as higher puncture force. The coated layer acts as an additional barrier against the protrusion of separator by solid particles while also restrict the motion of separator. The coated layer should have interconnected porous structure with optimized tortuosity and this can be measured indirectly by measuring the Gurley value. The Gurley value is inversely proportional to air permeability. Higher the Gurley value lower the air permeability. This Gurley value is also an indirect method predicting lithium-ion conductivity through electrolyte filled separator. Pristine polypropylene separator has the Gurley value of 622 and ionic conductivity is of 0.76 mScm^{-1} . Unlike polyolefin separator, ceramic coated separator should have lower Gurley value which attributes those pores in the coated layer are interconnected and the coated particles do not block even the smaller pores rather these micropores facilitates the air transport by capillary effects of interstitial void between nanoparticles. Higher ionic conductivity of $8.908 \times 10^{-4} \text{ Scm}^{-1}$ of AlO.OH coated separator also attributes that the pores in the coated layer is uniformly distributed with narrow pore size distribution in micron level, having well developed interconnectivity between the pores and facilitates ionic conductivity when filled with electrolyte.

4.2.5 Electrochemical Properties

The effect of AlO.OH coated separator (ALO-PP) with varying thickness on electrochemical performance of the cell has been investigated by assembling 2032-type coin cells using LiFePO₄ as cathode against Li/Li⁺ in half-cell configuration. The pristine PP based cells show an initial discharge capacity of ~140 mAhg⁻¹. Initial capacity decreases only slightly for the ALO-PP based cells within the range of 135-143 mAhg⁻¹ for the separator thickness range of 23-45 μm (**Figure 47a**). Among the coated separators, it is observed that ALO-PP-35 shows a maximum initial capacity of 143 mAhg⁻¹. The discharge capacity of ALO-PP-23 is almost equal to pristine PP as the thickness of the coated layer is very low or the overall thickness (~23 μm) is almost close to the thickness of pristine PP (~19 μm). Further, as the thickness of the coated layer increases, both the impedance with respect to Li⁺ ion migration across the separator and the electrolyte uptake also increases. However, initially, up to a thickness of 27 μm the impedance factor predominates resulting in a decrease in the initial capacity. With further increase in the thickness, the electrolyte uptake dominates the Li⁺ ion conductivity over its impedance and thus, the capacity becomes higher for ALO-PP-35. Again, with further increase of the thickness, the mass of the coated layer as well as the migration path of the Li⁺ increases resulting decrease in discharge capacity in ALO-PP-42 and ALO-PP-45 successively.

The rate performance and capacity restoration of the ALO-PP-35 have been tested and compared with PP for LiFePO₄/Li half cells (**Figure 47b**) as well as for LiFePO₄/MCMB full cells (**Figure 47c**). The performance of the cell while using γ-AlO.OH coated separator (ALO-PP-35) shows better capacity compared to that of uncoated separator (PP) at all current densities, particularly at higher current rate (C/5). The reason is that the porous AlO.OH coated PP membrane has improved

porosity and pore size distribution along with enhanced electrolyte wettability due to better electrolyte uptake. This increased electrolyte uptake acts as a reservoir of liquid electrolyte within the pores of the coated layer on both sides of the PP membrane providing a buffer source of Li^+ ions which provide better rate performance at all current densities and is significant at higher current rate (C/5) compared to that of uncoated PP membrane. It is observed that while at lower current rates of C/20 and C/10, the obtained capacity values are comparable, at higher current rate of C/5 and C/2, there is a significant improvement of capacity for ALO-PP-35. For $\text{LiFePO}_4//\text{Li}$ half cells at C/5 rate, the specific discharge capacity for the cells having commercial separator (PP) is $\sim 90 \text{ mAhg}^{-1}$ while the cells fabricated with the coated separator (ALO-PP-35) the value is $\sim 105 \text{ mAhg}^{-1}$ (Fig. 47b). Though the uncoated separator does not take part in improving electrochemical performance directly in the lithium-ion battery but coating makes the difference. In the present investigation, the AIO.OH coated layer on PP membrane increases the electrolyte uptake within the pores of the coated layer on both sides of the PP which enhance the Li^+ ion diffusivity; thus, provide better rate performance at higher current rate (C/5) as compared to uncoated PP membrane. The capacity fluctuation in $\text{LiFePO}_4//\text{Li}$ half cells at different current rate except at the initial rate of C/20 may be because of the capacity loss in a lithium-ion battery due to loss of active electrode material or loss of active lithium. It may also be possible due to some adverse side reactions at anode or cathode [315]. However, the exact reason for capacity fluctuation is required to be investigated [316]. The ALO-PP-35 composite membrane separator has its maximum capability in reserving liquid electrolyte inside the pores of the AIO.OH layer depending upon its overall porosity, liquid electrolyte uptake capacity and thickness of the AIO.OH layer on both side of the PP membrane. The capacity at C/5 rate is in coherence with the buffer source of Li^+ ions in AIO.OH layer on PP membrane. Thus, the capacity difference while using ALO-PP-35 at C/5 rate

is higher compared to that of uncoated PP. However, at even higher rate, i.e., at $C/2$, the difference in capacities is lower in-between ALO-PP-35 and uncoated PP in cell because of limited supply of Li^+ ions from the buffer source compared to the rate of Li^+ ions supply required at $C/2$ rate.

Similarly, for the $\text{LiFePO}_4/\text{MCMB}$ full cells at the same rate ($C/5$), the specific discharge capacity for the cell having commercial separator (PP) is $\sim 50 \text{ mAhg}^{-1}$ while cell having coated separator (ALO-PP-35) the value is $\sim 58 \text{ mAhg}^{-1}$ (Fig. 8c). The comparatively lower capacities of $\text{LiFePO}_4/\text{MCMB}$ cell may be due to the decomposition of LiPF_6 salt in electrolyte. The electrolyte decomposition product may be deposited on the electrode surface which results increase in cell impedance. The loss of cyclable lithium may also likely to originate on the negative MCMB electrode. Thus, both loss of cyclable lithium and increased cell impedance are the suggested source of lower capacities for $\text{LiFePO}_4/\text{MCMB}$ cell [317, 318]. However, the actual analysis for this lower capacity requires in-depth investigation. The capacity restoration is also found to be improved for ALO-PP-35 while columbic efficiency is comparable for both kinds of cells.

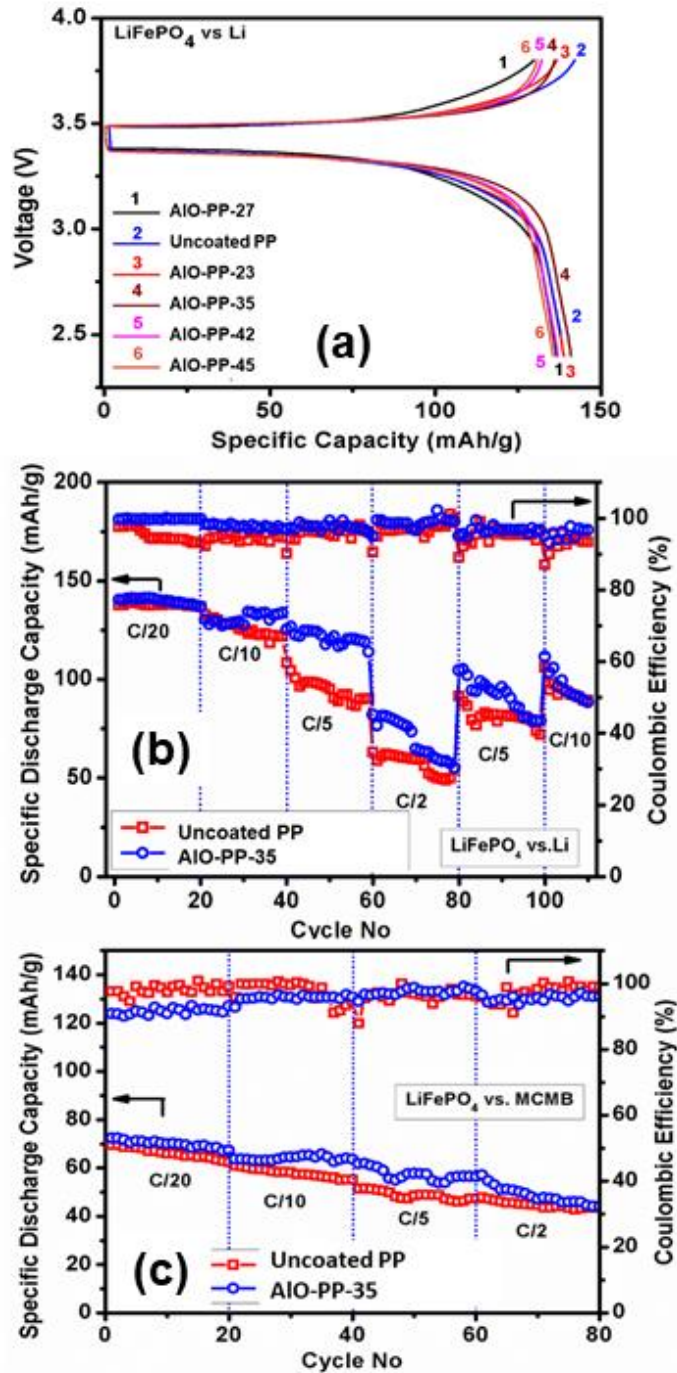


Figure 47. Comparison of Electrochemical Properties with ALO-PP and PP as Separator (a) Initial Charge-discharge Capacity of LiFePO₄//Li Cells at C/20 for Varying Coating Thickness (b) Rate Capability of LiFePO₄//Li Cells between C/20 and C/2 and (c) Rate Capability of LiFePO₄//MCMB Cells between C/20 and C/2

To understand the reasons for improved performance of ALO-PP-35, AC impedance spectroscopy was carried out on liquid electrolyte-soaked PP membrane and AIO-PP-35 membrane for determining the ionic conductivity of the separator material, which is an important parameter affecting the lithium-ion conduction of electrolyte material through the separator and the corresponding Nyquist plots are shown in **Figure 48**. The stainless steel (SS) supporting electrodes were used in two electrode system for the EIS measurement.

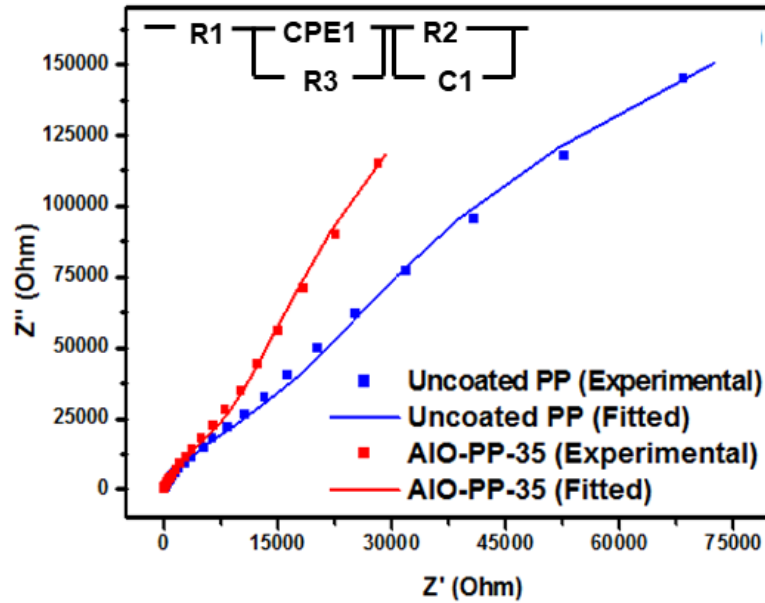


Figure 48. Nyquist Plots for PP and ALO-PP-35 Soaked in Liquid Electrolyte. The Equivalent Circuit used to fit the Impedance data is given in the Inset

The intercepts on the real axis gives the R_s ($R1$) values which are found to be 52.11 Ω and 15.44 Ω for PP and ALO-PP-35 respectively. Using Equation $\sigma = d/R_b \times S$, ionic conductivity of the ALO-PP-35 membrane has been calculated to be $8.908 \times 10^{-4} \text{ S cm}^{-1}$, while it is only $1.433 \times 10^{-4} \text{ S cm}^{-1}$ for the PP membrane. The improved ionic conductivity of the ALO.OH coated membrane (ALO-PP-35) may be explained in terms of its better electrolyte wettability with other contributing factors. The calculated impedance parameters are given in **Table 8**.

Table.8: Impedance Parameter for PP and ALO-PP-35 Membranes

Separator membrane	R ₁ (Ω)	R ₂ (Ω)	R ₃ (Ω)	C1 (F)	P1	n1
PP	52.97	4.87×10 ⁵	24269	9.707×10 ⁻⁶	1.021×10 ⁻⁵	0.85424
AIO-PP-35	15.31	8.67×10 ⁵	14582	1.349×10 ⁻⁵	2.161×10 ⁻⁵	0.8477

This has been observed that both in C/10 and C/20 rate that the separator with coating thickness of 35 μm, the specific discharge capacity is highest and is stable throughout the cycles. (Figure 49) This has been also noticed that with higher coating thickness (35 μm, 42 35 μm and 45 35 μm) the capacity decreases gradually.

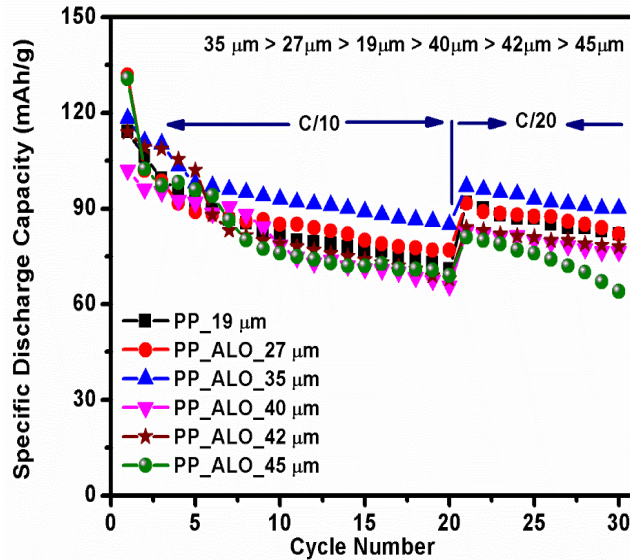


Figure 49. Cycling of LiFePO₄/Li Cell with PP and Coated Separators

The details of cycling performance have been studied at higher C rate (Figure 50). This has been observed that at higher C rate, the capacity decreases gradually with increasing cycle numbers but in all the higher C rates, the capacity is better in the cell with coated separator than that of uncoated

one. This is also noticeable that in all the cases the coulombic efficiencies are comparable in both coated and uncoated separator and which is around 100%. The following figures ((**Figure 50**) indicate that cells with coated separator is having better performance than that of uncoated pristine separators. However, the gradual decrease of capacity may be explained due to various reasons, mainly unstable LiFePO_4 coated layers.

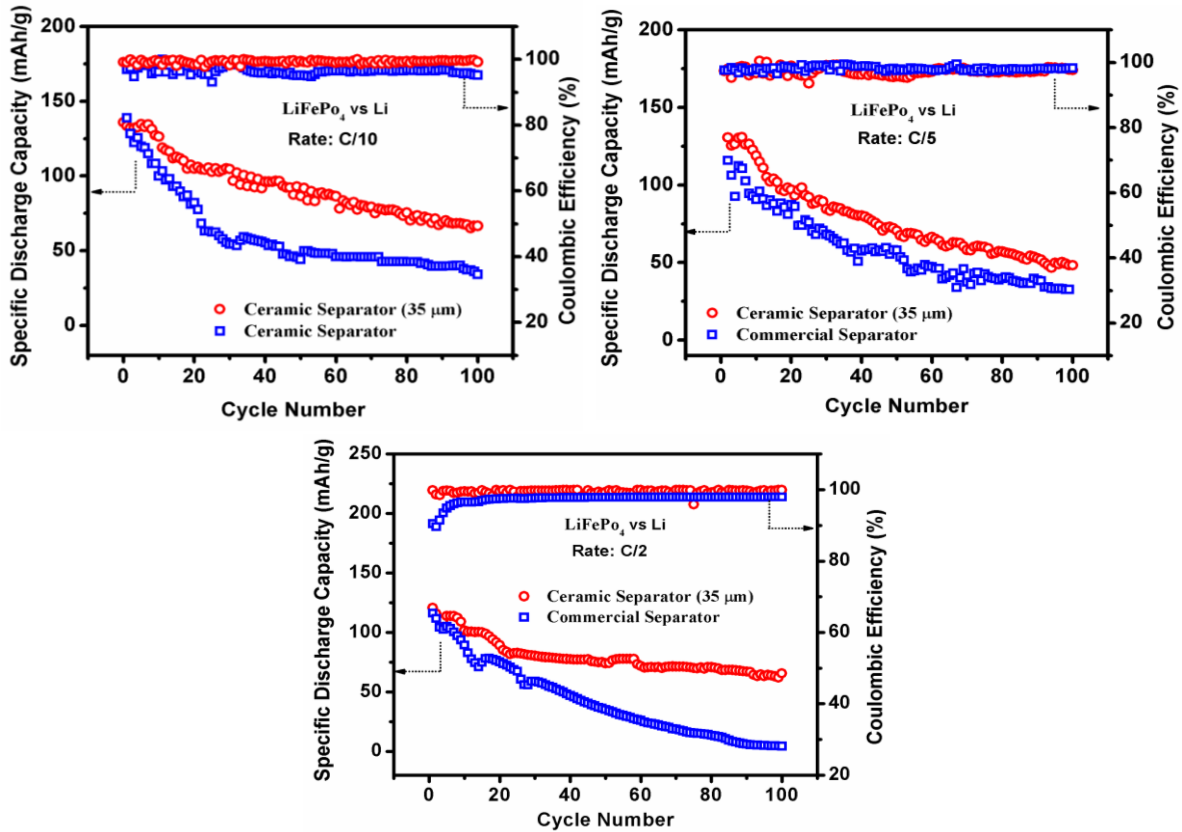


Figure 50. Cycling Performances of $\text{LiFePO}_4/\text{Li}$ Cell with Coated Separator (35 μm) with Conventional Polypropylene (19 μm) at Current Densities of (a) C/10, (b) C/5 and (c) C/2

The cycling efficiency of LiFePO_4 vs. CMS graphite cell has also been studied at higher C rate and it has been observed that though the overall specific capacity is low but the cell with coated separator performs better than uncoated one like $\text{LiFePO}_4/\text{Li}$ half cells while maintain the coulombic efficiency at 100%, which is comparable to uncoated one. (**Figure 51**)

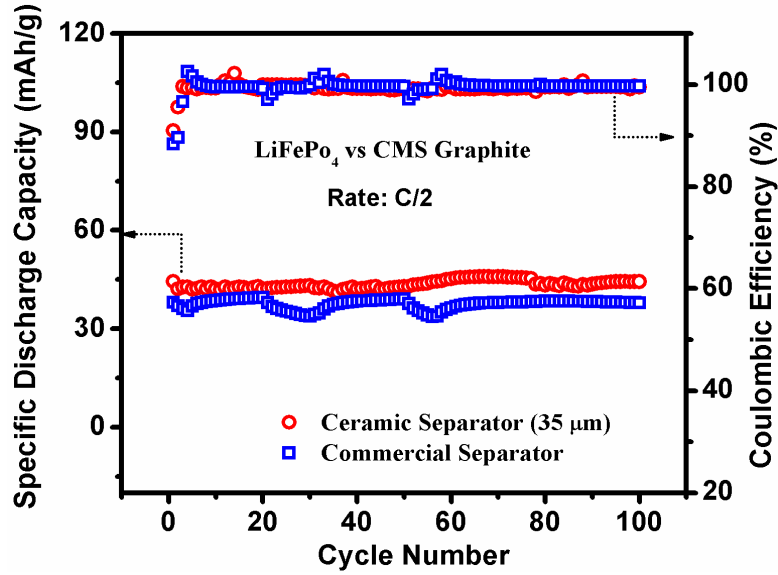


Figure 51. Cycling Performance of LiFePO₄/CMS Graphite Cell

The overall cell impedance has also been measured for LiFePO₄/Fe half-cell with coated separator. This has been found that after formation cycle cell resistance increases, which may be due to formation of SEI layers. The cell resistance decreases significantly after 20th cycle, which is conforming the general behaviour of the Lithium-ion battery cell. However, cell resistance increases more cycle numbers due to various side reactions in the cell.

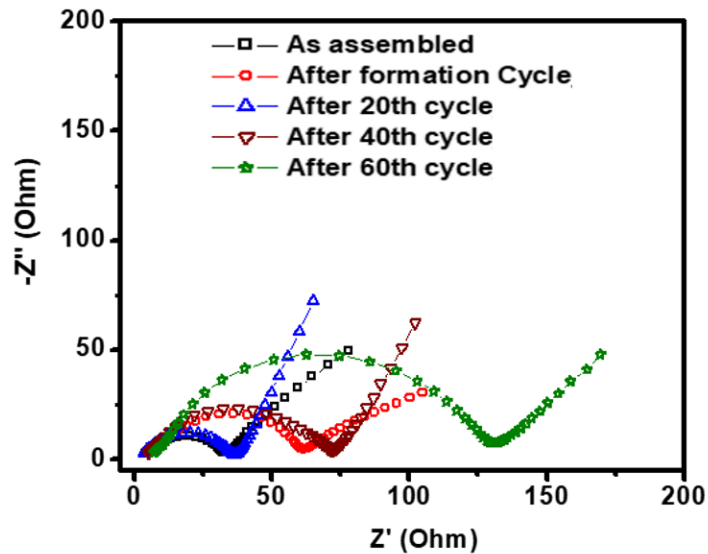


Figure 52. Cell Impedance of LiFePO₄/Li Half-cell with AIO-PP 35

Table 9: Properties of LiFePO₄/Li Half-cell with ALO-PP-35 Membranes

Properties	Celgard 2300 (PP)	Target (As recommended by RC)	Coated Separator (ALO-PP, nano)	Comment
Thickness	20 μm	$\geq 50 \mu\text{m}$	22, 27, 35, 40, 42 and 45 μm	√
Ionic Resistivity	NA	$\leq 5 \Omega\text{cm}^{-2}$	$5.4 \Omega\text{cm}^{-2}$	√
Porosity	39%	$\geq 30\text{-}40\%$	-	Under Study
Temperature Stability	$<130^\circ\text{C}$	$130^\circ\text{-}150^\circ\text{C}$	145°C (35 μm)	Yes
Wettability	Good	Good	Good	√
Electrolyte Uptake	1.76 mg/cm^2	Good	4.25 mg/cm^2 (36 μm)	√
Stability- LiPF_6 in EC: DMC	Stable	Stable	Stable	√
Puncture Strength	$>360 \text{ g/mil}$	$> 300 \text{ g/mill}$	-	Under Study
TD and MD Shrinkage @ 90°C /1 h	0.0% and $<5.0\%$	$\leq 5\%$ in MD and TD	0.0% and 0.0% (36 μm)	√

CHAPTER 5
CONCLUSIONS AND FUTURE WORK

CHAPTER 5

CONCLUSIONS AND FUTURE WORK

5.1 Conclusions

Cathode materials: The research focus on Li-ion battery at present is to achieve high-energy high-power density, which is required for the application in high end consumer electronic devices and electric vehicles. To achieve this major two properties along with stability and safety researchers have concentrated in major four challenging areas which include (i) electrode materials having high specific capacity and high voltage, (ii) nano materials to increase the reactivity and high lithium-ion diffusivity, (iii) use of non-carbonaceous anode materials to increase safety and (iv) structurally stable electrode materials. The specific approaches to meet these challenges are as follows. Energy density can be improved by selecting a positive electrode (cathode) that could either display higher redox potential or larger capacity or both in together. One of the ways to increase the power density is to use nanomaterials having structural stability. Coupling a highly oxidizing materials ($\text{Li}_4\text{Ti}_5\text{O}_{12}$ instead of C) in order to eliminate the formation of SEI layer at negative electrode when dealing with safety. The cost of Li-ion battery mainly dependent on the synthesis procedure of its component materials, particularly the cathode material, its raw materials abundance on earth crust and renewability. Hydrothermal / solvothermal processes are cheaper than other synthesis process due to its simplicity, water based and low temperature. Cathode materials are mainly responsible to improve the energy density and power density. Cathode material determines the voltage and capacity of the of Li-ion battery. Capacity is dependent on the number of extractable lithium from cathode during charge. Voltage is dependent on the redox potential of the transition metal element. The combined effect of voltage and capacity determines the energy density as well as power density of the cell. In Li-ion battery, the anode is well

developed and little improvements in electrochemical performance can be achieved in terms of design changes. However, cathode shows a great prospect for further enhancement of the battery properties. Battery research is therefore concentrating on cathode materials. The key challenges for developing Li-ion battery for electric vehicle applications are to achieve high energy densities and high power density. Olivine structured based cathode material LiMPO_4 is having high operating voltage around (4.1 - 5.1V) and a maximum theoretical capacity ($\sim 170 \text{ mAhg}^{-1}$). Compared to many commercialized compounds, this material can provide higher specific energy, which is $> 850 \text{ Whkg}^{-1}$.

Development of advanced Lithium-ion battery mainly requires the cathode materials having higher redox potential of its transition element to meet the high performance demand, particularly in electric vehicle. In this work a high energy LIB with high voltage cathode material is prepared based on olivine structured materials having general formula LiMPO_4 ($M = \text{Fe, Mn, Co \& Ni}$). Phosphates can provide higher voltages than oxides of same transition metal with similar thermal stability. In (PO_4^{3-}) polyanion, the strong P–O covalent bond stabilize the oxygen in fully charged state MPO_4 , thus making LiMPO_4 electrochemically excellent, thermally stable, and environmentally safe material. The strong P-O bond in the polyanion is responsible for lowering the $M^{2+/3+}$ redox energy and improving the battery voltage higher (V_{oc} vs. lithium) for that couple. The theoretical redox potential of LiFePO_4 , LiMnPO_4 , LiCoPO_4 and LiNiPO_4 are 3.5 V, 4.1 V, 4.8 V, and 5.1 V respectively and the corresponding specific energies are 578, 697, 816 and 867 Whkg^{-1} respectively. The major challenges of this materials include low ionic diffusivity, low electronic conductivity, anisotropic movement of Li ions within the materials in [010] direction, instability of the fully de-lithiated phase (i.e., MPO_4 & MVO_4), Jahn Teller effect (LiMnPO_4) and large

volume mismatch between lithiated and delithiated phases. Various approaches have been taken to meet these challenges. These are (a) growth of nano-sized material with desired morphology to decrease the Li^+ ion migration path and increase the Li^+ ion diffusivity (b) increasing ionic diffusivity and electronic conductivity by suitable addition of dopants in cation as well as anion sites (c) increasing inter-particle conductivity of the cathode materials by increasing the ratio of graphitic vs. amorphous carbon with suitable synthesis procedure (d) synthesis of $\text{Li}_y\text{MPO}_4\text{X}$ [$\text{X} = \text{S, F, N}$ etc., $y > 1$] to increase the specific capacity and also to make isotropic Li^+ ion diffusivity (e) increasing capacity by increasing the ratio of Mn^{2+} vs. Mn^{3+} with suitable synthesis procedure and (f) increasing energy density of Lithium-ion battery either by improving the voltage or increasing the capacity (or both together).

In this work we have successfully prepared LiMnPO_4 olivine structured cathode material at optimum pH condition. Optimum content of conducting carbon in cathode material is obtained based on electrochemical performance. Optimum percentage of La doping in carbon containing cathode material is obtained based on electrochemical performance. Physical and morphological characterization shows the structure and phase purity and their nano size morphology. The bulk conductivity is improved after substituting Mn^{2+} in LiMnPO_4 by La^{3+} ion. In La doped LiMnPO_4/C , electron transfer reaction would also become faster than that of in pure LiMnPO_4 . The maximum capacity for this material obtained is 129 mAhg^{-1} . In summary, we have demonstrated a facile low temperature solvothermal method for synthesizing single phase LiMnPO_4 and $\text{LiMn}_{0.99}\text{La}_{0.01}\text{PO}_4$ nano-structured materials. The physical and electrochemical properties of La-doped LiMnPO_4 cathode materials are systematically investigated. XRD studies confirmed the orthorhombic crystal structure of LiMnPO_4 and $\text{LiMn}_{0.99}\text{La}_{0.01}\text{PO}_4$. FESEM images

showed the formation of nanoparticles with spherical morphology for both LiMnPO_4 and $\text{LiMn}_{0.99}\text{La}_{0.01}\text{PO}_4$ materials. Among the materials studied, the $\text{LiMn}_{0.99}\text{La}_{0.01}\text{PO}_4/\text{C}$ composite demonstrated the best cell performance with higher electrochemical stability at higher C-rate.

Separator: Lithium-ion batteries with high energy density and high power output, long cycle life along with low self-discharge rate are presently the most preferred energy storage system for a wide range of applications. However, improving the battery safety remains a critical issue particularly for applications where high power is required, for example, in electric vehicles. In this respect, the separator, which is an integral component of Li-ion battery, plays a crucial role by providing a physical barrier between cathode and anode part; thus, preventing electrical short circuiting during battery operation while maintaining a steady flow of Li^+ ions through the electrolyte. Consequently, mechanical, thermal and electrochemical stability, porosity, wettability, electrolyte uptake and Li^+ ion permeability are the important parameters for a separator. The effect of these parameters on the electrochemical performance of Li-ion battery are summarized in recent articles. Polyolefin based micro-porous membranes such as polypropylene (PP), polyethylene (PE), polyethylene oxide (PEO), polyacrylonitrile (PAN), polyvinylidene fluoride (PVDF), polyvinylidene fluoride-co-hexafluoropropylene (PVDF-HFP) etc. or their combination are the most preferred composition of a separator used in commercial Li-ion battery at present. However, polyolefin membranes have several inherent disadvantages such as poor thermal stability, low porosity (~ 40%) and insufficient electrolyte wettability. Especially, because of low melting point of the polyolefin separators, it can easily result in shrinkage that leads to internal short-circuiting of the electrodes, causing fire or even an explosion. Moreover, being non-polar, polyolefin membranes have poor wettability in highly polar organic electrolytes; thus, a high electrical

resistance is developed as the pores of the separators are not completely filled with the liquid electrolyte.

In this respect, boehmite (γ -AlO.OH), which is a light weight, non-toxic and low-cost material, could be a suitable coating material. It has a favourable layered structure composed of AlO₆ octahedra and more importantly, it possesses a large number of -OH functional groups on the surface. Besides, it is a well-known flame retarding material. In fact, boehmite is widely used in several industrial applications such as catalysis, adsorbent, filler in plastic etc. Additionally, this material is having other advantages which include its better dispersity in aqueous slurries which would facilitate uniform coating on the polymer membrane.

In the present work, we have synthesized boehmite (γ -AlO.OH) nanofibers (length 90-140 nm; dia ~15 nm) by a simple low-temperature (180°C) hydrothermal method and coated onto both sides of surface modified polypropylene (Celgard). The prepared composite separator has been tested in LiFePO₄/Li half cells as well as in LiFePO₄/MCMB full cells in coin cell configuration for understanding the influence of this separator on electrochemical performance.

Ceramic coated composite separator shows enhanced thermal and dimensional stability over uncoated polypropylene. Optimum coating thickness is found to be 8 μ m in each side. Electrochemical performance is evaluated by investigating the essential properties of 2032-type coin cells using LiFePO₄ as cathode against Li/Li⁺ in half cell and MCMB in full cell configuration respectively. It is found that composite separator results in improved cell kinetics due to better electrolyte uptake and formation of a Li⁺ ions buffer reservoir facilitating fast ion transport at high

current rates. About 16% higher capacity is observed for coated polypropylene over one at a current rate of $C/5$. Present results show that nanostructured boehmite could be a promising coating material for surface modification of polyolefin separators not only with improved safety but also with enhanced rate performance.

In summary, we have demonstrated a facile hydrothermal technique for synthesizing single phase γ -AlO.OH nanostructured material. The surface coating of γ -AlO.OH on polypropylene membrane is shown to be a promising approach for the development of advanced separator for lithium-ion batteries with enhanced safety. The coated PP membrane showed significantly higher thermal stability up to 140°C with only $8\ \mu\text{m}$ coating thickness on each side of polypropylene. Such thin coatings are advantageous to save battery space and thereby gaining high energy density. The coated separator shows improved electrochemical performance in comparison to uncoated polypropylene at higher current densities. The hydrophilic nature of AlO.OH imparts higher wettability, which in-turn facilitating the formation of a reservoir of electrolyte within its pores on both sides of the separator providing a buffer source for Li^+ for faster cell kinetics.

5.2 Scope of Future Work

- Preparation of phase pure LiMPO_4 ($M - \text{Mn, Co \& Ni}$)
- Preparation of mixed transition metal material $\text{LiMM}'\text{PO}_4$ ($M \& M' - \text{Mn, Co \& Ni}$).
- Cation site doping: Substitution of $M \& M'$ by $A - \text{La, Sr, Mg, Ti, V}$ etc. [$\text{Li}(\text{MM}')_{1-x}\text{A}_x\text{PO}_4$]
- Anion site doping: B, S, N and P doping in anion sites [$\text{L}_z(\text{MM}')_{1-x}\text{A}_x\text{PO}_4\text{B}$]. [e.g., $\text{Li}_3\text{Mn}_{1-x}\text{M}_x\text{PO}_4\text{S}$, $\text{Li}_4\text{Mn}_{1-x}\text{M}_x\text{PO}_4\text{N}$, $\text{Li}_2\text{Mn}_{1-x}\text{M}_x\text{PO}_4\text{F}$ etc.]
- Preparation of $\text{Li}_3\text{V}_2(\text{PO}_4)_3$

- Optimization of each of the developed electrodes with electrolyte (LiPF_6 in EC:DMC = 1:2) and Li anode (Half Cell)
- The optimized composition is tested with Carbon (Half-cell) and also with $\text{Li}_4\text{Ti}_5\text{O}_{12}$ anode (Full Cell)
- Preparation of half-cell as well as full cell with the modified electrode and AlO.OH coated polypropylene separator with Li anode (Half Cell), with Carbon (Half-cell) and also with $\text{Li}_4\text{Ti}_5\text{O}_{12}$ anode (Full Cell)
- Electrochemical characterization of fabricated half-cell and full cell with the modified electrode and AlO.OH coated polypropylene separator

REFERENCES

- [1] IEA, 2022. Global EV Outlook 2022. International Energy Agency, Paris, France
- [2] P.J. Hall, E.J. Bain, Energy-storage technologies and electricity generation, *Energy Policy*, 36 (2008) 4352-4355.
- [3] R. Qi, B.D.L. Campeon, I. Konuma, Y. Sato, Y. Kaneda, M. Kondo, N. Yabuuchi, Metastable and nanosized $\text{Li}_{1.2}\text{Nb}_{0.2}\text{V}_{0.6}\text{O}_2$ for high-energy Li-ion batteries, *Electrochemistry*, 90 (2022) 037005-037005.
- [4] C.-C. Zhou, Z. Su, X.-L. Gao, R. Cao, S.-C. Yang, X.-H. Liu, Ultra-high-energy lithium-ion batteries enabled by aligned structured thick electrode design, *Rare Metals*, 41 (2022) 14-20.
- [5] A.S. Arico, P. Bruce, B. Scrosati, J.-M. Tarascon, W. Van Schalkwijk, Nanostructured materials for advanced energy conversion and storage devices, *Nat. Mater.*, 4 (2005) 366-377.
- [6] J. Park, H. Song, I. Jang, J. Lee, J. Um, S.-g. Bae, J. Kim, S. Jeong, H.-J. Kim, Three-dimensionalization via control of laser-structuring parameters for high energy and high power lithium-ion battery under various operating conditions, *J. Energy Chem.*, 64 (2022) 93-102.
- [7] M. Armand, J.M. Tarascon, Issues and challenges facing rechargeable lithium batteries, *Nature*, 414 (2001) 359-367.
- [8] Y. Wang, G. Cao, Developments in nanostructured cathode materials for high-performance lithium-ion batteries, *Adv. Mater.*, 20 (2008) 2251-2269.
- [9] M.S. Whittingham, Lithium batteries and cathode materials, *Chem. Rev.*, 104 (2004) 4271-4302.
- [10] M. Winter, R.J. Brodd, What are batteries, fuel cells, and supercapacitors? *Chem. Rev.*, 104 (2004) 4245-4270.
- [11] P. Arora, Z. Zhang, Battery separators, *Chem. Rev.*, 104 (2004) 4419-4462.

- [12] J. Choi, P.J. Kim, A roadmap of battery separator development: Past and future, *Curr. Opin. Electrochem.*, 31 (2022) 100858.
- [13] H. Lee, M. Yanilmaz, O. Toprakci, K. Fu, X. Zhang, A review of recent developments in membrane separators for rechargeable lithium-ion batteries, *Energy Environ. Sci.*, 7 (2014) 3857-3886.
- [14] M. Yang, J. Hou, Membranes in lithium ion batteries, *Membranes*, 2 (2012) 367-383.
- [15] W. Zhang, Z. Tu, J. Qian, S. Choudhury, L.A. Archer, Y. Lu, Design principles of functional polymer separators for high-energy, metal-based batteries, *Small*, 14 (2018) 1703001.
- [16] W. Xu, J. Wang, F. Ding, X. Chen, E. Nasybulin, Y. Zhang, J.-G. Zhang, Lithium metal anodes for rechargeable batteries, *Energy Environ. Sci.*, 7 (2014) 513-537.
- [17] B. Scrosati, J. Garche, Lithium batteries: Status, prospects and future, *J. Power Sources*, 195 (2010) 2419-2430.
- [18] X. Zhang, Z. Ju, Y. Zhu, K.J. Takeuchi, E.S. Takeuchi, A.C. Marschilok, G. Yu, Multiscale understanding and architecture design of high energy/power lithium-ion battery electrodes, *Adv. Energy Mater.*, 11 (2021) 2000808.
- [19] U.S. Energy Information Administration, Annual Energy Review 2011, U.S. Department of Energy, Washington, DC, 2012.
- [20] U.S. Energy Information Administration, Inventory of U.S. greenhouse gas emissions and sinks: 1990-2011, U.S. Environmental Protection Agency, Washington, DC, 2013.
- [21] M. Armand, J.M. Tarascon, Building better batteries, *Nature*, 451 (2008) 652-657.
- [22] X. Zhang, Z. Li, L. Luo, Y. Fan, Z. Du, A review on thermal management of lithium-ion batteries for electric vehicles, *Energy*, 238 (2022) 121652.
- [23] J. Larminie, J. Lowry, *Electric vehicle technology explained*, John Wiley and Sons 2012.

- [24] United Nations, Sustainable Development Goals, <https://www.un.org/sustainabledevelopment/>, 2022.
- [25] N. Nakamura, S. Ahn, T. Momma, T. Osaka, Future potential for lithium-sulfur batteries, *J. Power Sources*, 558 (2023) 232566-232581.
- [26] J.T. Frith, M.J. Lacey, U. Ulissi, A non-academic perspective on the future of lithium-based batteries, *Nat. Commun.*, 14 (2023) 420-437.
- [27] Y. Wang, X. Zhang, Z. Chen, Low temperature preheating techniques for lithium-ion batteries: Recent advances and future challenges, *Appl. Energy*, 313 (2022) 118832-118845.
- [28] L. Zhou, X. Lai, B. Li, Y. Yao, M. Yuan, J. Weng, Y. Zheng, State estimation models of lithium-ion batteries for battery management system: Status, challenges, and future trends, *Batteries*, 9 (2023) 131-154.
- [29] International Monetary Fund, Soaring Metal Prices May Delay Energy Transition, <https://blogs.imf.org/2021/11/10/soaring-metal-prices-may-delay-energy-transition/>, 2022.
- [30] T. Raj, K. Chandrasekhar, A.N. Kumar, P. Sharma, A. Pandey, M. Jang, B.-H. Jeon, S. Varjani, S.-H. Kim, Recycling of cathode material from spent lithium-ion batteries: Challenges and future perspectives, *J. Hazard. Mater.*, 429 (2022) 128312-128335.
- [31] X. Wu, J. Ma, J. Wang, X. Zhang, G. Zhou, Z. Liang, Progress, key issues, and future prospects for Li-ion battery recycling, *Global Chall.*, 6 (2022) 2200067-2200088.
- [32] K.D. Huang, S.-C. Tzeng, Development of a hybrid pneumatic-power vehicle, *Appl. Energ.*, 80 (2005) 47-59.
- [33] N. Xue, PhD Thesis: Design and optimization of lithium-ion batteries for electric-vehicle applications, University of Michigan, 2014.

- [34] A. Jarry, S.b. Gottis, Y.-S. Yu, J. Roque-Rosell, C. Kim, J. Cabana, J. Kerr, R. Kostecki, The formation mechanism of fluorescent metal complexes at the $\text{Li}_x\text{Ni}_{0.5}\text{Mn}_{1.5}\text{O}_4$ /carbonate ester electrolyte interface, *J. Am. Chem. Soc.*, 137 (2015) 3533-3539.
- [35] K. Xu, Nonaqueous liquid electrolytes for lithium-based rechargeable batteries, *Chem. Rev.*, 104 (2004) 4303-4418.
- [36] E. Castel, E.J. Berg, M. El Kazzi, P. Novak, C. Villevieille, Differential electrochemical mass spectrometry study of the interface of $x\text{Li}_2\text{MnO}_3 \cdot (1-x)\text{LiMO}_2$ (M= Ni, Co, and Mn) material as a positive electrode in Li-ion batteries, *Chem. Mater.*, 26 (2014) 5051-5057.
- [37] R. Imhof, P. Novak, Oxidative electrolyte solvent degradation in lithium-ion batteries: An In Situ differential electrochemical mass spectrometry investigation, *J. Electrochem. Soc.*, 146 (1999) 1702-1706.
- [38] J. Fischer, C. Adelhelm, T. Bergfeldt, K. Chang, C. Ziebert, H. Leiste, M. Stuber, S. Ulrich, D. Music, B. Hallstedt, Development of thin film cathodes for lithium-ion batteries in the material system Li-Mn-O by rf magnetron sputtering, *Thin Solid Films*, 528 (2013) 217-223.
- [39] Y.-M. Liu, B. G. Nicolau, J.L. Esbenshade, A.A. Gewirth, Characterization of the cathode electrolyte interface in lithium ion batteries by desorption electrospray ionization mass spectrometry, *Anal. Chem.*, 88 (2016) 7171-7177.
- [40] H.S. Lee, V. Ramar, S. Kuppan, M. Nagarathinam, M. Law, C. Wang, A. Tripathi, P. Balaya, Key design considerations for synthesis of mesoporous $\square\text{-Li}_3\text{V}_2(\text{PO}_4)_3/\text{C}$ for high power lithium batteries, *Electrochim. Acta.*, 372 (2021) 137831.
- [41] T. Trigg, P. Telleen, Global EV Outlook 2013 - Understanding the electric vehicle landscape to 2020, Technical report, International Energy Agency, 2013.

- [42] P.G. Bruce, S.A. Freunberger, L.J. Hardwick, J.-M. Tarascon, Li-O₂ and Li-S batteries with high energy storage, *Nat. Mater.*, 11 (2012) 19-29.
- [43] N.R. Van, The rechargeable revolution: A better battery, *Nature*, 507 (2014) 26-28.
- [44] W. Zeng, F. Xia, W. Tian, F. Cao, J. Chen, J. Wu, R. Song, S. Mu, Single-crystal high-nickel layered cathodes for lithium-ion batteries: Advantages, mechanism, challenges and approaches, *Curr. Opin. Electrochem.*, 31 (2022) 100831-100839.
- [45] G. Zheng, Ph.D. Thesis: Beyond lithium ion: Developing high energy density lithium sulfur batteries, Stanford University, 2014.
- [46] Y. Hu, X. Li, D. Geng, M. Cai, R. Li, X. Sun, Influence of paper thickness on the electrochemical performances of graphene papers as an anode for lithium ion batteries, *Electrochim. Acta.*, 91 (2013) 227-233.
- [47] G. Qian, J. Wang, H. Li, Z.-F. Ma, P. Pianetta, L. Li, X. Yu, Y. Liu, Structural and chemical evolution in layered oxide cathodes of lithium-ion batteries revealed by synchrotron techniques, *Natl. Sci. Rev.*, 9 (2022) nwab146-163.
- [48] V. Etacheri, R. Marom, R. Elazari, G. Salitra, D. Aurbach, Challenges in the development of advanced Li-ion batteries: A review, *Energy Environ. Sci.*, 4 (2011) 3243-3262.
- [49] A. Gomez-Martin, F. Reissig, L. Frankenstein, M. Heidebuchel, M. Winter, T. Placke, R. Schmuch, Magnesium substitution in Ni-rich NMC layered cathodes for high-energy lithium ion batteries, *Adv. Energy Mater.*, 12 (2022) 2103045-2103060.
- [50] H. Kim, S.-W. Kim, J. Hong, H.-D. Lim, H.S. Kim, J.-K. Yoo, K. Kang, Graphene-based hybrid electrode material for high-power lithium-ion batteries, *J. Electrochem. Soc.*, 158 (2011) A930.

- [51] M. Zhang, D. Lei, X. Yin, L. Chen, Q. Li, Y. Wang, T. Wang, Magnetite/graphene composites: microwave irradiation synthesis and enhanced cycling and rate performances for lithium ion batteries, *J. Mater. Chem.*, 20 (2010) 5538-5543.
- [52] J. Ren, Z. Wang, P. Xu, C. Wang, F. Gao, D. Zhao, S. Liu, H. Yang, D. Wang, C. Niu, Porous Co_2VO_4 nanodisk as a high-energy and fast-charging anode for lithium-ion batteries, *Nano-Micro Lett.*, 14 (2022) 1-14.
- [53] C. Ma, X. Shao, D. Cao, Nitrogen-doped graphene nanosheets as anode materials for lithium ion batteries: A first-principles study, *J. Mater. Chem.*, 22 (2012) 8911-8915.
- [54] P.G. Bruce, B. Scrosati, J.M. Tarascon, Nanomaterials for rechargeable lithium batteries, *Angew. Chem. Int. Edit.*, 47 (2008) 2930-2946.
- [55] C. Zhan, J. Lu, A. Jeremy Kropf, T. Wu, A.N. Jansen, Y.-K. Sun, X. Qiu, K. Amine, Mn (II) deposition on anodes and its effects on capacity fade in spinel lithium manganate-carbon systems, *Nat. Commun.*, 4 (2013) 1-8.
- [56] B. Scrosati, Recent advances in lithium ion battery materials, *Electrochim. Acta.*, 45 (2000) 2461-2466.
- [57] J. Lin, E. Fan, X. Zhang, R. Chen, F. Wu, L. Li, Sustainable recycling of cathode scrap towards high-performance anode materials for Li-ion batteries, *Adv. Energy Mater.*, 12 (2022) 2103288.
- [58] M.-H. Ryou, Y.M. Lee, J.-K. Park, J.W. Choi, Mussel-inspired polydopamine-treated polyethylene separators for high-power Li-ion batteries, *Adv. Mater.*, 23 (2011) 3066-3070.
- [59] K. Xu, Electrolytes and interphases in Li-ion batteries and beyond, *Chem. Rev.*, 114 (2014) 11503-11618.
- [60] J. Janek, W.G. Zeier, A solid future for battery development, *Nat. Energy*, 1 (2016) 16141.

- [61] J. Mindemark, M.J. Lacey, T. Bowden, D. Brandell, Beyond PEO-alternative host materials for Li⁺-conducting solid polymer electrolytes, *Prog. Polym. Sci.*, 81 (2018) 114-143.
- [62] G.N. Lewis, F.G. Keyes, The potential of the lithium electrode, *J. Am. Chem. Soc.*, 35 (1913) 340-344.
- [63] M.S. Whittingham, Electrical energy storage and intercalation chemistry, *Science*, 192 (1976) 1126-1127.
- [64] P. Touzain, R. Yazami, J. Maire, Insertion compounds of graphite with improved performances and electrochemical applications of those compounds, in: U.S. Patent (Ed.), Le Carbone Lorraine, S.A., France, USA, 1986.
- [65] R. Paravasthu, Ph. D. Thesis - Synthesis and characterization of lithium-ion cathode materials in the system $(1-x-y)\text{LiNi}_{1/3}\text{Mn}_{1/3}\text{Co}_{1/3}\text{O}_2 \cdot x\text{Li}_2\text{MnO}_3 \cdot y\text{LiCoO}_2$, Colorado State University, 2012.
- [66] K. Mizushima, P.C. Jones, P.J. Wiseman, J.B. Goodenough, Li_xCoO_2 ($0 < x < 1$): A new cathode material for batteries of high energy density, *Mater. Res. Bull.*, 15 (1980) 783-789.
- [67] T. Nagaura, K. Tozawa, *Progress in batteries and solar cells*, JEC Press, 9 (1990) 209-217.
- [68] K. Ozawa, Lithium-ion rechargeable batteries with LiCoO_2 and carbon electrodes: the LiCoO_2/C system, *Solid State Ionics*, 69 (1994) 212-221.
- [69] G.M. Ehrlich, *Lithium-ion batteries*, McGraw-Hill, New York, USA, 2002.
- [70] J. Wang, Z. Liang, Y. Zhao, J. Sheng, J. Ma, K. Jia, B. Li, G. Zhou, H.-M. Cheng, Direct conversion of degraded LiCoO_2 cathode materials into high-performance LiCoO_2 : A closed-loop green recycling strategy for spent lithium-ion batteries, *Energy Stor. Mater.*, 45 (2022) 768-776.
- [71] D. Linden, T.B. Reddy, *Handbook of Batteries*, 3rd ed., McGraw-Hill, New York, 2001.

- [72] M. Jeong, W. Lee, S. Yun, W. Choi, H. Park, E. Lee, J. Kim, S.J. Cho, N.-H. Lee, H.-J. Shin, W.-S. Yoon, Strategic approach to diversify design options for Li-ion batteries by utilizing low-Ni layered cathode materials, *Adv. Energy Mater.*, 12 (2022) 2103052.
- [73] R. Paravasthu, Synthesis and characterization of lithium-ion cathode materials in the system $(1-x-y)\text{LiNi}_{1/3}\text{Mn}_{1/3}\text{Co}_{1/3}\text{O}_2 \cdot x\text{Li}_2\text{MnO}_3 \cdot y\text{LiCoO}_2$, Department of Mechanical Engineering, Colorado State University, Fort Collins, Colorado, 2012.
- [74] Y. Chen, L. Yang, F. Guo, D. Liu, H. Wang, J. Lu, J. Zheng, X. Yu, H. Li, Mechanical-electrochemical modeling of silicon-graphite composite anode for lithium-ion batteries, *J. Power Sources*, 527 (2022) 231178.
- [75] G. Zheng, Beyond lithium ion: Developing high energy density lithium sulfur batteries, Department of Chemical Engineering, Stanford University, California, 2014.
- [76] R. Huggins, *Advanced batteries: Materials science aspects*, Springer Science and Business Media 2008.
- [77] P.G. Bruce, A. Robert Armstrong, R.L. Gitzendanner, New intercalation compounds for lithium batteries: layered LiMnO_2 , *J. Mater. Chem.*, 9 (1999) 193-198.
- [78] J.B. Goodenough, V. Manivannan, Cathodes for lithium-ion batteries: Some comparisons, *Denki Kagaku*, 66 (1998) 1173-1181.
- [79] J. Morales, C. Perez-Vicente, J.L. Tirado, Cation distribution and chemical deintercalation of $\text{Li}_{1-x}\text{Ni}_{1+x}\text{O}_2$, *Mater. Res. Bull.*, 25 (1990) 623-630.
- [80] T. Ohzuku, A. Ueda, Solid-state redox reactions of LiCoO_2 (R3m) for 4 volt secondary lithium cells, *J. Electrochem. Soc.*, 141 (1994) 2972-2977.
- [81] J.N. Reimers, J.R. Dahn, Electrochemical and in situ X-ray diffraction studies of lithium intercalation in Li_xCoO_2 , *J. Electrochem. Soc.*, 139 (1992) 2091-2097.

- [82] M. Broussely, F. Pertont, P. Biensan, J.M. Bodet, J. Labat, A. Lecerf, C. Delmas, A. Rougier, J.P. Peres, Li_xNiO_2 , a promising cathode for rechargeable lithium batteries, *J. Power Sources*, 54 (1995) 109-114.
- [83] J.R. Dahn, U. Von Sacken, M.W. Juzkow, H. Al-Janaby, Rechargeable LiNiO_2 /carbon cells, *J. Electrochem. Soc.*, 138 (1991) 2207-2211.
- [84] A.R. Armstrong, P.G. Bruce, Synthesis of layered LiMnO_2 as an electrode for rechargeable lithium batteries, *Nature*, 381 (1996) 499-500.
- [85] P.G. Bruce, A.R. Armstrong, H. Huang, New and optimised lithium manganese oxide cathodes for rechargeable lithium batteries, *J. Power Sources*, 68 (1997) 19-23.
- [86] F. Capitaine, P. Gravereau, C. Delmas, A new variety of LiMnO_2 with a layered structure, *Solid State Ionics*, 89 (1996) 197-202.
- [87] W.I.F. David, M.M. Thackeray, L.A. De Picciotto, J.B. Goodenough, Structure refinement of the spinel-related phases $\text{Li}_2\text{Mn}_2\text{O}_4$ and $\text{Li}_{0.2}\text{Mn}_2\text{O}_4$, *J. Solid State Chem.*, 67 (1987) 316-323.
- [88] M.M. Thackeray, W.I.F. David, P.G. Bruce, J.B. Goodenough, Lithium insertion into manganese spinels, *Mater. Res. Bull.*, 18 (1983) 461-472.
- [89] M.M. Thackeray, P.J. Johnson, L.A. De Picciotto, P.G. Bruce, J.B. Goodenough, Electrochemical extraction of lithium from LiMn_2O_4 , *Mater. Res. Bull.*, 19 (1984) 179-187.
- [90] A.K. Padhi, K.S. Nanjundaswamy, J.B. Goodenough, Phospho-olivines as positive-electrode materials for rechargeable lithium batteries, *J. Electrochem. Soc.*, 144 (1997) 1188.
- [91] M. Wakihara, Recent developments in lithium ion batteries, *Mat. Sci. Eng. R*, 33 (2001) 109-134.

- [92] R. Konno, Structure, phase relationship and electrochemical properties of cathode materials - Nickel, manganese and iron systems, International Open Seminar - High Energy Density Lithium Batteries for the Coming Generation Tokyo: Italian Institute of Culture, 1998.
- [93] Z.P. Guo, Investigation on cathode materials for lithium-ion batteries, Institute for Superconducting and Electronic Materials, Faculty of Engineering, University of Wollongong, New South Wales, Australia, 2003.
- [94] M. Broussely, P. Biensan, B. Simon, Lithium insertion into host materials: The key to success for Li ion batteries, *Electrochim. Acta.*, 45 (1999) 3-22.
- [95] Y.-I. Jang, W.D. Moorehead, Y.-M. Chiang, Synthesis of the monoclinic and orthorhombic phases of LiMnO_2 in oxidizing atmosphere, *Solid State Ionics*, 149 (2002) 201-207.
- [96] M. Tabuchi, C. Masquelier, T. Takeuchi, K. Ado, I. Matsubara, T. Shirane, R. Kanno, S. Tsutsui, S. Nasu, H. Sakaebe, $\text{Li}^+ \text{Na}^+$ exchange from $\square\text{-NaFeO}_2$ using hydrothermal reaction, *Solid State Ionics*, 90 (1996) 129-132.
- [97] S.-Y. Chung, J.T. Bloking, Y.-M. Chiang, Electronically conductive phospho-olivines as lithium storage electrodes, *Nat. Mater.*, 1 (2002) 123-128.
- [98] H. Huang, S.C. Yin, L.F.s. Nazar, Approaching theoretical capacity of LiFePO_4 at room temperature at high rates, *Electrochem. Solid-State Lett.*, 4 (2001) A170-A172.
- [99] J.B. Goodenough, Design considerations, *Solid State Ionics*, 69 (1994) 184-198.
- [100] C.M. Julien, A. Mauger, K. Zaghib, H. Groult, Comparative issues of cathode materials for Li-ion batteries, *Inorganics*, 2 (2014) 132-154.
- [101] M.S. Idris, Synthesis and characterization of lithium nickel manganese cobalt oxide as cathode material, Department of Materials Science and Engineering, University of Sheffield, Sheffield, United Kingdom, 2011.

- [102] A. Manthiram, An outlook on lithium ion battery technology, *ACS Cent. Sci.*, 3 (2017) 1063-1069.
- [103] R.C. Masse, C. Liu, Y. Li, L. Mai, G. Cao, Energy storage through intercalation reactions: Electrodes for rechargeable batteries, *Natl. Sci. Rev.*, 4 (2017) 26-53.
- [104] Y. Mekonnen, A. Sundararajan, A.I. Sarwat, A review of cathode and anode materials for lithium-ion batteries, *SoutheastCon 2016, IEEE*, 2016, pp. 1-6.
- [105] F. Schipper, D. Aurbach, A brief review: Past, present and future of lithium ion batteries, *Russ. J. Electrochem+*, 52 (2016) 1095-1121.
- [106] J.M. Tarascon, D. Guyomard, The $\text{Li}_{1+x}\text{Mn}_2\text{O}_4/\text{C}$ rocking-chair system: A review, *Electrochim. Acta.*, 38 (1993) 1221-1231.
- [107] N. Nitta, F. Wu, J.T. Lee, G. Yushin, Li-ion battery materials: Present and future, *Mater. Today*, 18 (2015) 252-264.
- [108] Y. Hu, Development of novel nanomaterials based on silicon and graphene for lithium ion battery applications, University of Western Ontario, London, Ontario, Canada, 2014.
- [109] K.M. Shaju, G.V.S. Rao, B.V.R. Chowdari, Performance of layered $\text{Li}(\text{Ni}_{1/3}\text{Co}_{1/3}\text{Mn}_{1/3})\text{O}_2$ as cathode for Li-ion batteries, *Electrochim. Acta.*, 48 (2002) 145-151.
- [110] J. Akimoto, Y. Gotoh, Y. Oosawa, Synthesis and structure refinement of LiCoO_2 single crystals, *J. Solid State Chem.*, 141 (1998) 298-302.
- [111] C. Madhu, J. Garrett, V. Manivannan, Synthesis and characterization of oxide cathode materials of the system $(1-x-y)\text{LiNiO}_2.x\text{Li}_2\text{MnO}_3.y\text{LiCoO}_2$, *Ionics*, 16 (2010) 591-602.
- [112] Y. Sun, Y. Shiosaki, Y. Xia, H. Noguchi, The preparation and electrochemical performance of solid solutions $\text{LiCoO}_2\text{-Li}_2\text{MnO}_3$ as cathode materials for lithium ion batteries, *J. Power Sources*, 159 (2006) 1353-1359.

- [113] J. Jiang, K.W. Eberman, L.J. Krause, J.R. Dahn, Structure, electrochemical properties, and thermal stability studies of cathode materials in the $x\text{Li}[\text{Mn}_{1/2}\text{Ni}_{1/2}]\text{O}_2 \cdot y\text{LiCoO}_2 \cdot z\text{Li}[\text{Li}_{1/3}\text{Mn}_{2/3}]\text{O}_2$ pseudoternary System ($x + y + z = 1$), *J. Electrochem. Soc.*, 152 (2005) A1879-A1889.
- [114] Q. Zhong, A. Bonakdarpour, M. Zhang, Y. Gao, J.R. Dahn, Synthesis and Electrochemistry of $\text{LiNi}_x\text{Mn}_{2-x}\text{O}_4$, *J. Electrochem. Soc.*, 144 (1997) 205-213.
- [115] S.-W. Zhong, Y.-J. Zhao, L. Fang, L.I. Yan, H.U. Yang, P.-Z. Li, M.E.I. Jia, Q.-G. Liu, Characteristics and electrochemical performance of cathode material Co-coated LiNiO_2 for Li-ion batteries, *Trans. Nonferrous Met. Soc. China*, 16 (2006) 137-141.
- [116] J.-S. Kim, C.S. Johnson, J.T. Vaughey, M.M. Thackeray, S.A. Hackney, W. Yoon, C.P. Grey, Electrochemical and structural properties of $x\text{Li}_2\text{M}'\text{O}_3 \cdot (1-x)\text{LiMn}_{0.5}\text{Ni}_{0.5}\text{O}_2$ electrodes for lithium batteries ($\text{M}'=\text{Ti}, \text{Mn}, \text{Zr}; 0 \leq x \leq 0.3$), *Chem. Mater.*, 16 (2004) 1996-2006.
- [117] Y. Makimura, T. Ohzuku, Lithium insertion material of $\text{LiNi}_{1/2}\text{Mn}_{1/2}\text{O}_2$ for advanced lithium-ion batteries, *J. Power Sources*, 119 (2003) 156-160.
- [118] E. Rossen, C.D.W. Jones, J.R. Dahn, Structure and electrochemistry of $\text{Li}_x\text{Mn}_y\text{Ni}_{1-y}\text{O}_2$, *Solid State Ionics*, 57 (1992) 311-318.
- [119] M.E. Spahr, P. Novak, B. Schnyder, O. Haas, R. Nesper, Characterization of layered lithium nickel manganese oxides synthesized by a novel oxidative coprecipitation method and their electrochemical performance as lithium insertion electrode materials, *J. Electrochem. Soc.*, 145 (1998) 1113-1121.
- [120] T. Ohzuku, Y. Makimura, Layered lithium insertion material of $\text{LiNi}_{1/2}\text{Mn}_{1/2}\text{O}_2$: A possible alternative to LiCoO_2 for advanced lithium-ion batteries, *Chem. Lett.*, 30 (2001) 744-745.
- [121] Z. Liu, A. Yu, J.Y. Lee, Synthesis and characterization of $\text{LiNi}_{1-x-y}\text{Co}_x\text{Mn}_y\text{O}_2$ as the cathode materials of secondary lithium batteries, *J. Power Sources*, 81 (1999) 416-419.

- [122] T. Ohzuku, Y. Makimura, Layered lithium insertion material of $\text{LiCo}_{1/3}\text{Ni}_{1/3}\text{Mn}_{1/3}\text{O}_2$ for lithium-ion batteries, *Chem. Lett.*, 30 (2001) 642-643.
- [123] M. Yoshio, H. Noguchi, J.-i. Itoh, M. Okada, T. Mouri, Preparation and properties of $\text{LiCo}_y\text{Mn}_x\text{Ni}_{1-x-y}\text{O}_2$ as a cathode for lithium ion batteries, *J. Power Sources*, 90 (2000) 176-181.
- [124] N. Yabuuchi, T. Ohzuku, Novel lithium insertion material of $\text{LiCo}_{1/3}\text{Ni}_{1/3}\text{Mn}_{1/3}\text{O}_2$ for advanced lithium-ion batteries, *J. Power Sources*, 119 (2003) 171-174.
- [125] I. Belharouak, Y.K. Sun, J. Liu, K. Amine, $\text{Li}(\text{Ni}_{1/3}\text{Co}_{1/3}\text{Mn}_{1/3})\text{O}_2$ as a suitable cathode for high power applications, *J. Power Sources*, 123 (2003) 247-252.
- [126] Z. Lu, D.D. MacNeil, J.R. Dahn, Layered $\text{Li}[\text{Ni}_x\text{Co}_{1-2x}\text{Mn}_x]\text{O}_2$ cathode materials for lithium-ion batteries, *Electrochem. Solid-State Lett.*, 4 (2001) A200-A203.
- [127] J.K. Ngala, N.A. Chernova, M. Ma, M. Mamak, P.Y. Zavalij, M.S. Whittingham, The synthesis, characterization and electrochemical behavior of the layered $\text{LiNi}_{0.4}\text{Mn}_{0.4}\text{Co}_{0.2}\text{O}_2$ compound, *J. Mater. Chem.*, 14 (2004) 214-220.
- [128] W.-S. Yoon, K.Y. Chung, J. McBreen, X.-Q. Yang, A comparative study on structural changes of $\text{LiCo}_{1/3}\text{Ni}_{1/3}\text{Mn}_{1/3}\text{O}_2$ and $\text{LiNi}_{0.8}\text{Co}_{0.15}\text{Al}_{0.05}\text{O}_2$ during first charge using in situ XRD, *Electrochem. Commun.*, 8 (2006) 1257-1262.
- [129] J. Choi, A. Manthiram, Role of chemical and structural stabilities on the electrochemical properties of layered $\text{LiNi}_{1/3}\text{Mn}_{1/3}\text{Co}_{1/3}\text{O}_2$ cathodes, *J. Electrochem. Soc.*, 152 (2005) A1714-A1718.
- [130] R. Chen, M.S. Whittingham, Cathodic behavior of alkali manganese oxides from permanganate, *J. Electrochem. Soc.*, 144 (1997) L64-L67.
- [131] M.M. Thackeray, Structural considerations of layered and spinel lithiated oxides for lithium ion batteries, *J. Electrochem. Soc.*, 142 (1995) 2558-2563.

- [132] G. Amatucci, A. Du Pasquier, A. Blyr, T. Zheng, J.M. Tarascon, The elevated temperature performance of the $\text{LiMn}_2\text{O}_4/\text{C}$ system: Failure and solutions, *Electrochim. Acta.*, 45 (1999) 255-271.
- [133] R.J. Gummow, A. De Kock, M.M. Thackeray, Improved capacity retention in rechargeable 4 V lithium/lithium-manganese oxide (spinel) cells, *Solid State Ionics*, 69 (1994) 59-67.
- [134] N. Krins, F. Hatert, K. Traina, L. Dusoulier, I. Molenberg, J.F. Fagnard, P. Vanderbemden, A. Rulmont, R. Cloots, B. Vertruyen, $\text{LiMn}_{2-x}\text{Ti}_x\text{O}_4$ spinel-type compounds ($x \leq 1$): Structural, electrical and magnetic properties, *Solid State Ionics*, 177 (2006) 1033-1040.
- [135] Y. Shao-Horn, R.L. Midaugh, Redox reactions of cobalt, aluminum and titanium substituted lithium manganese spinel compounds in lithium cells, *Solid State Ionics*, 139 (2001) 13-25.
- [136] B. Ammundsen, J. Paulsen, I. Davidson, R.-S. Liu, C.-H. Shen, J.-M. Chen, L.-Y. Jang, J.-F. Lee, Local structure and first cycle redox mechanism of layered $\text{Li}_{1.2}\text{Cr}_{0.4}\text{Mn}_{0.4}\text{O}_2$ cathode material, *J. Electrochem. Soc.*, 149 (2002) A431-A436.
- [137] C.S. Johnson, J.S. Kim, C. Lefief, N. Li, J.T. Vaughey, M.M. Thackeray, The significance of the Li_2MnO_3 component in 'composite' $x\text{Li}_2\text{MnO}_3 \cdot (1-x)\text{LiMn}_{0.5}\text{Ni}_{0.5}\text{O}_2$ electrodes, *Electrochem. Commun.*, 6 (2004) 1085-1091.
- [138] M.M. Thackeray, C.S. Johnson, J.T. Vaughey, N. Li, S.A. Hackney, Advances in manganese-oxide 'composite' electrodes for lithium-ion batteries, *J. Mater. Chem.*, 15 (2005) 2257-2267.
- [139] C.S. Johnson, S.D. Korte, J.T. Vaughey, M.M. Thackeray, T.E. Bofinger, Y. Shao-Horn, S.A. Hackney, Structural and electrochemical analysis of layered compounds from Li_2MnO_3 , *J. Power Sources*, 81 (1999) 491-495.

- [140] Y. Sun, C. Ouyang, Z. Wang, X. Huang, L. Chen, Effect of Co content on rate performance of $\text{LiMn}_{0.5-x}\text{Co}_{2x}\text{Ni}_{0.5-x}\text{O}_2$ cathode materials for lithium-ion batteries, *J. Electrochem. Soc.*, 151 (2004) A504-A508.
- [141] Z. Lu, L.Y. Beaulieu, R.A. Donabarger, C.L. Thomas, J.R. Dahn, Synthesis, structure, and electrochemical behavior of $\text{Li}[\text{Ni}_x\text{Li}_{1/3-2x/3}\text{Mn}_{2/3-x/3}]\text{O}_2$, *J. Electrochem. Soc.*, 149 (2002) A778-A791.
- [142] Z. Lu, D.D. MacNeil, J.R. Dahn, Layered cathode materials $\text{Li}[\text{Ni}_x\text{Li}_{(1/3-2x/3)}\text{Mn}_{(2/3-x/3)}]\text{O}_2$ for lithium-ion batteries, *Electrochem. Solid-State Lett.*, 4 (2001) A191-A194.
- [143] S.S. Shin, Y.K. Sun, K. Amine, Synthesis and electrochemical properties of $\text{Li}[\text{Li}_{(1-2x)/3}\text{Ni}_x\text{Mn}_{(2-x)/3}]\text{O}_2$ as cathode materials for lithium secondary batteries, *J. Power Sources*, 112 (2002) 634-638.
- [144] L. Zhang, H. Noguchi, M. Yoshio, Synthesis and electrochemical properties of layered Li-Ni-Mn-O compounds, *J. Power Sources*, 110 (2002) 57-64.
- [145] K. Numata, C. Sakaki, S. Yamanaka, Synthesis and characterization of layer structured solid solutions in the system of $\text{LiCoO}_2\text{-Li}_2\text{MnO}_3$, *Solid State Ionics*, 117 (1999) 257-263.
- [146] C.S. Johnson, J.-S. Kim, A.J. Kropf, A.J. Kahaian, J.T. Vaughey, M.M. Thackeray, The role of Li_2MO_2 structures (M = metal ion) in the electrochemistry of $(x)\text{LiMn}_{0.5}\text{Ni}_{0.5}\text{O}_2\cdot(1-x)\text{Li}_2\text{TiO}_3$ electrodes for lithium-ion batteries, *Electrochem. Commun.*, 4 (2002) 492-498.
- [147] J.S. Kim, C.S. Johnson, M.M. Thackeray, Layered $x\text{LiMO}_2\cdot(1-x)\text{Li}_2\text{M}'\text{O}_3$ electrodes for lithium batteries: A study of $0.95\text{LiMn}_{0.5}\text{Ni}_{0.5}\text{O}_2\cdot0.05\text{Li}_2\text{TiO}_3$, *Electrochem. Commun.*, 4 (2002) 205-209.
- [148] L. Zhang, H. Noguchi, Novel layered Li-Cr-Ti-O cathode materials for lithium rechargeable batteries, *Electrochem. Commun.*, 4 (2002) 560-564.

- [149] L. Zhang, H. Noguchi, Novel layered Li Cr Ti O cathode materials related to the LiCrO_2 Li_2TiO_3 solid solution, *J. Electrochem. Soc.*, 150 (2003) A601-A607.
- [150] L. Zhang, T. Muta, H. Noguchi, X. Wang, M. Zhou, M. Yoshio, Peculiar electrochemical behaviors of $(1-x)\text{LiNiO}_2 \cdot x\text{Li}_2\text{TiO}_3$ cathode materials prepared by spray drying, *J. Power Sources*, 117 (2003) 137-142.
- [151] L. Zhang, X. Wang, H. Noguchi, M. Yoshio, K. Takada, T. Sasaki, Electrochemical and ex situ XRD investigations on $(1-x)\text{LiNiO}_2 \cdot x\text{Li}_2\text{TiO}_3$ ($0.05 \leq x \leq 0.5$), *Electrochim. Acta.*, 49 (2004) 3305-3311.
- [152] M. Tabuchi, A. Nakashima, H. Shigemura, K. Ado, H. Kobayashi, H. Sakaebe, H. Kageyama, T. Nakamura, M. Kohzaki, A. Hirano, Synthesis, cation distribution, and electrochemical properties of Fe-substituted Li_2MnO_3 as a novel 4 V positive electrode material, *J. Electrochem. Soc.*, 149 (2002) A509-A524.
- [153] M. Tabuchi, H. Shigemura, K. Ado, H. Kobayashi, H. Sakaebe, H. Kageyama, R. Kanno, Preparation of lithium manganese oxides containing iron, *J. Power Sources*, 97 (2001) 415-419.
- [154] K. Xu, Secondary batteries - Lithium rechargeable systems | Electrolytes: Overview, *Encyclopedia of Electrochemical Power Sources*, Elsevier, Amsterdam, 2009, pp. 51-70.
- [155] S. Goriparti, E. Miele, F. De Angelis, E. Di Fabrizio, R.P. Zaccaria, C. Capiglia, Review on recent progress of nanostructured anode materials for Li-ion batteries, *J. Power Sources*, 257 (2014) 421-443.
- [156] G.-A. Nazri, G. Pistoia, *Lithium Batteries: Science and Technology*, Springer, USA, 2009.
- [157] T.-H. Park, J.-S. Yeo, M.-H. Seo, J. Miyawaki, I. Mochida, S.-H. Yoon, Enhancing the rate performance of graphite anodes through addition of natural graphite/carbon nanofibers in lithium-ion batteries, *Electrochim. Acta.*, 93 (2013) 236-240.

- [158] Y. Xie, Y. Qiu, L. Tian, T. Liu, X. Su, Ultrafine hollow Fe₃O₄ anode material modified with reduced graphene oxides for high-power lithium-ion batteries, *J. Alloy. Compd.*, 894 (2022) 162384.
- [159] L. Pauling, The structure and properties of graphite and boron nitride, *Proc. Natl. Acad. Sci.*, 56 (1966) 1646-1652.
- [160] A.C. Neto, F. Guinea, N.M. Peres, Drawing conclusions from graphene, *Phys. World*, 19 (2006) 33-37.
- [161] R.F. Nelson, Power requirements for batteries in hybrid electric vehicles, *J. Power Sources*, 91 (2000) 2-26.
- [162] J.W.F. To, Z. Chen, H. Yao, J. He, K. Kim, H.-H. Chou, L. Pan, J. Wilcox, Y. Cui, Z. Bao, Ultrahigh surface area three-dimensional porous graphitic carbon from conjugated polymeric molecular framework, *ACS Cent. Sci.*, 1 (2015) 68-76.
- [163] D.A.C. Brownson, D.K. Kampouris, C.E. Banks, An overview of graphene in energy production and storage applications, *J. Power Sources*, 196 (2011) 4873-4885.
- [164] M. Liang, L. Zhi, Graphene-based electrode materials for rechargeable lithium batteries, *J. Mater. Chem.*, 19 (2009) 5871-5878.
- [165] D. Pan, S. Wang, B. Zhao, M. Wu, H. Zhang, Y. Wang, Z. Jiao, Li storage properties of disordered graphene nanosheets, *Chem. Mater.*, 21 (2009) 3136-3142.
- [166] P. Lian, X. Zhu, S. Liang, Z. Li, W. Yang, H. Wang, Large reversible capacity of high quality graphene sheets as an anode material for lithium-ion batteries, *Electrochim. Acta.*, 55 (2010) 3909-3914.
- [167] Z.-L. Wang, D. Xu, H.-G. Wang, Z. Wu, X.-B. Zhang, In situ fabrication of porous graphene electrodes for high-performance energy storage, *ACS Nano*, 7 (2013) 2422-2430.

- [168] T. Bhardwaj, A. Antic, B. Pavan, V. Barone, B.D. Fahlman, Enhanced electrochemical lithium storage by graphene nanoribbons, *J. Am. Chem. Soc.*, 132 (2010) 12556-12558.
- [169] V.H. Pham, K.-H. Kim, D.-w. Jung, K. Singh, E.-S. Oh, J.S. Chung, Liquid phase co-exfoliated MoS₂-graphene composites as anode materials for lithium ion batteries, *J. Power Sources*, 244 (2013) 280-286.
- [170] Y. Wu, Y. Wei, J. Wang, K. Jiang, S. Fan, Conformal Fe₃O₄ sheath on aligned carbon nanotube scaffolds as high-performance anodes for lithium ion batteries, *Nano Lett.*, 13 (2013) 818-823.
- [171] H. Xia, D. Zhu, Y. Fu, X. Wang, CoFe₂O₄-graphene nanocomposite as a high-capacity anode material for lithium-ion batteries, *Electrochim. Acta.*, 83 (2012) 166-174.
- [172] A. Hu, X. Chen, Y. Tang, Q. Tang, L. Yang, S. Zhang, Self-assembly of Fe₃O₄ nanorods on graphene for lithium ion batteries with high rate capacity and cycle stability, *Electrochem. Commun.*, 28 (2013) 139-142.
- [173] D. Fauteux, R. Koksang, Rechargeable lithium battery anodes: Alternatives to metallic lithium, *J. Appl. Electrochem.*, 23 (1993) 1-10.
- [174] Y. Ma, P. Guo, M. Liu, P. Cheng, T. Zhang, J. Liu, D. Liu, D. He, To achieve controlled specific capacities of silicon-based anodes for high-performance lithium-ion batteries, *J. Alloy. Compd.*, 905 (2022) 164189.
- [175] T. Masanao, Ph. D. Thesis - Studies on the novel nonwoven separators for high power and large-scale lithium-ion battery, Kobe University, 2012.
- [176] C.M. Hayner, X. Zhao, H.H. Kung, Materials for rechargeable lithium-ion batteries, *Annu. Rev. Chem. Biomol.*, 3 (2012) 445-471.

- [177] M. Nie, D.P. Abraham, Y. Chen, A. Bose, B.L. Lucht, Silicon solid electrolyte interphase (SEI) of lithium ion battery characterized by microscopy and spectroscopy, *J. Phys. Chem. C*, 117 (2013) 13403-13412.
- [178] B.M.L. Rao, R.W. Francis, H.A. Christopher, Lithium-aluminum electrode, *J. Electrochem. Soc.*, 124 (1977) 1490-1492.
- [179] M. Winter, J.O. Besenhard, Electrochemical lithiation of tin and tin-based intermetallics and composites, *Electrochim. Acta.*, 45 (1999) 31-50.
- [180] G. Derrien, J. Hassoun, S. Panero, B. Scrosati, Nanostructured Sn-C composite as an advanced anode material in high-performance lithium-ion batteries, *Adv. Mater.*, 19 (2007) 2336-2340.
- [181] H. Kim, B. Han, J. Choo, J. Cho, Three-dimensional porous silicon particles for use in high-performance lithium secondary batteries, *Angew. Chem. Int. Edit.*, 47 (2008) 10151-10154.
- [182] K.D. Kepler, J.T. Vaughey, M.M. Thackeray, $\text{Li}_x\text{Cu}_6\text{Sn}_5$ ($0 < x < 13$): An intermetallic insertion electrode for rechargeable lithium batteries, *Electrochem. Solid-State Lett.*, 2 (1999) 307.
- [183] Y. Idota, T. Kubota, A. Matsufuji, Y. Maekawa, T. Miyasaka, Tin-based amorphous oxide: A high-capacity lithium-ion-storage material, *Science*, 276 (1997) 1395-1397.
- [184] T.L. Kulova, New electrode materials for lithium-ion batteries, *Russ. J. Electrochem.*, 49 (2013) 1-25.
- [185] J. Morales, L. Sanchez, Improving the electrochemical performance of SnO_2 cathodes in lithium secondary batteries by doping with Mo, *J. Electrochem. Soc.*, 146 (1999) 1640.
- [186] S.-L. Chou, J.-Z. Wang, H.-K. Liu, S.-X. Dou, SnO_2 meso-scale tubes: One-step, room temperature electrodeposition synthesis and kinetic investigation for lithium storage, *Electrochem. Commun.*, 11 (2009) 242-246.

- [187] Z.Y. Zeng, J.P. Tu, X.H. Huang, X.L. Wang, X.B. Zhao, K.F. Li, Electrochemical properties of a mesoporous Si/TiO₂ nanocomposite film anode for lithium-ion batteries, *Electrochem. Solid-State Lett.*, 11 (2008) A105.
- [188] Y. Liang, J. Fan, X.-h. Xia, Y.-s. Luo, Z.-j. Jia, Modified hydrothermal synthesis of SnO_y-SiO₂ for lithium-ion battery anodes, *Electrochim. Acta.*, 52 (2007) 5891-5895.
- [189] G. Wang, X.P. Gao, P.W. Shen, Hydrothermal synthesis of Co₂SnO₄ nanocrystals as anode materials for Li-ion batteries, *J. Power Sources*, 192 (2009) 719-723.
- [190] T. Zhang, L.J. Fu, J. Gao, Y.P. Wu, R. Holze, H.Q. Wu, Nanosized tin anode prepared by laser-induced vapor deposition for lithium ion battery, *J. Power Sources*, 174 (2007) 770-773.
- [191] C. Arbizzani, S. Beninati, M. Lazzari, M. Mastragostino, Carbon paper as three-dimensional conducting substrate for tin anodes in lithium-ion batteries, *J. Power Sources*, 141 (2005) 149-155.
- [192] P. Poizot, S. Laruelle, S. Grugeon, L. Dupont, J.M. Tarascon, Nano-sized transition-metal oxides as negative-electrode materials for lithium-ion batteries, *Nature*, 407 (2000) 496-499.
- [193] P. Poizot, S. Laruelle, S. Grugeon, L. Dupont, J.M. Tarascon, Searching for new anode materials for the Li-ion technology: Time to deviate from the usual path, *J. Power Sources*, 97 (2001) 235-239.
- [194] A. Debart, L. Dupont, P. Poizot, J.B. Leriche, J.M. Tarascon, A transmission electron microscopy study of the reactivity mechanism of tailor-made CuO particles toward lithium, *J. Electrochem. Soc.*, 148 (2001) A1266.
- [195] S. Grugeon, S. Laruelle, R. Herrera-Urbina, L. Dupont, P. Poizot, J.M. Tarascon, Particle size effects on the electrochemical performance of copper oxides toward lithium, *J. Electrochem. Soc.*, 148 (2001) A285.

- [196] F. Badway, I. Plitz, S. Grugeon, S. Laruelle, M. Dolle, A.S. Gozdz, J.M. Tarascon, Metal oxides as negative electrode materials in Li-ion cells, *Electrochem. Solid-State Lett.*, 5 (2002) A115.
- [197] J.-S. Xu, Y.-J. Zhu, Monodisperse Fe₃O₄ and α -Fe₂O₃ magnetic mesoporous microspheres as anode materials for lithium-ion batteries, *ACS Appl. Mater. Inter.*, 4 (2012) 4752-4757.
- [198] L. Zhang, P. Hu, X. Zhao, R. Tian, R. Zou, D. Xia, Controllable synthesis of core-shell Co@CoO nanocomposites with a superior performance as an anode material for lithium-ion batteries, *J. Mater. Chem.*, 21 (2011) 18279-18283.
- [199] J.-K. Hwang, H.-S. Lim, Y.-K. Sun, K.-D. Suh, Monodispersed hollow carbon/Fe₃O₄ composite microspheres for high performance anode materials in lithium-ion batteries, *J. Power Sources*, 244 (2013) 538-543.
- [200] I.T. Kim, A. Magasinski, K. Jacob, G. Yushin, R. Tannenbaum, Synthesis and electrochemical performance of reduced graphene oxide/maghemite composite anode for lithium ion batteries, *Carbon*, 52 (2013) 56-64.
- [201] X. Zhu, W. Wu, Z. Liu, L. Li, J. Hu, H. Dai, L. Ding, K. Zhou, C. Wang, X. Song, A reduced graphene oxide-nanoporous magnetic oxide iron hybrid as an improved anode material for lithium ion batteries, *Electrochim. Acta.*, 95 (2013) 24-28.
- [202] S.H. Lee, C. Huang, P.S. Grant, Multi-layered composite electrodes of high power Li₄Ti₅O₁₂ and high capacity SnO₂ for smart lithium ion storage, *Energy Stor. Mater.*, 38 (2021) 70-79.
- [203] Z. Deng, Z. Xu, W. Deng, X. Wang, Ultrafine Li₄Ti₅O₁₂ nanocrystals as building blocks for ultrahigh-power lithium-ion battery anodes, *J. Power Sources*, 521 (2022) 230970.
- [204] I. Exnar, L. Kavan, S.Y. Huang, M. Gratzel, Novel 2 V rocking-chair lithium battery based on nano-crystalline titanium dioxide, *J. Power Sources*, 68 (1997) 720-722.

- [205] M. Inaba, Y. Oba, F. Niina, Y. Murota, Y. Ogino, A. Tasaka, K. Hirota, TiO₂ (B) as a promising high potential negative electrode for large-size lithium-ion batteries, *J. Power Sources*, 189 (2009) 580-584.
- [206] L. Kavan, M. Gratzel, S.E. Gilbert, C. Klemenz, H.J. Scheel, Electrochemical and photoelectrochemical investigation of single-crystal anatase, *J. Am. Chem. Soc.*, 118 (1996) 6716-6723.
- [207] M. Wagemaker, G.J. Kearley, A.A. Van Well, H. Mutka, F.M. Mulder, Multiple Li positions inside oxygen octahedra in lithiated TiO₂ anatase, *J. Am. Chem. Soc.*, 125 (2003) 840-848.
- [208] M. Winter, J.O. Besenhard, *Handbook of Battery Materials*, Wiley, New York, 1999.
- [209] Y. Surace, D. Leanza, M. Mirolo, L. Kondracki, C.A.F. Vaz, M. El Kazzi, P. Novak, S. Trabesinger, Evidence for stepwise formation of solid electrolyte interphase in a Li-ion battery, *Energy Stor. Mater.*, 44 (2022) 156-167.
- [210] A. Banerjee, Y. Shilina, B. Ziv, J.M. Ziegelbauer, S. Luski, D. Aurbach, I.C. Halalay, Multifunctional materials for enhanced Li-ion batteries durability: A brief review of practical options, *J. Electrochem. Soc.*, 164 (2017) A6315-A6323.
- [211] X.-B. Cheng, R. Zhang, C.-Z. Zhao, F. Wei, J.-G. Zhang, Q. Zhang, A review of solid electrolyte interphases on lithium metal anode, *Adv. Sci.*, 3 (2016) 1500213.
- [212] N. Dupre, M. Cuisinier, J.F. Martin, D. Guyomard, Interphase evolution at two promising electrode materials for Li-ion batteries: LiFePO₄ and LiNi_{1/2}Mn_{1/2}O₂, *ChemPhysChem*, 15 (2014) 1922-1938.
- [213] K. Edstrom, M. Herstedt, D.P. Abraham, A new look at the solid electrolyte interphase on graphite anodes in Li-ion batteries, *J. Power Sources*, 153 (2006) 380-384.

- [214] P. Lu, C. Li, E.W. Schneider, S.J. Harris, Chemistry, impedance, and morphology evolution in solid electrolyte interphase films during formation in lithium ion batteries, *J. Phys. Chem. C*, 118 (2014) 896-903.
- [215] P. Verma, P. Maire, P. Novak, A review of the features and analyses of the solid electrolyte interphase in Li-ion batteries, *Electrochim. Acta.*, 55 (2010) 6332-6341.
- [216] R. Pan, O. Cheung, Z. Wang, P. Tammela, J. Huo, J. Lindh, K. Edstrom, M. Stromme, L. Nyholm, Mesoporous Cladophora cellulose separators for lithium-ion batteries, *J. Power Sources*, 321 (2016) 185-192.
- [217] J. Zhang, D. Shao, L. Jiang, G. Zhang, H. Wu, R. Day, W. Jiang, Advanced thermal management system driven by phase change materials for power lithium-ion batteries: A review, *Renew. Sustain. Energy Rev.*, 159 (2022) 112207.
- [218] X. Huang, Separator technologies for lithium-ion batteries, *J. Solid State Electr.*, 15 (2011) 649-662.
- [219] R. Pan, X. Xu, R. Sun, Z. Wang, J. Lindh, K. Edstrom, M. Stromme, L. Nyholm, Nanocellulose modified polyethylene separators for lithium metal batteries, *Small*, 14 (2018) 1704371.
- [220] M.-H. Ryou, D.J. Lee, J.-N. Lee, Y.M. Lee, J.-K. Park, J.W. Choi, Excellent cycle life of lithium-metal anodes in lithium-ion batteries with mussel-inspired polydopamine-coated separators, *Adv. Energy Mater.*, 2 (2012) 645-650.
- [221] J. Dai, C. Shi, C. Li, X. Shen, L. Peng, D. Wu, D. Sun, P. Zhang, J. Zhao, A rational design of separator with substantially enhanced thermal features for lithium-ion batteries by the polydopamine-ceramic composite modification of polyolefin membranes, *Energy Environ. Sci.*, 9 (2016) 3252-3261.

- [222] H. Li, D. Wu, J. Wu, L.-Y. Dong, Y.-J. Zhu, X. Hu, Flexible, high-wettability and fire-resistant separators based on hydroxyapatite nanowires for advanced lithium-ion batteries, *Adv. Mater.*, 29 (2017) 1703548.
- [223] C. Man, P. Jiang, K.-w. Wong, Y. Zhao, C. Tang, M. Fan, W.-m. Lau, J. Mei, S. Li, H. Liu, Enhanced wetting properties of a polypropylene separator for a lithium-ion battery by hyperthermal hydrogen induced cross-linking of poly (ethylene oxide), *J. Mater. Chem. A*, 2 (2014) 11980-11986.
- [224] D. Aurbach, Y. Talyosef, B. Markovsky, E. Markevich, E. Zinigrad, L. Asraf, J.S. Gnanaraj, H.-J. Kim, Design of electrolyte solutions for Li and Li-ion batteries: A review, *Electrochim. Acta.*, 50 (2004) 247-254.
- [225] M.R. Palacin, Recent advances in rechargeable battery materials: a chemist's perspective, *Chem. Soc. Rev.*, 38 (2009) 2565-2575.
- [226] Z.W. Seh, Y. Sun, Q. Zhang, Y. Cui, Designing high-energy lithium-sulfur batteries, *Chem. Soc. Rev.*, 45 (2016) 5605-5634.
- [227] H. Buqa, D. Goers, M. Holzapfel, M.E. Spahr, P. Novak, High rate capability of graphite negative electrodes for lithium-ion batteries, *J. Electrochem. Soc.*, 152 (2005) A474-A481.
- [228] V.R. Koch, Status of the secondary lithium electrode, *J. Power Sources*, 6 (1981) 357-370.
- [229] M. Petzl, M. Kasper, M.A. Danzer, Lithium plating in a commercial lithium-ion battery - A low-temperature aging study, *J. Power Sources*, 275 (2015) 799-807.
- [230] D. Lin, Y. Liu, Y. Cui, Reviving the lithium metal anode for high-energy batteries, *Nat. Nanotechnol.*, 12 (2017) 194-206.
- [231] H. Yang, C. Guo, A. Naveed, J. Lei, J. Yang, Y. Nuli, J. Wang, Recent progress and perspective on lithium metal anode protection, *Energy Stor. Mater.*, 14 (2018) 199-221.

- [232] R. Jin, L. Fu, H. Zhou, Z. Wang, Z. Qiu, L. Shi, J. Zhu, S. Yuan, High Li⁺ ionic flux separator enhancing cycling stability of lithium metal anode, *ACS Sustain. Chem. Eng.*, 6 (2018) 2961-2968.
- [233] X. Mao, L. Shi, H. Zhang, Z. Wang, J. Zhu, Z. Qiu, Y. Zhao, M. Zhang, S. Yuan, Polyethylene separator activated by hybrid coating improving Li⁺ ion transference number and ionic conductivity for Li-metal battery, *J. Power Sources*, 342 (2017) 816-824.
- [234] Y. Saito, W. Morimura, R. Kuratani, S. Nishikawa, Ion transport in separator membranes of lithium secondary batteries, *J. Phys. Chem. C*, 119 (2015) 4702-4708.
- [235] J.-Q. Huang, T.-Z. Zhuang, Q. Zhang, H.-J. Peng, C.-M. Chen, F. Wei, Permselective graphene oxide membrane for highly stable and anti-self-discharge lithium-sulfur batteries, *ACS Nano*, 9 (2015) 3002-3011.
- [236] B.G. Kim, J.-S. Kim, J. Min, Y.-H. Lee, J.H. Choi, M.C. Jang, S.A. Freunberger, J.W. Choi, A moisture- and oxygen- impermeable separator for aprotic Li-O₂ batteries, *Adv. Funct. Mater.*, 26 (2016) 1747-1756.
- [237] Y. Pan, J. Hao, X. Zhu, Y. Zhou, S.-L. Chou, Ion selective separators based on graphene oxide for stabilizing lithium organic batteries, *Inorg. Chem. Front.*, 5 (2018) 1869-1875.
- [238] B. Aktekin, M.J. Lacey, T. Nordh, R. Younesi, C. Tengstedt, W. Zipprich, D. Brandell, K. Edstrom, Understanding the capacity loss in LiNi_{0.5}Mn_{1.5}O₄-Li₄Ti₅O₁₂ lithium-ion cells at ambient and elevated temperatures, *J. Phys. Chem. C*, 122 (2018) 11234-11248.
- [239] A. Banerjee, B. Ziv, Y. Shilina, S. Luski, D. Aurbach, I.C. Halalay, Acid-scavenging separators: A novel route for improving Li-ion batteries' durability, *ACS Energy Lett.*, 2 (2017) 2388-2393.

- [240] J.-H. Kim, J.-H. Kim, J.-M. Kim, Y.-G. Lee, S.-Y. Lee, Superlattice crystals-mimic, flexible/functional ceramic membranes: Beyond polymeric battery separators, *Adv. Energy Mater.*, 5 (2015) 1500954.
- [241] K.W. Leitner, H. Wolf, A. Garsuch, F. Chesneau, M. Schulz-Dobrick, Electroactive separator for high voltage graphite/LiNi_{0.5}Mn_{1.5}O₄ lithium ion batteries, *J. Power Sources*, 244 (2013) 548-551.
- [242] Z. Li, A.D. Pauric, G.R. Goward, T.J. Fuller, J.M. Ziegelbauer, M.P. Balogh, I.C. Halalay, Manganese sequestration and improved high-temperature cycling of Li-ion batteries by polymeric aza-15-crown-5, *J. Power Sources*, 272 (2014) 1134-1141.
- [243] S.-H. Chung, A. Manthiram, High-performance Li-S batteries with an ultra-lightweight MWCNT-coated separator, *J. Phys. Chem. Lett.*, 5 (2014) 1978-1983.
- [244] Y.-H. Lee, J.-H. Kim, J.-H. Kim, J.-T. Yoo, S.-Y. Lee, Spiderweb-mimicking anion-exchanging separators for Li-S batteries, *Adv. Funct. Mater.*, 28 (2018) 1801422.
- [245] Y.-S. Su, A. Manthiram, A new approach to improve cycle performance of rechargeable lithium-sulfur batteries by inserting a free-standing MWCNT interlayer, *Chem. Commun.*, 48 (2012) 8817-8819.
- [246] T.M. Bandhauer, S. Garimella, T.F. Fuller, A critical review of thermal issues in lithium-ion batteries, *J. Electrochem. Soc.*, 158 (2011) R1-R25.
- [247] Y. Yang, X. Huang, Z. Cao, G. Chen, Thermally conductive separator with hierarchical nano/microstructures for improving thermal management of batteries, *Nano Energy*, 22 (2016) 301-309.

- [248] L. Yue, J. Zhang, Z. Liu, Q. Kong, X. Zhou, Q. Xu, J. Yao, G. Cui, A heat resistant and flame-retardant polysulfonamide/polypropylene composite nonwoven for high performance lithium ion battery separator, *J. Electrochem. Soc.*, 161 (2014) A1032-A1038.
- [249] J. Zhang, Q. Kong, Z. Liu, S. Pang, L. Yue, J. Yao, X. Wang, G. Cui, A highly safe and inflame retarding aramid lithium ion battery separator by a papermaking process, *Solid State Ionics*, 245 (2013) 49-55.
- [250] K. Liu, W. Liu, Y. Qiu, B. Kong, Y. Sun, Z. Chen, D. Zhuo, D. Lin, Y. Cui, Electrospun core-shell microfiber separator with thermal-triggered flame-retardant properties for lithium-ion batteries, *Sci. Adv.*, 3 (2017) e1601978.
- [251] W. Zichen, D. Changqing, A comprehensive review on thermal management systems for power lithium-ion batteries, *Renew. Sustain. Energy Rev.*, 139 (2021) 110685.
- [252] K.-H. Choi, S.-J. Cho, S.-J. Chun, J.T. Yoo, C.K. Lee, W. Kim, Q. Wu, S.-B. Park, D.-H. Choi, S.-Y. Lee, Heterolayered, one-dimensional nanobuilding block mat batteries, *Nano Lett.*, 14 (2014) 5677-5686.
- [253] K.-H. Choi, J. Yoo, C.K. Lee, S.-Y. Lee, All-inkjet-printed, solid-state flexible supercapacitors on paper, *Energy Environ. Sci.*, 9 (2016) 2812-2821.
- [254] S. Leijonmarck, A. Cornell, G. Lindbergh, L. Wagberg, Single-paper flexible Li-ion battery cells through a paper-making process based on nano-fibrillated cellulose, *J. Mater. Chem. A*, 1 (2013) 4671-4677.
- [255] W. Liu, M.-S. Song, B. Kong, Y. Cui, Flexible and stretchable energy storage: Recent advances and future perspectives, *Adv. Mater.*, 29 (2017) 1603436.
- [256] L. Nyholm, G. Nystrom, A. Mihranyan, M. Stromme, Toward flexible polymer and paper-based energy storage devices, *Adv. Mater.*, 23 (2011) 3751-3769.

- [257] V.L. Pushparaj, M.M. Shaijumon, A. Kumar, S. Murugesan, L. Ci, R. Vajtai, R.J. Linhardt, O. Nalamasu, P.M. Ajayan, Flexible energy storage devices based on nanocomposite paper, *Proc. Natl. Acad. Sci.*, 104 (2007) 13574-13577.
- [258] Z. Wang, R. Pan, C. Ruan, K. Edstrom, M. Stromme, L. Nyholm, Redox-active separators for lithium-ion batteries, *Adv. Sci.*, 5 (2018) 1700663.
- [259] P. Zuo, J. Hua, M. He, H. Zhang, Z. Qian, Y. Ma, C. Du, X. Cheng, Y. Gao, G. Yin, Facilitating the redox reaction of polysulfides by an electrocatalytic layer-modified separator for lithium-sulfur batteries, *J. Mater. Chem. A*, 5 (2017) 10936-10945.
- [260] D. Lin, D. Zhuo, Y. Liu, Y. Cui, All-integrated bifunctional separator for Li dendrite detection via novel solution synthesis of a thermostable polyimide separator, *J. Am. Chem. Soc.*, 138 (2016) 11044-11050.
- [261] H. Wu, D. Zhuo, D. Kong, Y. Cui, Improving battery safety by early detection of internal shorting with a bifunctional separator, *Nat. Commun.*, 5 (2014) 5193.
- [262] G. Chen, T.J. Richardson, Overcharge protection for rechargeable lithium batteries using electroactive polymers, *Electrochem. Solid-State Lett.*, 7 (2003) A23-A26.
- [263] J.K. Feng, X.P. Ai, Y.L. Cao, H.X. Yang, Polytriphenylamine used as an electroactive separator material for overcharge protection of rechargeable lithium battery, *J. Power Sources*, 161 (2006) 545-549.
- [264] B. Wang, T.J. Richardson, G. Chen, Electroactive polymer fiber separators for stable and reversible overcharge protection in rechargeable lithium batteries, *J. Electrochem. Soc.*, 161 (2014) A1039-A1044.

- [265] D. Hubble, D.E. Brown, Y. Zhao, C. Fang, J. Lau, B.D. McCloskey, G. Liu, Liquid electrolyte development for low-temperature lithium-ion batteries, *Energy Environ. Sci.*, 15 (2022) 550-578.
- [266] D. Aurbach, Y. Ein-Eli, B. Markovsky, A. Zaban, S. Luski, Y. Carmeli, H. Yamin, The study of electrolyte solutions based on ethylene and diethyl carbonates for rechargeable Li batteries: II. Graphite electrodes, *J. Electrochem. Soc.*, 142 (1995) 2882-2889.
- [267] J.M. Tarascon, D. Guyomard, New electrolyte compositions stable over the 0 to 5 V voltage range and compatible with the $\text{Li}_{1+x}\text{Mn}_2\text{O}_4$ /carbon Li-ion cells, *Solid State Ionics*, 69 (1994) 293-305.
- [268] G.H. Newman, R.W. Francis, L.H. Gaines, B.M.L. Rao, Hazard investigations of LiClO_4 /dioxolane electrolyte, *J. Electrochem. Soc.*, 127 (1980) 2025.
- [269] K.i. Takata, M. Morita, Y. Matsuda, K. Matsui, Cycling characteristics of secondary Li electrode in LiBF_4 /mixed ether electrolytes, *J. Electrochem. Soc.*, 132 (1985) 126-128.
- [270] A. Hofmann, M. Schulz, T. Hanemann, Effect of conducting salts in ionic liquid based electrolytes: Viscosity, conductivity, and Li-ion cell studies, *Int. J. Electrochem. Sc.*, 8 (2013) 10170-10189.
- [271] H. Yang, G.V. Zhuang, P.N. Ross Jr, Thermal stability of LiPF_6 salt and Li-ion battery electrolytes containing LiPF_6 , *J. Power Sources*, 161 (2006) 573-579.
- [272] L. Larush-Asraf, M. Biton, H. Teller, E. Zinigrad, D. Aurbach, On the electrochemical and thermal behavior of lithium bis (oxalato) borate (LiBOB) solutions, *J. Power Sources*, 174 (2007) 400-407.
- [273] W. Xu, C.A. Angell, A fusible orthoborate lithium salt with high conductivity in solutions, *Electrochem. Solid-State Lett.*, 3 (2000) 366.

- [274] W. Xu, C.A. Angell, Weakly coordinating anions, and the exceptional conductivity of their nonaqueous solutions, *Electrochem. Solid-State Lett.*, 4 (2000) E1-E4.
- [275] D.T. Hallinan Jr, N.P. Balsara, Polymer electrolytes, *Annu. Rev. Mater. Res.*, 43 (2013) 503-525.
- [276] C. Cao, Z.-B. Li, X.-L. Wang, X.-B. Zhao, W.-Q. Han, Recent advances in inorganic solid electrolytes for lithium batteries, *Front. Energy Res.*, 2 (2014) 25.
- [277] H.Y.P. Hong, Crystal structure and ionic conductivity of $\text{Li}_{14}\text{Zn}(\text{GeO}_4)_4$ and other new Li^+ superionic conductors, *Mater. Res. Bull.*, 13 (1978) 117-124.
- [278] A. Dumon, M. Huang, Y. Shen, C.-W. Nan, High Li ion conductivity in strontium doped $\text{Li}_7\text{La}_3\text{Zr}_2\text{O}_{12}$ garnet, *Solid State Ionics*, 243 (2013) 36-41.
- [279] H. Aono, E. Sugimoto, Y. Sadaoka, N. Imanaka, G.y. Adachi, Ionic conductivity of solid electrolytes based on lithium titanium phosphate, *J. Electrochem. Soc.*, 137 (1990) 1023-1027.
- [280] A. Yamauchi, A. Sakuda, A. Hayashi, M. Tatsumisago, Preparation and ionic conductivities of $(100-x)(0.75\text{Li}_2\text{S} \cdot 0.25\text{P}_2\text{S}_5) \cdot x\text{LiBH}_4$ glass electrolytes, *J. Power Sources*, 244 (2013) 707-710.
- [281] Y. Seino, T. Ota, K. Takada, A. Hayashi, M. Tatsumisago, A sulphide lithium super ion conductor is superior to liquid ion conductors for use in rechargeable batteries, *Energy Environ. Sci.*, 7 (2014) 627-631.
- [282] H. Yamin, A. Gorenshtein, J. Penciner, Y. Sternberg, E. Peled, Lithium sulfur battery: Oxidation/reduction mechanisms of polysulfides in THF solutions, *J. Electrochem. Soc.*, 135 (1988) 1045-1048.
- [283] S.S. Zhang, Liquid electrolyte lithium/sulfur battery: Fundamental chemistry, problems, and solutions, *J. Power Sources*, 231 (2013) 153-162.

- [284] J.-W. Park, K. Ueno, N. Tachikawa, K. Dokko, M. Watanabe, Ionic liquid electrolytes for lithium-sulfur batteries, *J. Phys. Chem. C*, 117 (2013) 20531-20541.
- [285] J. Scheers, S. Fantini, P. Johansson, A review of electrolytes for lithium-sulphur batteries, *J. Power Sources*, 255 (2014) 204-218.
- [286] M. Barghamadi, A.S. Best, A.I. Bhatt, A.F. Hollenkamp, M. Musameh, R.J. Rees, T. Ruther, Lithium-sulfur batteries - The solution is in the electrolyte, but is the electrolyte a solution?, *Energy Environ. Sci.*, 7 (2014) 3902-3920.
- [287] S. Zhang, K. Ueno, K. Dokko, M. Watanabe, Recent advances in electrolytes for lithium-sulfur batteries, *Adv. Energy Mater.*, 5 (2015) 1500117.
- [288] B.H. Jeon, J.H. Yeon, I.J. Chung, Preparation and electrical properties of lithium-sulfur-composite polymer batteries, *J. Mater. Process. Tech.*, 143 (2003) 93-97.
- [289] J. Wang, S.Y. Chew, Z.W. Zhao, S. Ashraf, D. Wexler, J. Chen, S.H. Ng, S.L. Chou, H.K. Liu, Sulfur-mesoporous carbon composites in conjunction with a novel ionic liquid electrolyte for lithium rechargeable batteries, *Carbon*, 46 (2008) 229-235.
- [290] Y.V. Mikhaylik, J.R. Akridge, Polysulfide shuttle study in the Li/S battery system, *J. Electrochem. Soc.*, 151 (2004) A1969-A1976.
- [291] Z.W. Seh, Q. Zhang, W. Li, G. Zheng, H. Yao, Y. Cui, Stable cycling of lithium sulfide cathodes through strong affinity with a bifunctional binder, *Chem. Sci.*, 4 (2013) 3673-3677.
- [292] M. Barghamadi, A. Kapoor, C. Wen, A review on Li-S batteries as a high efficiency rechargeable lithium battery, *J. Electrochem. Soc.*, 160 (2013) A1256-A1263.
- [293] D. Aurbach, Review of selected electrode-solution interactions which determine the performance of Li and Li ion batteries, *J. Power Sources*, 89 (2000) 206-218.

- [294] U. Kasavajjula, C. Wang, A.J. Appleby, Nano-and bulk-silicon-based insertion anodes for lithium-ion secondary cells, *J. Power Sources*, 163 (2007) 1003-1039.
- [295] H. Wu, G. Yu, L. Pan, N. Liu, M.T. McDowell, Z. Bao, Y. Cui, Stable Li-ion battery anodes by in-situ polymerization of conducting hydrogel to conformally coat silicon nanoparticles, *Nat. Commun.*, 4 (2013) 1943.
- [296] K.M. Abraham, Z. Jiang, A polymer electrolyte-based rechargeable lithium/oxygen battery, *J. Electrochem. Soc.*, 143 (1996) 1-5.
- [297] G. Girishkumar, B. McCloskey, A.C. Luntz, S. Swanson, W. Wilcke, Lithium - Air battery: Promise and challenges, *J. Phys. Chem. Lett.*, 1 (2010) 2193-2203.
- [298] C. Shi, J. Zhu, X. Shen, F. Chen, F. Ning, H. Zhang, Y.-Z. Long, X. Ning, J. Zhao, Flexible inorganic membranes used as a high thermal safety separator for the lithium-ion battery, *RSC Adv.*, 8 (2018) 4072-4077.
- [299] D. Wu, L. Deng, Y. Sun, K.S. Teh, C. Shi, Q. Tan, J. Zhao, D. Sun, L. Lin, A high-safety PVDF/Al₂O₃ composite separator for Li-ion batteries via tip-induced electrospinning and dip-coating, *RSC Adv.*, 7 (2017) 24410-24416.
- [300] M. Yanilmaz, Evaluation of electrospun PVA/SiO₂ nanofiber separator membranes for lithium-ion batteries, *J. Text. I.*, 111 (2020) 447-452.
- [301] B. Chen, X. Xu, X. Chen, L. Kong, D. Chen, Transformation behavior of gibbsite to boehmite by steam-assisted synthesis, *J. Solid State Chem.*, 265 (2018) 237-243.
- [302] V.P. Pakharukova, D.A. Yatsenko, E.Y. Gerasimov, A.S. Shalygin, O.N. Martyanov, S.V. Tsybulya, Coherent 3D nanostructure of γ -Al₂O₃: Simulation of whole X-ray powder diffraction pattern, *J. Solid State Chem.*, 246 (2017) 284-292.

- [303] B. Sun, X. Li, R. Zhao, M. Yin, Z. Wang, Z. Jiang, C. Wang, Hierarchical aminated PAN/ γ -AlOOH electrospun composite nanofibers and their heavy metal ion adsorption performance, *J. Taiwan Inst. Chem. E.*, 62 (2016) 219-227.
- [304] K. Feng, D. Rong, W. Ren, X. Wen, Hierarchical flower-like γ -AlOOH and γ -Al₂O₃ microspheres: Synthesis and adsorption properties, *Mater. Express*, 5 (2015) 371-375.
- [305] P.-H. Huang, S.-J. Chang, C.-C. Li, C.-A. Chen, Boehmite-based microcapsules as flame-retardants for lithium-ion batteries, *Electrochim. Acta.*, 228 (2017) 597-603.
- [306] A. Laachachi, M. Ferriol, M. Cochez, J.M.L. Cuesta, D. Ruch, A comparison of the role of boehmite (AlOOH) and alumina (Al₂O₃) in the thermal stability and flammability of poly (methyl methacrylate), *Polym. Degrad. Stabil.*, 94 (2009) 1373-1378.
- [307] A.M. Baccarella, R. Garrard, M.L. Beauvais, U. Bednarski, S. Fischer, A.M. Abeykoon, K.W. Chapman, B.L. Phillips, J.B. Parise, J.W. Simonson, Cluster mediated conversion of amorphous Al(OH)₃ to γ -AlOOH, *J. Solid State Chem.*, 301 (2021) 122340.
- [308] R. Xu, X. Lin, X. Huang, J. Xie, C. Jiang, C. Lei, Boehmite-coated microporous membrane for enhanced electrochemical performance and dimensional stability of lithium-ion batteries, *J. Solid State Electr.*, 22 (2018) 739-747.
- [309] C. Yang, H. Tong, C. Luo, S. Yuan, G. Chen, Y. Yang, Boehmite particle coating modified microporous polyethylene membrane: A promising separator for lithium ion batteries, *J. Power Sources*, 348 (2017) 80-86.
- [310] G. Zhong, Y. Wang, C. Wang, Z. Wang, S. Guo, L. Wang, X. Liang, H. Xiang, An AlOOH-coated polyimide electrospun fibrous membrane as a high-safety lithium-ion battery separator, *Ionics*, 25 (2019) 2677-2684.

- [311] K. Rajaram, J. Kim, Surfactant assisted fabrication of different nanostructures of boehmite by hydrothermal process, *Int. J. Appl. Eng. Res.*, 12 (2017) 2781-2787.
- [312] P.S. Santos, A.C.V. Coelho, H.d.S. Santos, P.K. Kiyohara, Hydrothermal synthesis of well-crystallised boehmite crystals of various shapes, *Mater. Res.*, 12 (2009) 437-445.
- [313] Z. Tang, J. Liang, X. Li, J. Li, H. Guo, Y. Liu, C. Liu, Synthesis of flower-like Boehmite (γ -AlOOH) via a one-step ionic liquid-assisted hydrothermal route, *J. Solid State Chem.*, 202 (2013) 305-314.
- [314] A. Varesano, A. Belluati, D.O. Sanchez Ramirez, R.A. Carletto, C. Vineis, C. Tonetti, M. Bianchetto Songia, G. Mazzuchetti, A systematic study on the effects of doping agents on polypyrrole coating of fabrics, *J. Appl. Polym. Sci.*, 133 (2016) 42831.
- [315] S. Gantenbein, M. Schonleber, M. Weiss, E. Ivers-Tiffée, Capacity fade in lithium-ion batteries and cyclic aging over various state-of-charge ranges, *Sustainability*, 11 (2019) 6697-6712.
- [316] C.J. Patridge, C.T. Love, K.E. Swider-Lyons, M.E. Twigg, D.E. Ramaker, In-situ X-ray absorption spectroscopy analysis of capacity fade in nanoscale-LiCoO₂, *J. Solid State Chem.*, 203 (2013) 134-144.
- [317] M. Herstedt, D.P. Abraham, J.B. Kerr, K. Edstrom, X-ray photoelectron spectroscopy of negative electrodes from high-power lithium-ion cells showing various levels of power fade, *Electrochim. Acta.*, 49 (2004) 5097-5110.
- [318] D.D. MacNeil, D. Larcher, J.R. Dahn, Comparison of the reactivity of various carbon electrode materials with electrolyte at elevated temperature, *J. Electrochem. Soc.*, 146 (1999) 3596-3602.

APPENDIX

APPENDIX

CHARACTERIZATION INSTRUMENTS FOR LI-ION BATTERY

Fabrication & Casting Process of Li-Ion Coin Cell (Type 2032)

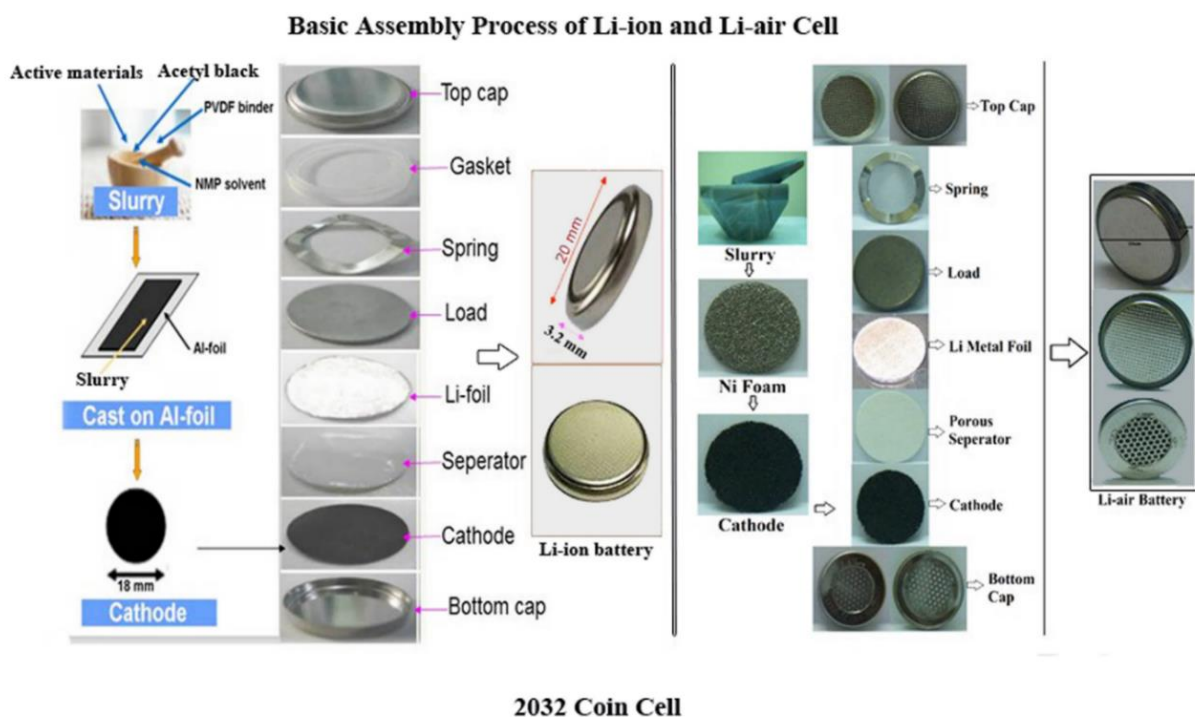


Fig. I: Basic Assembly Process of Coin Cell

During the reporting period a large number of 2032 type coin cells have been fabricated. For electrode preparation standard slurry casting technique was used. An optimized slurry was prepared by mixing the active material (like 80 wt %) with acetylene black (like 10 wt %) and binder (like 10 wt %) polyvinylidene fluoride (PVDF), dissolved in n-methyl-2-pyrrolidone (NMP). The mixed slurry was coated on an aluminum or a copper foil of 20 μm thickness for Li-ion Battery. The coated films or foam were then dried at 120°C for 12 hours, pressed and punched into circular disk (diameter \sim 15 mm) which is used either as cathode or anode. The thicknesses of various kinds of electrodes were in the range of 50-200 μm (excluding Al-foil). 2032 coin cells were assembled in a glove box (MBRAUN, Germany) where both oxygen and moisture levels were kept below 1.0

ppm. A complete cell comprises of a working electrode (cathode/anode), cellgard 2300 as the separator and lithium metal foil as counter electrode. 1M LiPF₆ dissolved in a mixture of ethylene carbonate (EC) and dimethyl carbonate (DMC) (1:2 by volume ratio) was used as the electrolyte. Basic cathode electrode casting and cell assembly process is shown in fig.(i) Each cell voltage is ~ 3.5V and ~2mAh capacity for Li-ion and 2.7V 600mAh for Li-air Battery.

1. Glove Box (Make: M'Braun, Germany, Model: Unilab)

For smooth running of the Atmosphere Controlled Glove-Box which is used routinely for coin cell fabrication. Li foil can catch fire easily in moisture and electrolyte is highly hygroscopic; so inert Ar gas atmosphere is used. Periodically regeneration of the catalyst bed is required to maintain the level of O₂ and H₂O to < 0.1 PPM.



Fig. II: Glove Box

2. Equipment for Electrode Preparation & Testing of Li-Ion Battery (MTI corporation, USA)

Vacuum slurry mixture, benchtop ball mill, film coater, hot rolling press (calendaring), and cutting & crimping tools, test cell etc. Optimization of slurry casting process etc for different electrodes and ceramic powder coated on poly propylene separators.



Fig. III: Equipment for Electrode Preparation

3. Laboratory Autoclave (Make: Parker autoclave Engineers, USA and Amar equipment, India)

Maximum vessel volume: 100 ml and 250 ml, Max. Pressure: 200 Bar, Max. Temperature: 230 °C and 200 °C, rotor speeds: 3000 rpm and 1450 rpm respectively. These are used 90% of max value of temperature and pressure.



Fig. IV: Laboratory Autoclaves

4. Galvanostat-Potentiostat Instruments (2nos) (Make: Autolab, Netherland, Model: N30 & N302)

Many electrochemical tests like Impedance, CV and Charge-Discharge for Li-ion have been done by these instruments. Outputs range 10 nA to 1A, 10V and 10nA to 10A, 30V



Fig. V: Galvanostat-Potentiostat Instrument

5. Automatic Battery Tester Instrument (Make: Arbin, USA, Model: BT2000)

Electrical performance test (Charge-Discharge) of the Li-ion cells has been done by these instruments. Output range is 6V, 1 μ A to 500mA (16 channels) and 10V, 1 μ A to 500mA (32 channels)



Fig. VI: Automatic Battery Tester Instrument

6. Hydraulic Press (Make Poly hydron Pvt. Ltd, Belgaum)

It is used for compressing casted electrode. Its capacity is 10 ton (320 Kg/cm^2), effective area is 31.185 cm^2 .



Fig. VII: Hydraulic Press

7. Electrical Heated Oven Driers [(Spac-N-Service, India), (Sangling, China)]

For preparation of LIB electrode, the casted samples were kept at different temperatures (ie.80⁰C-130⁰C) in vacuum. Therefore, regular maintenance of the oven was required and carried out.



Fig. VIII: Electrical Heated Oven Driers

8. Furnaces & Controller

Different type of furnaces with various temperature ranges are used for calcination of cathode powder. The following furnaces & controllers have been operated:

Kanthal furnace (1700 °C, 950 °C), India / Laboratory Muffle Furnaces, Nabertherm- P320 (1200 °C) Germany / Applied Test System INC (ATS) vertical type furnace (1200 °C), USA, CM furnaces inc. (1400-1650 °C), USA / Controlled atmosphere CVD Furnaces, (1200 °C) MTI Corporation, USA, and Controllers are Eurotherm (818, 2416), Honeywell (DC1040) etc.



Fig. IX: Furnaces & Controller

9. Separator Coating Unit and Thickness Measuring Gauge

Elcometer 3560, 4 gap film applicator is precision engineered from hardened stainless steel to provide four film thickness 50 μm , 100 μm . 150 μm and 200 μm respectively in one gauge.



Fig. X: Coating Device with Digital Thickness Gauge

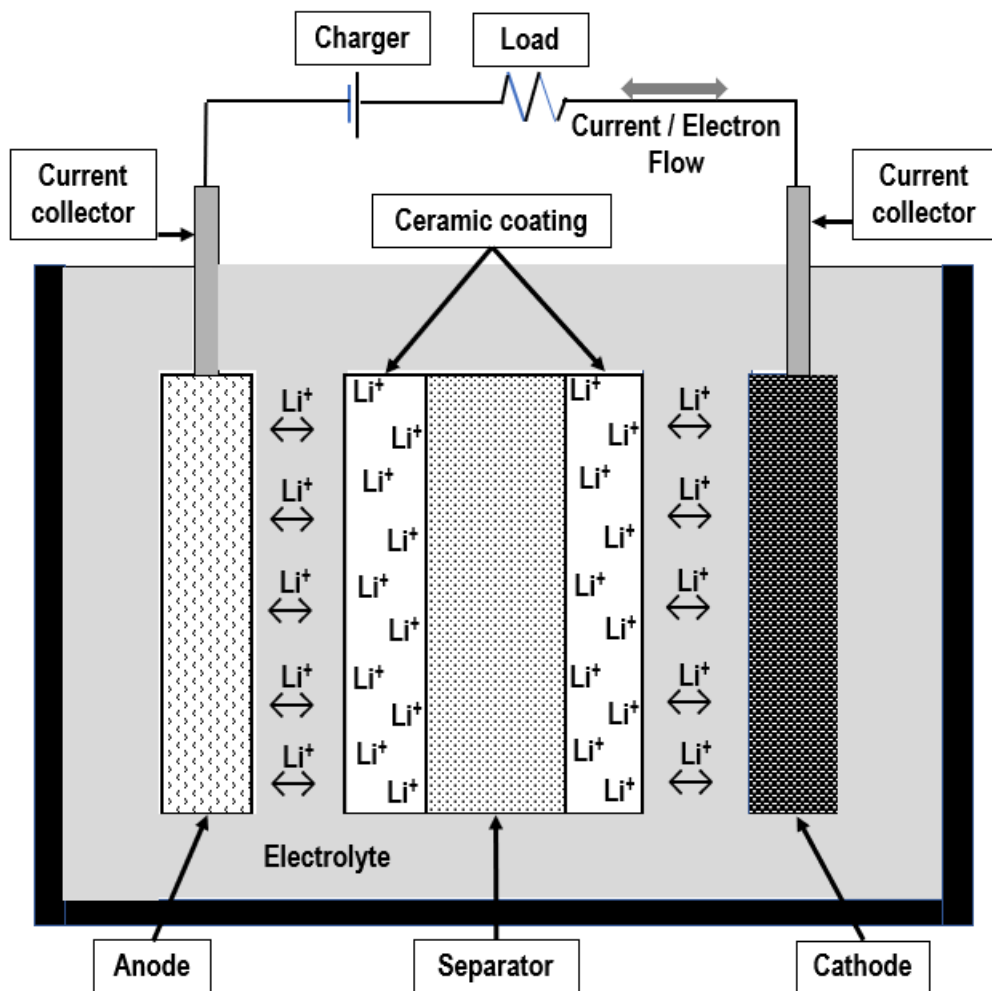


Fig. XI: Schematic Representation of Future Work

BIODATA

Name of student: Mr. Sourav Nag

Email: souravnag@cgcri.res.in

Contact: 90070 91905 / 86177 85737 (M)

Father's name: Late Pronay Kumar Nag

Nationality: Indian

Religion: Hindu

Present Address: 44/III SIRSA, 59 Lake Road, Kolkata – 700 029

Academic Qualifications

Qualification: B. Sc. (Tech), Ceramic Technology, 71.7%, Calcutta University, 1999

Award: GATE, Engineering Sciences, 80.41 Percentile, AIR – 212, 2003

Ph.D Course Work: In Engg. & Technology, CGPA – 7.75, Jadavpur University

Work Experience:

1. Principal Scientist, CSIR-CGCRI, Kolkata, From 2021 to Till date
2. Senior Scientist, CSIR-CGCRI, Kolkata, From 2015 to 2021
3. Scientist, CSIR-CGCRI, Kolkata, From 2010 to 2015
4. Junior Scientist, CSIR-CGCRI, Kolkata, From 2008 to 2010
5. Junior Scientist, CSIR-NAL, Bangalore, From 2006 to 2008
6. CSIR-JRF, CSIR-CGCRI, Kolkata, From 2004 to 2006
7. JRF (Project), CSIR-CGCRI, Kolkata, From 2001 to 2003
8. Asst. Manager (Operation), M/s RCI, New Delhi, From 2000 to 2001
9. Graduate Engineer Trainee, M/s SVM CTB Ltd., Gujarat, From 1999 to 2000

Publication:

Publications included in Thesis

1. **S. Nag**, S. Roy, Conventional Cathode Materials for Advanced Lithium-ion Battery: A Review, *Journal of Materials Science* (2023) Manuscript Under Review.
2. **S. Nag**, S. Roy, La-doped LiMnPO₄/C cathode material for Lithium-ion battery, *Chemical Engineering Science*, 272 (2023) 118600 - 118606.
3. **S. Nag**, A. Pramanik, S. Roy, S. Mahanty, Enhancement of Li⁺ ion kinetics in boehmite nanofiber coated polypropylene separator in LiFePO₄ cells, *Journal of Solid State Chemistry*, 312 (2022) 123214–123223.
4. **S. Nag**, S. Mahanty, Electrochemical properties of La-doped LiMnPO₄/C as lithium-ion battery cathode, Feb. 18-20, 2016, 27th Annual General Meeting of MRSI on Advanced Materials for Sustainable Application held at CSIR-NEIST, Jorhat, Assam.

Other publications

1. S. Mandal, S. Manna, K. Biswas, **S. Nag**, B. Ambade, Effect of gamma ray irradiation on optical and luminescence properties of CeO₂ doped bismuth glass, *Ceramics International*, (2023) DOI: <https://doi.org/10.1016/j.ceramint.2023.04.231>
2. S. Mandal, R. Chatterjee, **S. Nag**, S. Manna, S. Jana, K. Biswas, B. Ambade, Low Expansion Glass-Ceramics Using Industrial Waste and Low-cost Aluminosilicate Minerals: Fabrication and Characterizations, *Transaction of Indian Ceramic Society*, 82 (1) (2023) 46-55
3. **S. Nag**, S. Jana, M. Adhikary, S. Barik, A. Roy Chowdhury, S. Ghorui, B. Haldar, A. Ghosh, H. S. Tripathi and S. Mandal, Development of Mullite Based Refractory Pot for High Lead Containing Glass Melting, *Transaction of Indian Ceramic Society*, 80 (2) (2021) 150–156.

4. Q.A. Islam, **S. Nag**, R.N. Basu, Chemical Stability and Electrical Conductivity of $\text{Ba}_{0.8}\text{Ce}_{0.85-x}\text{Zr}_x\text{Tb}_{0.15}\text{O}_{3.8}$ Proton Conductors with ZnO as Sintering Aid, *Transaction of Indian Ceramic Society*, 75 (1) (2016) 25–32.
5. Q.A. Islam, S. Nag, R.N. Basu, Electrical properties of Tb-doped barium cerate, *Ceramics International*, 39 (6) (2013) 6433–6440.
6. Q.A. Islam, **S. Nag**, R.N. Basu, Study of electrical conductivity of Ca-substituted $\text{La}_2\text{Zr}_2\text{O}_7$, *Materials Research Bulletin*, 48 (2013) 3103–3107.
7. **S. Nag**, S. Mukhopadhyay, R.N. Basu, Development of mixed conducting dense nickel/Ca-doped lanthanum zirconate cermet for gas separation application, *Materials Research Bulletin*, 47 (2012) 925–929.

THE END